

NOTICES PAGE

Foreign Nation Release

This information is furnished upon the condition that it will not be released to another Nation without specific authority of the cognizant agency (Military or NASA) of the United States Government, and that the information be provided substantially the same degree of protection afforded it by the Department of Defense of the United States.

Disclaimer of Liability from Act of Transmittal

When Government drawings, specifications, or other data are used for any purpose other than in connection with a definitely related Government procurement operation, the United States Government thereby incurs no responsibility nor any obligation whatsoever; and the fact that the Government may have formulated, furnished, or in any way supplied the said drawings, specification, or other data, is not to be regarded by implication or otherwise as in any manner licensing the holder or any other person or corporation, or conveying and rights or permission to manufacture, use, or sell any patented invention that may in any be related thereto.

Any information disseminated by the Data Distribution Centers of the Interagency Data Exchange Program is intended to promote test data utilization in the National interest among groups engaged in Ballistic Missile, Space Vehicle and related programs.

Dissemination of said information does not imply verification or endorsement of the information. The originator, in submitting the material is acting in accordance with the requirements of his contract, and neither the originator nor the disseminator assumes any liability to parties adopting any product, process or practice based upon the usage of the information. Its presenting the success or failure of one (or several) part number(s), model(s), lot(s) under specific environment and output requirements, does not imply that other products not herein reported on are either inferior or superior.

Omission of Charges for Follow-on Actions

Any compliance by the report originator with requests from recipients for more detailed information on IDEP reports originated under Government contracts will be considered within the scope of present contractual obligations. Compliance with such requests will be at the discretion of the report originator and will be performed without cost or obligation to the requestor unless otherwise negotiated in advance.

Reproduction of this Report

Reproduction or duplication of any portion of this report is expressly forbidden, except by those contractors receiving it directly from the Data Centers or originator, for their internal use or the use of their sub-contractors. Reproduction or display of all or any portion of this material for any sales, advertising or publicity purposes is prohibited.

NASA CR-159717
PWA-5512-46

(NASA-CR-159717) EXPANDED STUDY OF
FEASIBILITY OF MEASURING IN-FLIGHT 747/JT9D
LOADS, PERFORMANCE, CLEARANCE, AND THERMAL
DATA (Pratt and Whitney Aircraft Group)
107 p HC A06/MF A01

N80-16063

Unclas
46991

CSCL 21E G3/07



EXPANDED STUDY OF FEASIBILITY OF MEASURING IN-FLIGHT 747/JT9D
LOADS, PERFORMANCE, CLEARANCE, AND THERMAL DATA

JT9D JET ENGINE DIAGNOSTICS PROGRAM

G. P. Sallee and R. L. Martin

UNITED TECHNOLOGIES CORPORATION
Pratt & Whitney Aircraft Group, Commercial Products Division
and
THE BOEING COMPANY
Boeing Commercial Airplane Company

Prepared for

NATIONAL AERONAUTICS AND SPACE ADMINISTRATION

Lewis Research Center
Cleveland, Ohio 44135

Contract NAS3-20632



TABLE OF CONTENTS

<u>Section</u>	<u>Page</u>
1.0 SUMMARY	1
2.0 INTRODUCTION	3
3.0 OBJECTIVES	5
4.0 FLIGHT LOADS BACKGROUND	6
4.1 Classification of Flight Loads	6
4.2 Current Estimate of Impact of Flight Loads on Engine Performance	6
4.3 Status of JT9D Flight Load Knowledge	23
5.0 FEASIBILITY	27
5.1 RA001 Airplane Instrumentation Capability	27
5.2 Pressure Loads	32
5.3 Inertia Loads	34
5.4 Engine Clearance Changes	37
5.5 Feasibility of Using NASA Space Shuttle Carrier Aircraft	47
6.0 INSTRUMENTATION SELECTION AND MEASUREMENT ACCURACY	53
6.1 Aerodynamic Pressure Load Instrumentation System	53
6.2 Inertia Load Instrumentation System	53
6.3 Clearance Measurement Instrumentation	61
6.4 Engine Performance and Case Temperature Instrumentation	64
7.0 PROGRAM OPTIONS	81
7.1 Use of NASA 747 as Flight Test Vehicle	81
7.2 RA001 747 Potential Program Configuration Matrix	81
7.2.1 Flight Loads Instrumentation Options	82
7.2.2 Engine Preparation and Instrumentation	84
7.2.3 Flight Program Scenario Elements	86
7.3 Selected Options	88
7.4 Program Relative Cost	89
7.5 Cost Effectiveness	90
8.0 RECOMMENDATIONS	97
APPENDIX A Program Schedule and Milestones	99
APPENDIX B List of Acronyms and Symbols	102

SECTION 1.0

SUMMARY

This report documents the results of studies concerning the feasibility of measuring 747/JT9D propulsion system aerodynamic and inertia loads and the critical engine clearance and performance changes during 747 flight and ground operation. In the course of the study, a number of technical options were examined including:

- o the potential use of the NASA-owned space shuttle carrier 747 (NASA 905) airplane as the flight test vehicle in lieu of the Boeing-owned (RA001) airplane;
- o variations in flight test program scenarios and objectives; and
- o variations in instrumentation levels on inboard and outboard engine and nacelle locations.

These options were examined to determine the most cost effective programs for NASA consideration. Only relative program costs are reported herein for each option, due to the proprietary nature of such cost data.

It is concluded that a flight test program meeting the overall objective of determining the levels of aerodynamic and inertia load levels to which the engine is exposed during the initial flight acceptance test and normal flight maneuvers is feasible and desirable. The concurrent measurement of engine clearance changes in the fan and first-stage high-pressure turbine, performance changes, and case thermal environment are also feasible and equally desirable.

While the use of the NASA-owned space shuttle carrier 747 aircraft is technically feasible, there are technical, schedular, and financial considerations that make the use of the aircraft undesirable. To effectively utilize the NASA-owned 747, the airplane would have to be taken out of service for installation of required data acquisition/recording equipment, instrumentation wiring, and removal of the space shuttle carrier support struts and stabilizer tip fins. At the conclusion of the flight test program, the original airplane configuration would be restored. The NASA airplane would be essentially unavailable to conduct a space shuttle carrier mission for a minimum period of five to six months. The estimated cost of conducting the test program effort utilizing the NASA 747 would be approximately twice the cost of conducting the program on the Boeing-owned RA001 airplane.

The recommended program consists of the following:

- o A 15-hour dedicated flight test program on RA001 airplane covering the acceptance flight, variations in take-off/landing conditions, and wind-up (high g) turns.
- o Pressure loads instrumentation consisting of 252 static pressure taps on the inboard and 45 static pressure taps on the outboard nacelle.
- o Primary inertia load instrumentation consisting of a three-dimensional rate gyro, six accelerometers on both inboard and outboard nacelles, and two accelerometers at the wing-strut intersection of each nacelle.
- o Clearance change instrumentation on the fan and high-pressure turbine of the inboard engine and on the fan of the outboard engine.
- o Expanded engine instrumentation and 20 high-pressure turbine thermocouples on the inboard engine.

This recommendation is based on the contractor (P&WA) and subcontractor (BCAC) evaluation of cost effectiveness. Optional programs studied and discussed herein, which include variations in airplane or engine instrumentation, flight time, and related analysis efforts, are considered to be less cost effective than the recommended program.

SECTION 2.0

INTRODUCTION

Pratt & Whitney Aircraft (P&WA) and the Boeing Commercial Airplane Company (BCAC) have conducted this Expanded Feasibility Study of measuring: 1) propulsion system flight aerodynamic and inertia loads, 2) engine performance and clearance changes, and 3) engine case thermal environment conditions during typical aircraft acceptance test and other flight and ground maneuver conditions that are typical of revenue service on the JT9D propulsion system of the 747 airplane.

This particular study is an expansion of a similar study conducted early in 1977 which considered the feasibility of measuring only inertia loads. This previous study is reported in NASA CR-135395, dated October 15, 1977. The conclusion of this previous study was that it was feasible and practical to measure flight inertia loads; however, the recommendation at the time of completion of the study was to postpone a flight test program until other test and analytical studies were completed to define the relative importance of inertia loads to engine performance deterioration.

These test and analytical studies have been completed and indicate that flight aerodynamic pressure loads are responsible for the major portion (87 percent) of the performance deterioration estimated to be caused by flight loads. Further analysis of the engine test data suggest that losses in the low-pressure compressor and high-pressure turbine module performance are the main contributors to engine TSFC increases. However, analysis of engine structural response to flight loads indicates that fan, low-pressure compressor, and high-pressure turbine clearance changes should be expected during typical flight acceptance testing. These data and results suggested the need to re-evaluate the JT9D/747 flight loads flight test program plans presented in the original feasibility study to include in-flight measurement of: 1) aerodynamic pressure loads, and 2) engine fan, low-pressure compressor, and high-pressure turbine clearance changes simultaneously with the measurement of load levels. The measurement of engine and module performance changes would improve the development of cause and effect relationships. The simultaneous measurement of loads, clearance, and performance data would lead to:

- o A better appreciation of the potential for avoiding deterioration by identification and revision of pertinent engine and aircraft operating procedures, and
- o The provision of data from which corrective design action might be initiated for current and future engines.

The reasons for measuring in-service flight loads are:

- o To improve knowledge of normal propulsion system operating flight loads and the influence of variations in normal aircraft operating factors (take-off gross weight, rotation angles, landing sink rate, etc.) on load levels;
- o To establish the relative importance of various types of typical aircraft maneuvers on load levels and engine performance deterioration;
- o To provide quantitative data for ground testing and analytical studies of the effects of propulsion system flight loads; and
- o To provide design data for new propulsion system designs related to the NASA Energy Efficient Engine Program and other new engine design and development programs. This is of particular importance because powerplant installations designed by strength and safety criteria (ultimate loads) still show significant performance deterioration under the much lower operational loads.

The reasons for measuring critical clearance and engine/module performance changes are:

- o To improve knowledge of engine rotor and structural response to various types of dynamic and steady flight loads;
- o To provide quantitative data to permit validation and/or refinement of previous analytical study results and performance deterioration models; and
- o To provide design data for new engines as well as current engines upon which to base development of performance retention concepts.

SECTION 3.0

OBJECTIVES

The study objectives included examination of:

- o The feasibility of measuring aerodynamic pressure loads on both inboard and outboard nacelles;
- o The appropriateness of the location of inertia load instrumentation as well as the desirability of obtaining such load data on inboard and/or outboard propulsion systems in conjunction with aerodynamic loads;
- o The feasibility of installing flight-worthy clearance measurement instrumentation in inboard and/or outboard engines to monitor fan, low-pressure compressor, and high-pressure turbine blade tip to outer air-seal clearances during flight on a real time basis;
- o The feasibility of installing expanded engine performance instrumentation suitable for determining module performance changes and engine case temperature instrumentation to provide a clearer picture of case operating temperatures as they relate to operating clearances;
- o The technical and economic merits of utilizing the NASA-owned 747 space shuttle carrier aircraft; and
- o Several combinations of load, clearance, and performance instrumentation on inboard and outboard propulsion systems as well as flight test program scenarios to permit evaluation and selection of the most cost-effective overall flight loads test program.

The evaluation of cost effectiveness of the various proposed programs is based on a relative ranking of:

- o The technical value of each type of data based on engineering judgement of the data element in understanding and quantifying the causes for short-term engine performance deterioration;
- o The completeness and quantity of similar existing data from other parts of the NASA JT9D Jet Engine Diagnostics Program or previous contractor/subcontractor testing; and
- o The overall importance of specific types of flights or flight maneuver events and their relative frequency of occurrence in typical airline service.

Based on full consideration of the program cost and effectiveness, the overall objective of the study was to recommend several potential program options to the NASA Engine Component Improvement Project Office for consideration.

SECTION 4.0

FLIGHT LOADS BACKGROUND

Prior to discussing the results of this feasibility study, a review of the various types of engine loads which occur in flight is presented. This material is followed by a review of the current understanding concerning the potential effects of flight loads on engine performance. Finally, a review and evaluation of the available flight loads data is presented.

4.1 CLASSIFICATION OF FLIGHT LOADS

Engine performance deterioration is influenced by two classes of loads: 1) engine loads, and 2) airplane loads. This distinction must be made because both kinds of loads must be measured, each with the appropriate instrumentation.

- 1) Engine loads, being directly related to engine power level, are relatively independent of the airplane flight environment. They include:
 - o Internal engine pressures,
 - o Thermal loads due to temperature differentials,
 - o Thrust loads, both forward and reverse, and
 - o Centrifugal loads.
- 2) Airplane loads are loads imposed on the propulsion system by airplane flight environment. These loads include:
 - o Aerodynamic pressures, both steady state and transient, due to gust and maneuvers, and
 - o Inertia forces due to gust, maneuvers, landing impact, and runway roughness.

A direct measurement of transient aerodynamic pressures is, in general, not feasible with flight test instrumentation. However, their effect, that is, dynamic loads due to nacelle vibrations with respect to the wing, as well as wing motion, will be measured by the inertial instrumentation.

4.2 CURRENT ESTIMATE OF IMPACT OF FLIGHT LOADS ON ENGINE PERFORMANCE

4.2.1 Introduction

This section summarizes the major findings related to levels, trends, and causes of performance deterioration. The knowledge gained and

outstanding issues from these tasks provide the basis for structuring and evaluating the various flight loads test program options discussed in later sections of this report.

Efforts conducted to date in the NASA JT9D Jet Engine Diagnostics Program have established four generic causes of engine performance deterioration, namely: 1) flight load induced clearance changes, 2) erosion of fan/compressor airfoils and seals, 3) thermal distortion of hot section parts, and 4) variations in airline repair standards. Performance deterioration trends may be divided into two distinct time periods: 1) short-term, and 2) long-term deterioration. The majority of the short-term deterioration is believed to be caused by flight load induced rubs which increase the gas-path clearance and influence both new and rebuilt engines, resulting in a TSFC deterioration of about 1 percent in the initial 50 flights. Performance deterioration then proceeds at a slower rate, dominated by erosion of cold section airfoils and thermal distortion of hot section parts. Short-term deterioration has a dominant effect on fleet fuel consumption due to its early occurrence, magnitude, and reoccurrence after repair.

4.2.2 Historical Data

The initial task in the multiple-task NASA JT9D Jet Engine Diagnostics Program involved the collection and analysis of historical JT9D engine performance and maintenance data from five airlines, two airplane manufacturers, and Pratt & Whitney Aircraft records. The purpose of this effort was to establish short- and long-term performance deterioration trends, establish probable causes of deterioration, and identify where corrective actions could be taken.

The data collected included:

- o Prerepair and postrepair engine test stand performance from airline and engine manufacturer repair facility testing;
- o Special back-to-back testing of specific engines from airline and engine manufacturers;
- o In-flight monitoring data on a fleet average basis from airline engine condition monitoring including pertinent operating procedures and changes;
- o Airframe manufacturer fleet performance audits accomplished at the request of specific airlines;
- o Engine manufacturer production performance records to serve as a base line from which to assess deterioration; and
- o Airframe manufacturer records pertaining to clearance and performance changes that occurred during certification flight testing.

The study provided a significant amount of short-term data (first flight to 250 flight cycles) and long-term data (1000 to 4000 flight cycles) but was lacking in data in the 300 to 1000 flight cycle range.

Most of the short-term data were from engines involved in aircraft certification testing at Boeing and Douglas and, therefore, represented engines with low numbers of flight hours per flight cycle. Figure 4.2-1 shows the change in thrust specific fuel consumption (TSFC) from these engines plotted as a function of flight hours. A slightly better correlation is obtained by plotting deterioration as a function of flight cycles as shown in Figure 4.2-2. Typical airline delivery occurs at about 12 hours or after four cycles. It can be seen that a significant loss in performance occurs very early followed by a more gradual, but continuing, deterioration over the first 250 flights.

Much more historical data were available for evaluating long-term deterioration than for short-term deterioration data. The bulk of the data was obtained during postrepair engine testing. However, at least a limited amount of data was available for prerepair testing. Figure 4.2-3 shows the trends for long-term deterioration. The average engine TSFC increase relative to new ranges from 3.2 to 4.5 percent between 1000 and 3500 flight cycles. Note that the individual airline curve and average trend curve all show a significant deterioration has occurred in the initial 1000 flight cycles followed by a more gradual deterioration during the next 3000 flights.

Analyses of these short- and long-term performance data, as well as repair records and parts inspection data, established that causes for performance deterioration fall into four generic categories, namely:

1. Effect of flight loads on running clearances;
2. Erosion of airfoils and seals which causes roughness and bluntness and increases running clearances;
3. Thermal distortion of turbine airfoils due to changing temperature levels and patterns; and
4. Operator repair practices which establish the depth of repair and repaired engine gas-path build clearances.

The performance deterioration contribution of the first three generic causes are estimated on Figure 4.2-4, based on these historical data. The flight load effects are shown to occur early and account for over 50 percent of the total increase in TSFC at 3000 cycles. This early loss is believed to be caused by clearance increases associated with nacelle aerodynamic and propulsion system inertia loading changes that occur during take-off rotation, flight maneuvers, and landing and thrust reversal. Engine power transients concurrent with these events may also contribute to rotor/case interferences that produce increases in clearances. However, power transient engine testing under static conditions does not produce these losses in performance or clearances.

Based on the analyses of the historical performance data, short term engine performance losses appear to be primarily due to losses in the low-pressure compressor and high-pressure turbine module performance.

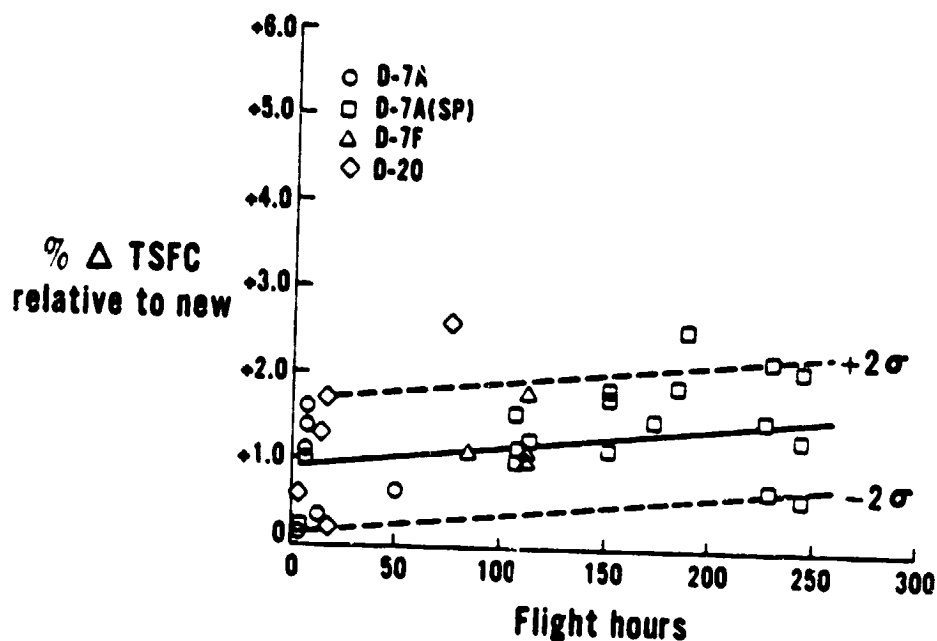


Figure 4.2-1 Short-Term TSFC Deterioration Trends as a Function of Flight Hours at Sea Level Static Take-Off Conditions - The ± 2 sigma range of the data is also shown.

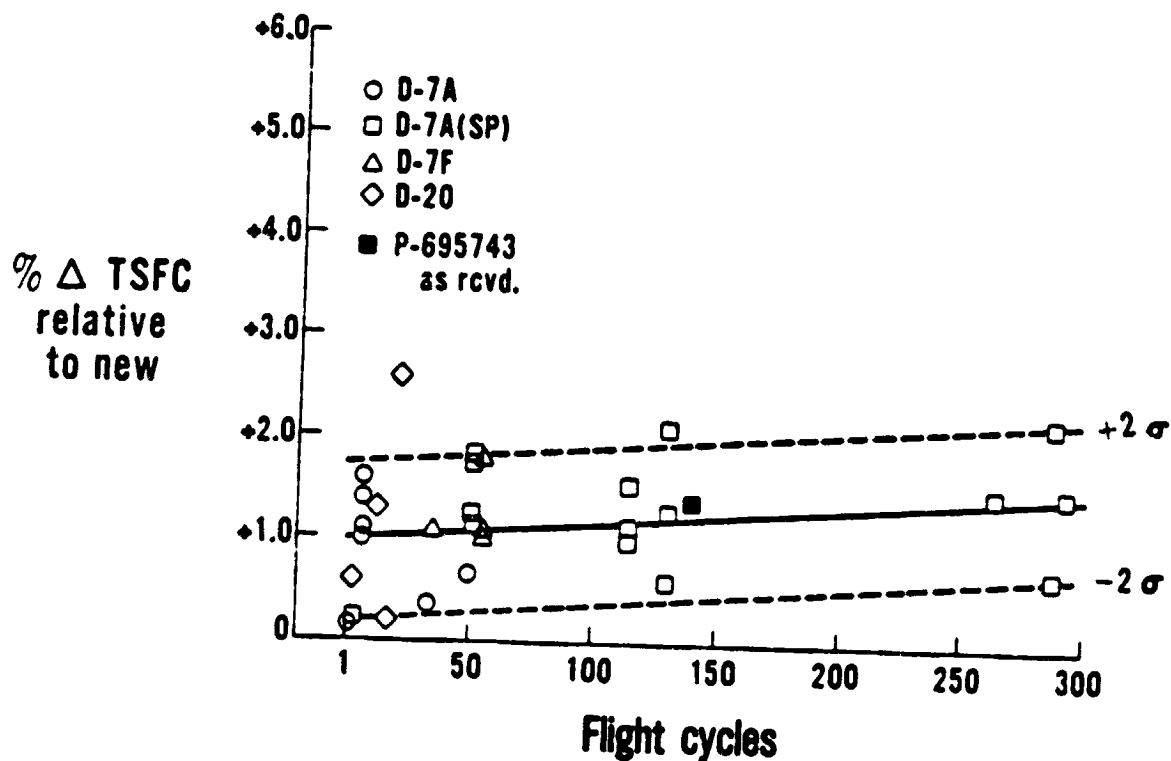


Figure 4.2-2 Short-Term TSFC Deterioration Trends as a Function of Flight Cycles at Sea Level Static Take-Off Conditions - The ± 2 sigma range of the data is also shown.

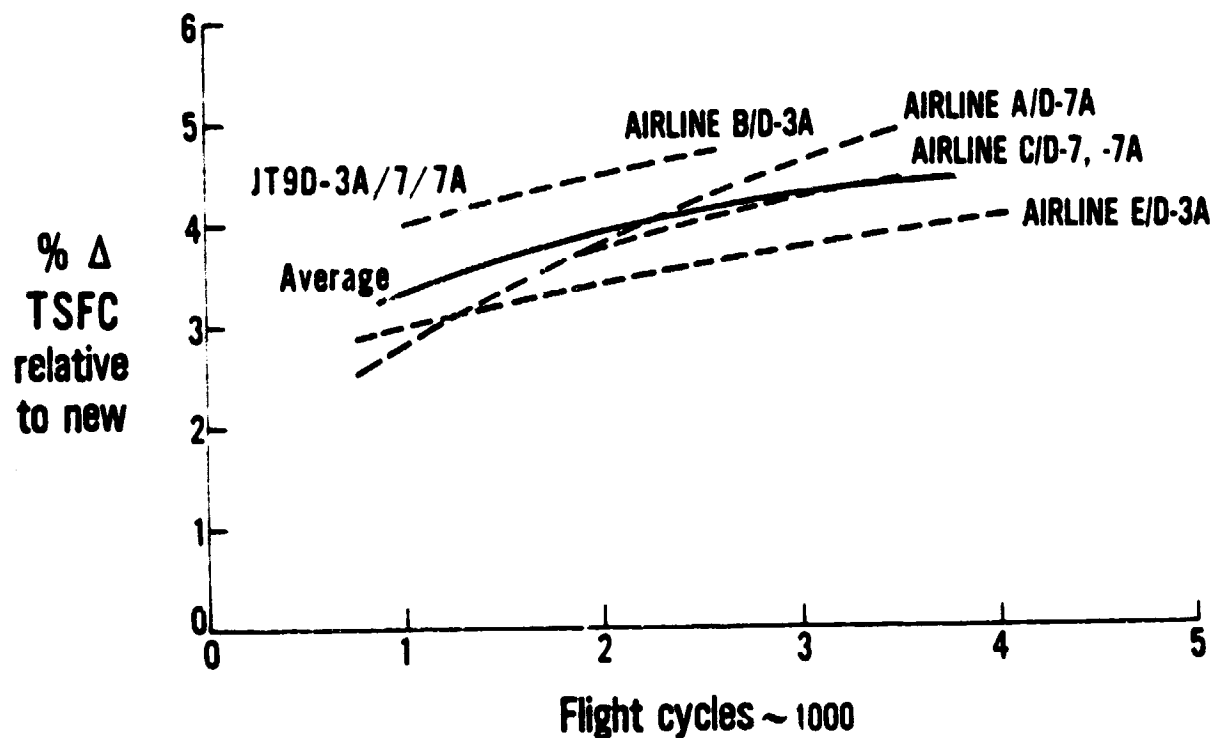


Figure 4.2-3 Take-Off Thrust TSFC Deterioration for Average Fleet Prerepair Engines Relative to New Engine Performance Levels at Sea Level Static Conditions - Average engine TSFC deterioration ranges from 3.2 to 4.5 percent between 1000 and 3500 flight cycles.

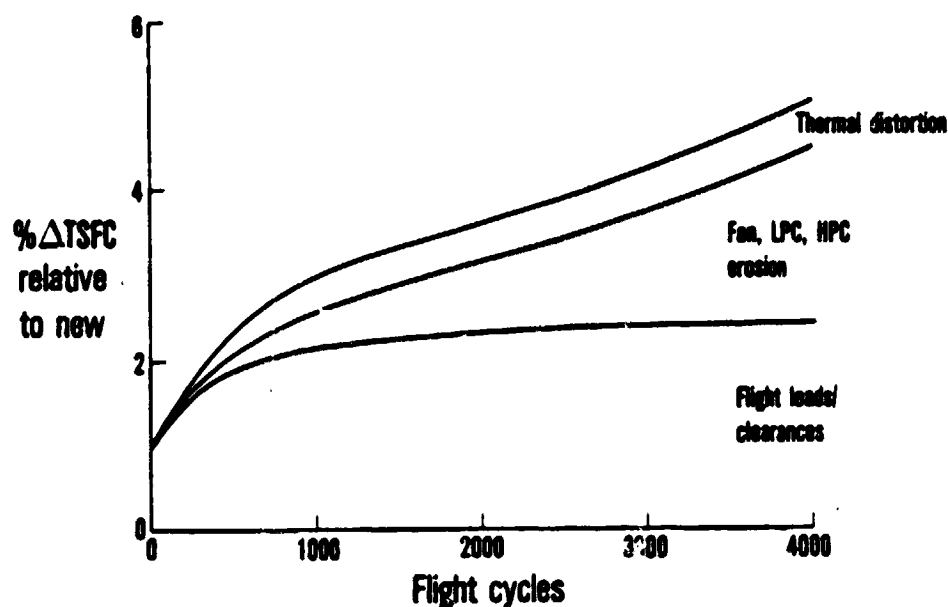


Figure 4.2-4 Take-Off Thrust TSFC Deterioration at Sea Level Static Conditions by Damage Mechanism - Flight load induced clearance changes are estimated to have the greatest influence below 500 cycles and to be significant over the longer term.

4.2.3 In-Service Engine Data

A study of In-Service Engine Performance Deterioration, under the NASA JT9D Jet Engine Diagnostics Program was completed in February 1979. This study expanded on the results of the historical data effort to enhance the understanding of the levels and trends of JT9D engine performance deterioration. The collection of in-flight and ground performance data from a selected sample of Pan American World Airways JT9D-7A(SP) engines, starting prior to the first flight, provided a better controlled data sample. This was especially true in the analysis of short-term deterioration where a combination of Plug-In Console (PIC) tests and in-flight calibrations were used to monitor engine performance. PIC testing is a system recently developed by Pratt & Whitney Aircraft for ground testing engines installed on the airplane using expanded instrumentation. A series of PIC tests were conducted on two engines on each of two airplanes in the Pan American 747SP fleet, with the first test accomplished prior to the first flight of the airplane. Additional PIC tests were then performed at intervals to determine how the performance changed with usage from the first flight to beyond 500 flights on each of the four engines. This additional PIC testing was supplemented by the in-flight calibrations conducted during the flights immediately following each PIC test. Thus, the short-term performance deterioration trends of these engines were well documented. A relationship between ground and flight performance trends also was achieved.

The 15 engine performance parameters measured by the PIC test system permitted analyses of module performance changes as well as overall engine performance. Estimation of the short-term engine deterioration based on the PIC tests results is shown in Figure 4.2-5. The two plots show the changes in exhaust gas temperature (EGT) and TSFC with succeeding flights. Both plots are normalized to the first PIC test which was conducted during a ground test prior to the first flight. Overall engine deterioration based on module deterioration and influence coefficients, shows a rapid deterioration of 1 percent TSFC and 60°C EGT in the first 50 cycles followed by a long-term deterioration at a much slower rate to 2.2 percent TSFC and 220°C EGT at 1000 cycles. The measured engine exhaust gas temperature necessary to achieve rated thrust is shown to increase in like fashion.

The individual module performance analyses, made possible by the PIC system, showed that the TSFC loss in the first 50 engine flight cycles was dominated by performance losses in the low-pressure compressor and high-pressure turbine modules. The fan, high-pressure compressor, and low-pressure turbine also contributed to the overall performance loss. The refined analytical model plots of changes in flow capacity and module efficiency as functions of usage for the fan, low-pressure compressor, and high-pressure turbine modules, as shown in Figures 4.2-6, 4.2-7, and 4.2-8, show these early module performance deterioration effects.

This in-service engine study further supports the initial conclusion that significant performance deterioration occurs early in the engine life. The test data also indicated no significant differences in deterioration between the inboard and outboard engines. The analysis of the data suggested that provisions to monitor clearance changes in the fan/low-pressure compressor and the high-pressure turbine during flight should be included in any flight test program.

4.2.4 Short-Term Performance Deterioration

This effort was directed toward the development of a better understanding of the causes for short-term engine performance deterioration. The effort was divided into the following: 1) testing and an analytical teardown of a short-term JT9D-7A(SP) engine, 2) analytical studies of the effects of steady flight loads on performance deterioration, and 3) an analytical study of the effect of typical dynamic flight load events on performance deterioration.

4.2.4.1 Short-Term Engine Performance Test

The short-term engine performance test and analytical teardown program was conducted on one of the Pan American 747SP/JT9D-7A(SP) engines which had been closely monitored starting before first flight. The objective of extensive testing and complete analytical teardown was to determine the level and module contribution to performance loss and the specific causative factors.

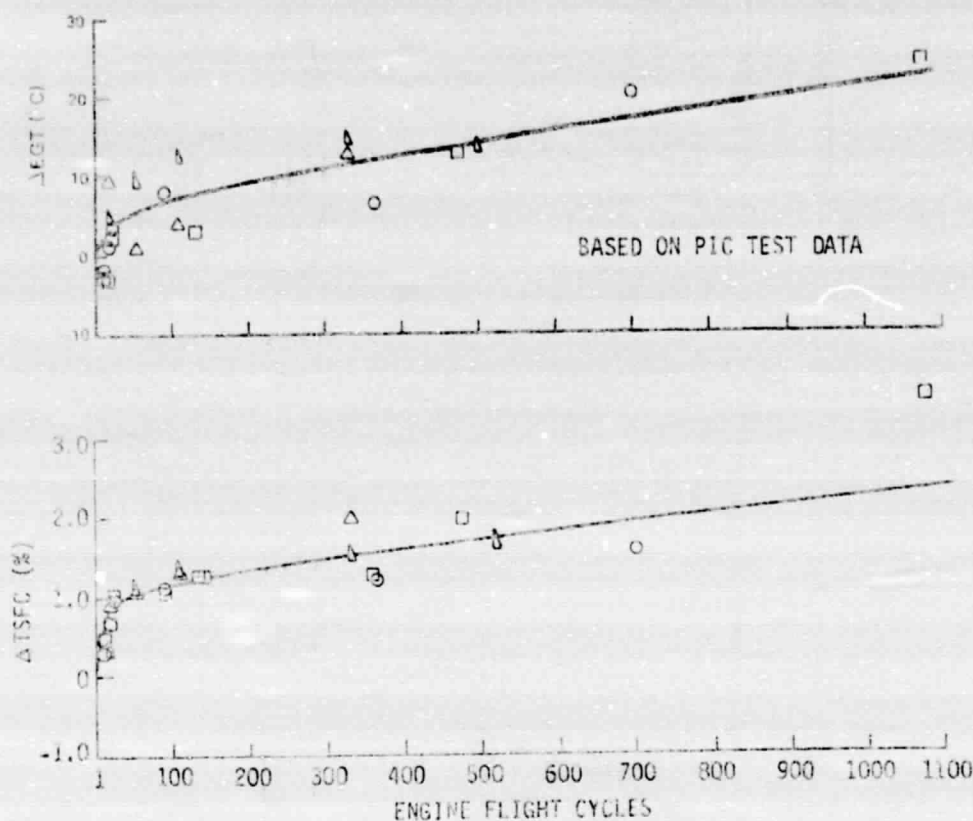


Figure 4.2-5 Estimated Sea Level Static Performance Deterioration Based on PIC Data at Take-Off Thrust - Overall engine deterioration, based on module deterioration and influence coefficients, shows a rapid deterioration of 1 percent TSFC and 6°C EGT in the first 50 cycles followed by a long-term deterioration at a much slower rate to 2.2 percent TSFC and 22°C EGT at 1000 cycles.

ORIGINAL PAGE IS
OF POOR QUALITY

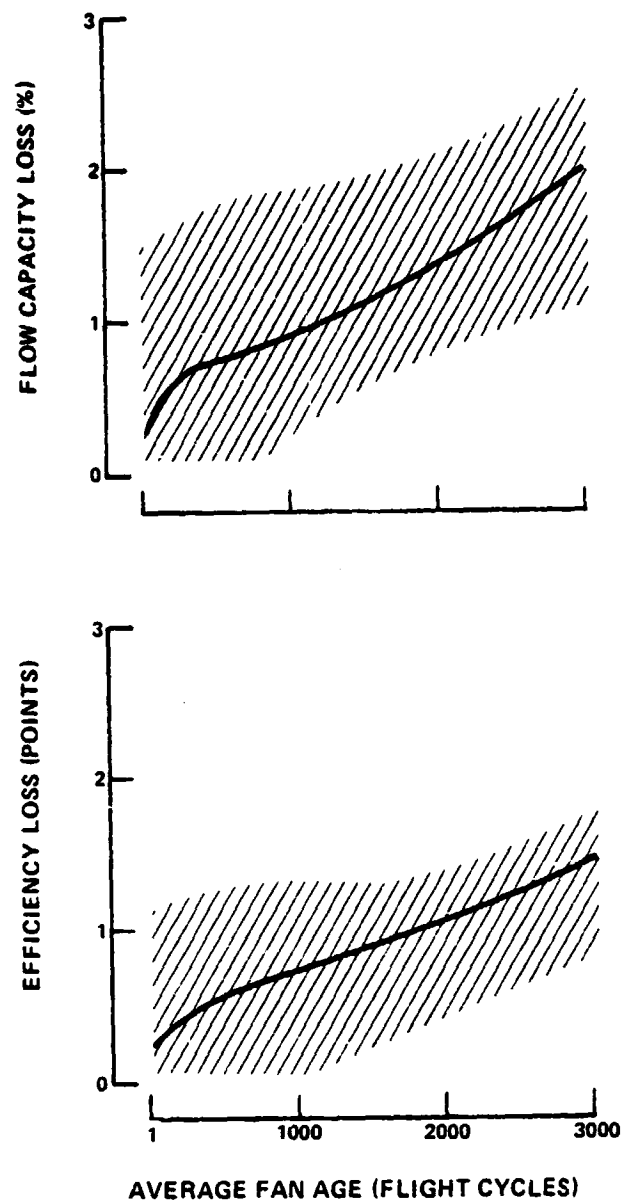


Figure 4.2-6 Refined Fan Performance Deterioration Model and Variation Band - The model shows the average and variation range of fan module deterioration as a function of average fan age.

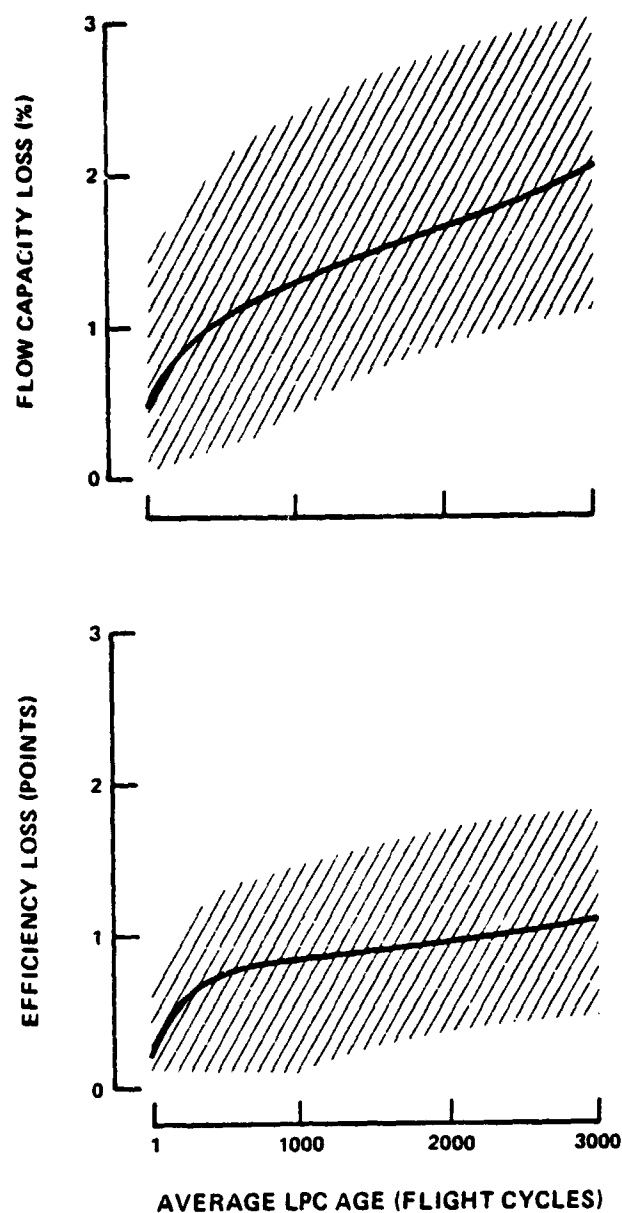


Figure 4.2-7 Refined Low-Pressure Compressor Performance Deterioration Model and Variation Band - The model shows the average and variation range of low-pressure compressor module deterioration as a function of average low-pressure compressor age.

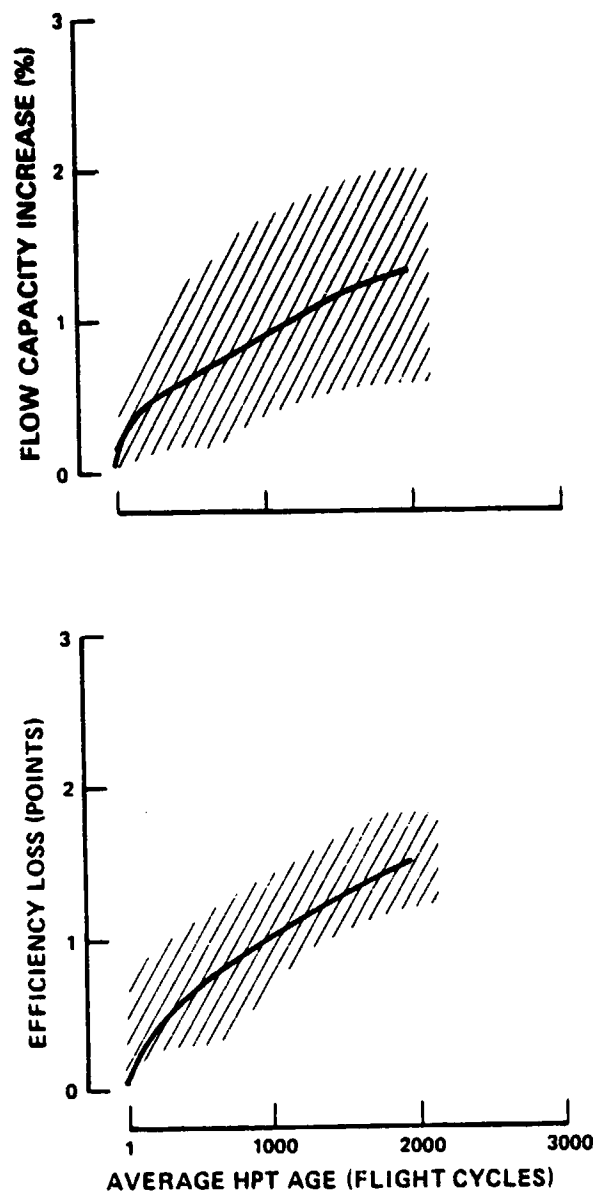


Figure 4.2-8 Refined High-Pressure Turbine Performance Deterioration Model and Variation Band - The model shows average and variation range of high-pressure turbine module deterioration as a function of average high-pressure turbine age.

Engine S/N 695743, which had been tracked with PIC and in-flight calibration tests since prior to the first flight, was removed from the wing at 141 flight cycles and 1079 flight hours. It was returned to Pratt & Whitney Aircraft and tested "as received". Table 4.2-I compares the results of this "as received" test with average short-term deterioration analysis results from the historical data and in-service engine PIC data.

The engine was retested after engine vane control (EVC) trim and water and detergent washing to remove surface contamination, reducing the level of TSFC deterioration by 0.3 percent. The engine was then disassembled to permit the installation of fully instrumented engine cases and was retested in an experimental test stand to permit the evaluation of modular performance.

A complete analytical teardown of the engine was conducted, and the condition of all seals and parts affecting performance was documented, from which the performance of each module was estimated. These results were then compared with analysis of the engine test data to achieve a final assessment of the causes for short-term deterioration at the module level. The performance testing of the engine showed that the overall short-term deterioration was distributed by module as tabulated in the right-hand column on Table 4.2-I. This level of deterioration correlated well with specific hardware deterioration in the engine and with other historical short-term deterioration data.

Modular contributions to short-term deterioration were distributed among all of the modules or components of the engine, and the summation of these individual losses make up the total short-term engine performance deterioration. Based on the parts inspection and test data analysis, the major fundamental cause of this deterioration is increased clearances in the engine associated with the aircraft operating environment and, to a lesser extent, second-stage turbine vane distortion and increased roughness of fan and low-pressure compressor airfoils.

These results thus support the prior conclusions that the low-pressure compressor and high-pressure turbine performance loss are the most important contributors to short-term deterioration and that clearance changes caused by flight loads play a major role. The results of this study are presented in NASA CR-135431.

TABLE 4.2-1
COMPARISON OF MODULE CONTRIBUTION TO
SHORT-TERM TSFC DETERIORATION

	Data Source		
	Historical Data	In-Service Engine	P&WA Testing of P-695743
	Analysis (149 Cycles)	PIC Analysis (150 Cycles)	(As Received With 141 Cycles) (Instrumented, After Washing)
		Change in TSFC (%)	
Fan	+0.15	+0.25	+0.05
Low-Pressure Compressor	+0.15	+0.40	+0.40
High-Pressure Compressor	+0.30	+0.20	+0.35
High-Pressure Turbine	+0.35	+0.40	+0.60
Low-Pressure Turbine	+0.50	+0.05	+0.10
Total	+1.45	+1.30	+1.19
Low-Pressure Spool	+0.80	+0.70	+0.55
High-Pressure Spool	+0.65	+0.60	+0.95
Cold Section	+0.60	+0.85	+0.80
Hot Section	+0.85	+0.45	+0.70

4.2.4.2 Steady Flight Loads Analysis

An analysis of the effects of steady state and quasi-steady (slowly varying with time) flight loads on engine and module performance was conducted using a computerized NASTRAN finite element analytical model of the JT9D/747 propulsion system.

The flight loads considered were steady state aerodynamic loads, steady state maneuver loads, internal engine loads due to thrust, gyroscopic loads, thermal loads, and engine thrust reversal loads.

Functionally, the model was used to compute the change in thrust specific fuel consumption (TSFC) that resulted from the sequence of events which defined an airplane flight profile or mission. A given flight profile was broken down into a large number of short segments, called time points, for which airplane and engine operating conditions were known. Internal and external flight loads that acted at each time point gave rise to structural deflections which may or may not exceed the local gap between static seals and rotating blades. When an interference (rub) was found to occur, wear on both blade tips and rub strips was calculated and added to the clearances available for succeeding time points. After all time points in a given flight profile had been considered, average clearance changes for all stages were computed and combined with performance influence coefficients to produce values of changes of TSFC with respect to standard steady state engine operating conditions such as sea level take-off and cruise. The manner in which these inputs were combined to relate causes and effects can be seen in Figure 4.2-9.

The analytical model predicted a 1 percent TSFC increase due to the aircraft acceptance flight test induced flight loads as shown by the first point on Figure 4.2-10. A revenue service flight profile was also simulated to determine further deterioration caused by flight loads through 5000 flights of the engine. In the simulation of the 747 revenue service experience, the previously defined flight acceptance test was refined to include only those maneuvers which are typical of a revenue flight. For the simulation, relative values of the loads remained unchanged, but the absolute values were increased to account for the probability of encountering larger loads during the life of the airplane. The effect of these simulated revenue flight loads on engine TSFC are also shown on Figure 4.2-10 out to 5000 flight cycles. The results from this analysis show strong support of the earlier conclusions as to the importance of flight loads (see Figure 4.2-4).

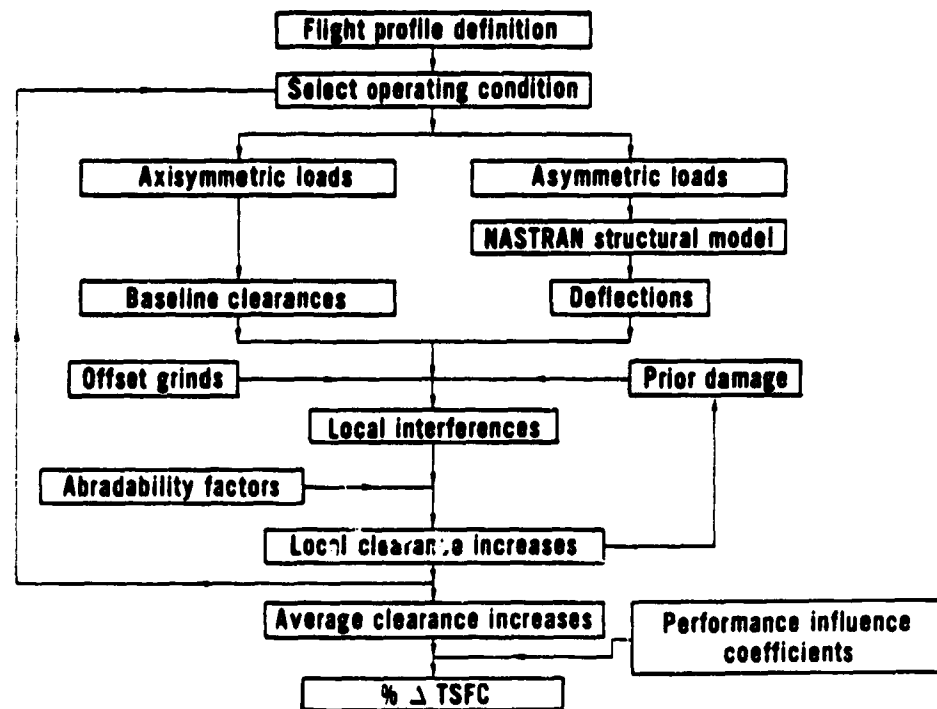


Figure 4.2-9 Flow Chart for the Analytical Model - The steps in the analytical process for predicting the effect of flight loads on engine performance loss are illustrated.

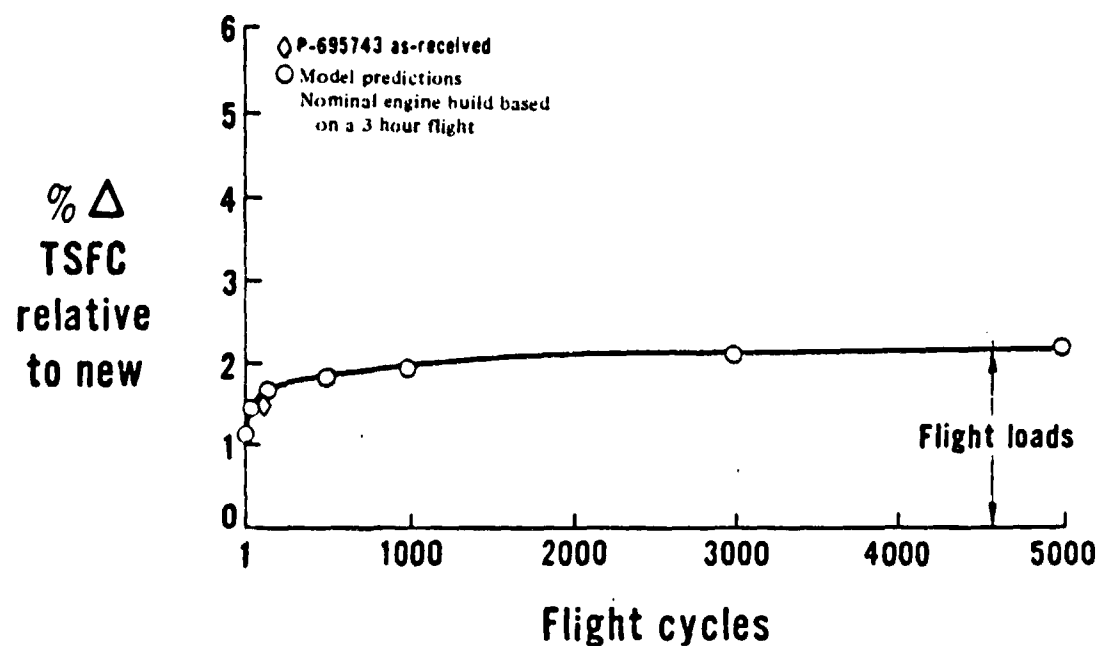


Figure 4.2-10 Analytically Predicted Loss in TSFC at Sea Level Static Take-Off Thrust Caused by Flight Loads - A loss of 1 percent in TSFC is predicted to occur during the acceptance flight and the losses are predicted to increase as the number of flights increases.

Figure 4.2-10 includes the "as received" test performance of the S/N 695743 engine at 141 flight cycles and demonstrates good agreement with the model prediction.

From these analyses, it was estimated that aerodynamic cowl loads account for 87 percent of the overall "loads contribution" to deterioration. Gyroscopic and gravitational loads contribute 5 and 8 percent, respectively, of the total loss in performance due to loads. Thrust and thermal loads account for clearance closure, but contribute to permanent clearance changes only in conjunction with the flight loads. The analysis also shows that certain engine components are particularly sensitive to certain types of loads. The fan stage is very sensitive to gyroscopic (gyro) loadings and relatively insensitive to varying gravitational (g) loading levels. The high-pressure turbine stages are relatively insensitive to gyro loadings but sensitive to g loadings.

The effects of different running clearances resulting from various engine build standards were also evaluated. An engine built with comparatively open clearances would be expected to have poorer initial performance but be less susceptible to rub damage. Conversely, an engine built with comparatively tight clearances would perform better before application of flight loads but the clearances would open up more after initial flights. The model compared engines built to the minimum and maximum clearances in accordance with Pratt & Whitney Aircraft's allowable build tolerances. The predicted band of TSFC change due to flight loads versus engine usage as defined by these two extremes of clearance is shown on Figure 4.2-11. Predicted bands bracket the historical short-term data (see also Figure 4.2-2) quite well. The results of these studies are reported in NASA CR-135407.

4.2.4.3 Response to Dynamic Flight Loads

In conjunction with the task of analytically simulating the short-term performance deterioration process, a transient dynamic analysis of typical dynamic load events on the JT9D-7 engine was conducted. The response of the engine to typical gust encounters and hard landings was examined. The dynamic response of the engine to a once-per-flight vertical gust and a normal revenue service landing produced negligible performance loss relative to the steady loads analysis. The response to a once-per-airframe-life hard landing indicated the possibility for very high local rub strip wear. However, the lack of a dynamic rotor/rub strip damage prediction system prohibits a rigorous quantitative evaluation of this particular event. The results from

the analyses of typical flight dynamic load events support the conclusion reached in the steady load analyses. The major impact of flight loads on engine performance is the steady aerodynamic pressure load on the engine inlet cowl. This finding further suggests that the planned flight loads program consider the measurement of aerodynamic loads as well as inertia loads and secondly, that measurement of engine clearance changes in conjunction with these loads would materially improve our understanding of the causes for short term deterioration.

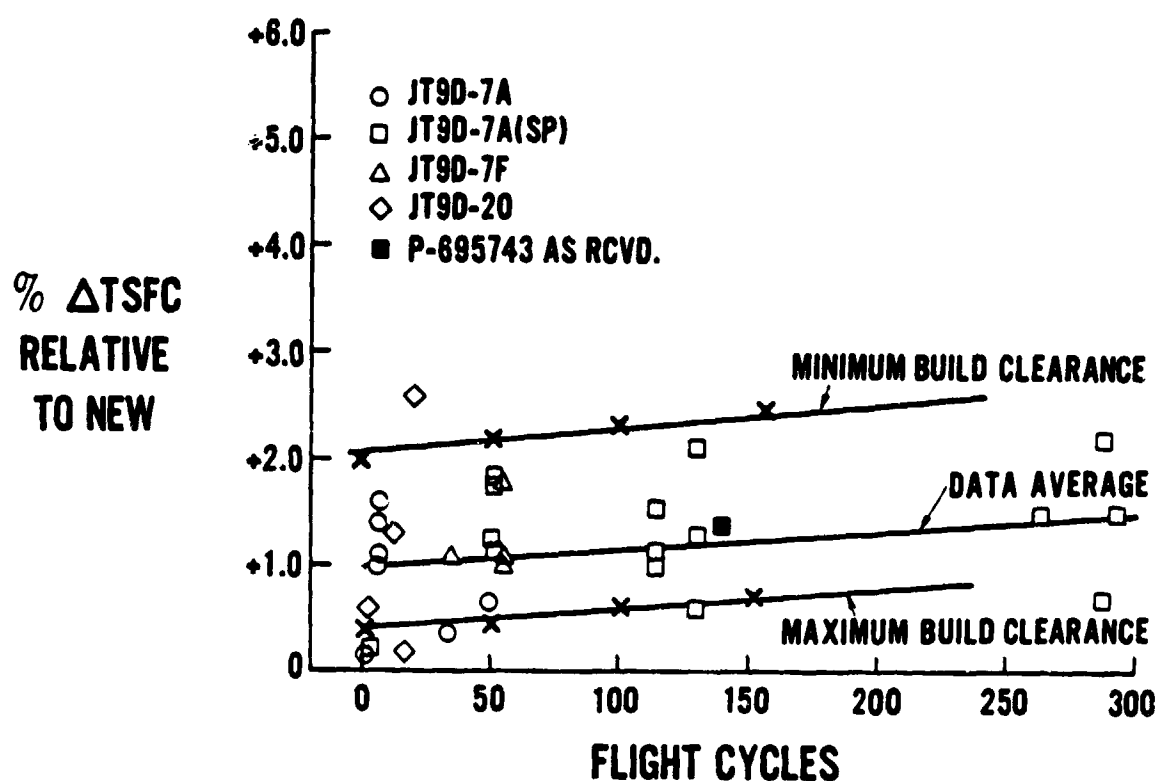


Figure 4.2-11 Comparison of Predicted TSFC Changes with Short-Term Deterioration Test Data for Maximum and Minimum Build Clearances at Sea Level Static Take-Off Conditions - The predicted short-term deterioration due to variation in initial build clearances provides a possible explanation for the variation in engine test data.

4.2.5 Summary

The JT9D Jet Engine Diagnostics Program efforts to date have established the levels and rates of performance deterioration, have identified the major causes, and have defined the modules most severely affected.

The engine exhibits a TSFC loss of about 1 percent in the initial 50 flight cycles of a new engine. Similar performance losses occur in the initial flights of rebuilt engines. These early losses are caused by seal wear induced opening of running clearances in the primary gas path. The early wear and module performance loss were primarily in the low-pressure compressor and high-pressure turbine modules.

The causes of seal wear were identified as flight induced loads which deflected either the engine case or rotor, causing the rotating blades to rub against and wear down the seal surfaces. Transient and

quasi-steady aerodynamic forces on the nacelle deformed the fan and engine cases against the rotating blades. Gravitational and gyroscopic forces on the fan and cantilevered high-pressure turbine rotors during flight maneuvers caused them to deflect against the cases. The case and rotor deflections, individually and combined, caused the observed seal rubs. Finite element analyses modeling of flight loads indicate that the aerodynamic loads are the prime cause of performance losses.

The on-going X-Ray Facility Load Test Program is a first step toward accurately measuring the direct effect of simulated flight loads on running clearances. This effort will provide a matrix of data on the effect of aerodynamic load direction and magnitude on engine running clearance and performance deterioration. There remains, however, uncertainty as to the real level of normal flight loads encountered during airplane acceptance testing and revenue service. The status of knowledge concerning these flight loads is addressed next.

4.3 STATUS OF JT9D FLIGHT LOADS KNOWLEDGE

A considerable amount of measured flight test data on 747/JT9D nacelle flight loads is available from previous testing conducted by BCAC. These data were gained from a series of flight pressure tests, flight flutter tests, and flight loads surveys. Aerodynamic pressures were measured on nine flight pressure tests, devoted to obtaining nacelle loads, while nacelle inertia measurements were obtained from approximately 160 flight flutter tests and a series of flight loads surveys conducted on the total airplane. Even though considerable data have been obtained previously, the data are inadequate for accurate prediction of performance deterioration, and the reasons for the inadequacy will be discussed in the following paragraphs.

4.3.1 Flight Pressure Tests

The pressure distribution over the JT9D-7 is very complex because it is influenced by a number of factors such as:

- o Thrust Level - This parameter influences the mass flow through the inlet and, consequently, the entire distribution of Mach numbers and static pressures between the hi-lite and the fan.
- o Angle of Attack - Strong asymmetries in pressure distribution, both outside and inside the inlet, occur at high angle of attack, especially if local separation should be present.
- o Spanwise Flow Due to Wing Sweep; Fuselage and Strut Interference - These effects cause strong lateral (outboard) forces even in unyawed flight.
- o Flap Setting and Yaw Angle.

An example of a typical highly asymmetric pressure distribution in the inlet during take-off rotation is shown in Figure 4.3-1.

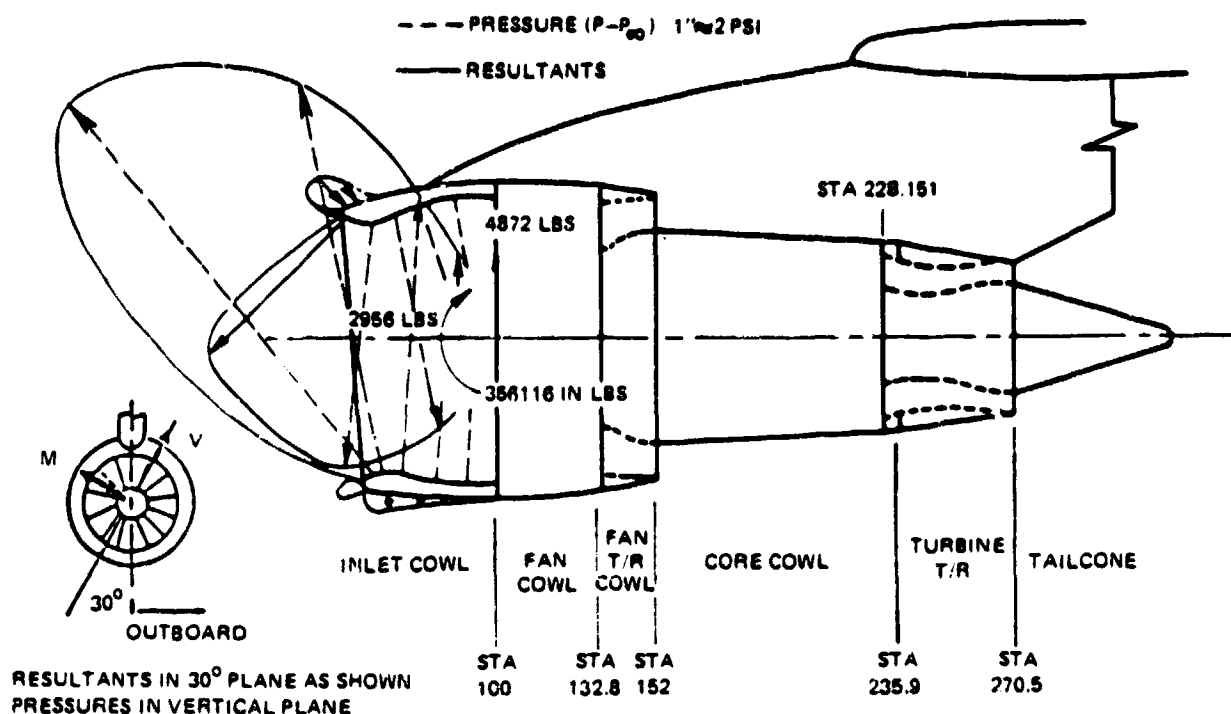


Figure 4.3-1 Inlet Pressure Distribution Case 101 for Take-Off Rotation.

It is apparent that the aerodynamic forces on the inlet will vary considerably with flight condition and that, due to the complex interaction of the above mentioned factors, no extrapolation is possible from one condition to another. None of the available theories can fully account for all phenomena that affect the inlet forces, and even wind tunnel tests cannot properly scale both the geometry and the mass flow.

Thus, actual flight tests, for the same condition that must be analyzed, are the only reliable sources of aerodynamic loads.

4.3.2 Flight Flutter Tests

Flight flutter test programs were conducted in which vertical and lateral accelerations were measured at the inlet lip. Only limited information on inertia loads is obtainable from these tests since it is not possible to establish the nacelle's c.g. acceleration, pitch rates, and yaw rates. Turbulence conditions were intentionally avoided in these tests; therefore, the nacelle acceleration data may not have been typical of in-service experience.

4.3.3 Flight Loads Surveys

Two types of flight loads surveys were conducted, one for maneuver loads and one for gust loads. The nacelles were instrumented with strain gage bridges to obtain only total nacelle/strut loads and accelerometers to measure vertical and lateral accelerations at a few locations. The gust load survey was severely limited as to conditions obtained, which, coupled with the minimum instrumentation, again preclude a complete description of the nacelle inertia loads.

4.3.4 Summary

None of the previously conducted 747 flight test programs had sufficient instrumentation to adequately measure the exceedingly complex aerodynamic pressure distributions on the inlet. Consequently, the circumferential pressure distribution on the inlet had to be represented by means of an interpolation formula.

Similarly for g and gyro loads, neither the instrumentation nor the flight conditions were sufficient to provide an adequate description of these loads during typical revenue service.

SECTION 5.0

FEASIBILITY

ORIGINAL PAGE IS
OF POOR QUALITY

Prior to discussing the feasibility of installing loads and engine clearance instrumentation, the current capability of the Boeing RA001 airplane, Figure 5.0-1, will be discussed to provide a sound basis for an understanding of what may or may not be feasible. As a note, the capability of installing expanded engine performance instrumentation or case thermocouples currently exists in RA001.



Figure 5.0-1 Boeing RA001 747 Research Test Airplane.

5.1 RA001 AIRPLANE INSTRUMENTATION CAPABILITY

The Boeing owned 747, RA001 airplane, is a highly sophisticated, extensively instrumented, research test aircraft. Considerable instrumentation, recording, and monitoring equipment are currently installed and are described in the following subsections.

5.1.1 Data Acquisition and Monitoring System

The RA001 Data Acquisition System consists of four Remote Multiplexer/De-Multiplexer Units (RMDU), one distribution box, one tape recorder, signal conditioning units, and analog and high accuracy digital transducers, as shown in Figure 5.1-1. Information from various sensors throughout the airplane such as positions, accelerations, voltages, pressures, etc., is routed through the signal conditioning which converts the information to a form acceptable to

the RMDU and presents the information to the RMDU. The RMDU accepts the information and places it into a measurement matrix which in turn is normally recorded on one track of the tape recorder in a Pulse Code Modulation (PCM) bit stream of 128K to 1024K bits/second. Normal sample rates vary from five to 100 samples per second depending upon the frequency range of interest and the number of measurements required. Supercommutating techniques can increase the sample rate to 800 samples per second without adversely affecting the rest of the format. Also with four tracks available, different mixes of sample rates may be employed. The maximum number of measurements per RMDU (track) is 256. The basic word size of the system is 10 bits with 20 or 30 bit words available for extra precision.

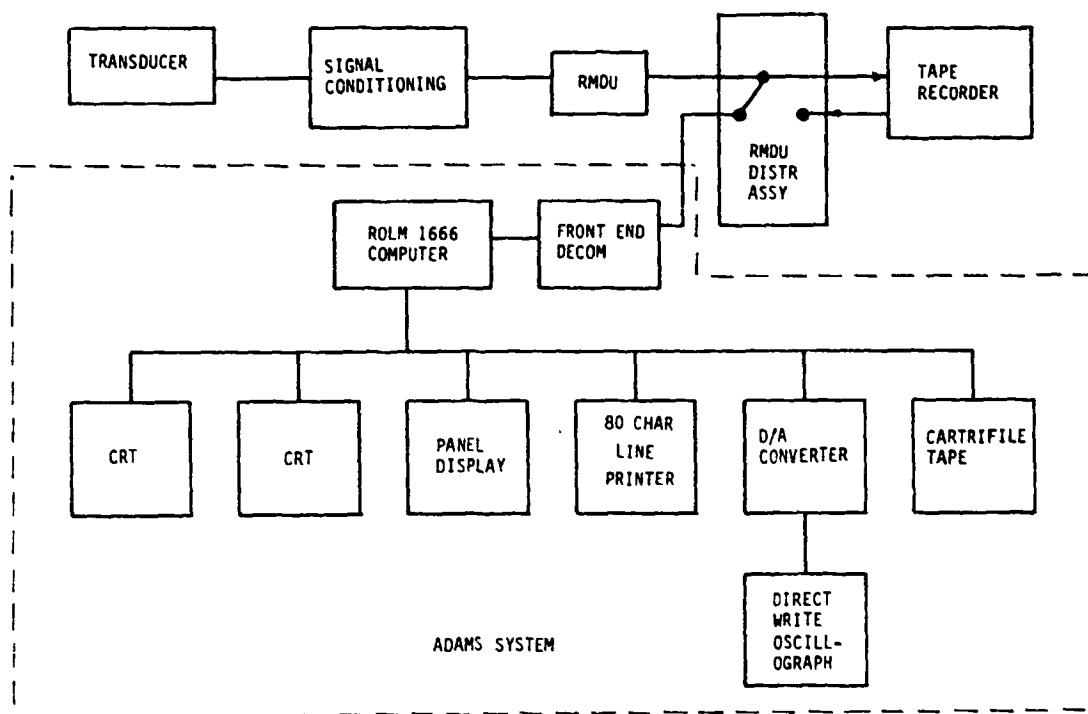


Figure 5.1-1 RA001 Airplane Flight-Test High-Speed Instrumentation System.

The Airborne Data Analysis and Monitor System (ADAMS), shown in Figures 5.1-1 and 5.1-2, provides the capability to perform functional tests, calibrations, preflight checkout, in-flight status monitoring, and real time data computation and analysis. This system is controlled by a minicomputer with two cathode ray tube (CRT)/keyboard operator stations, a line printer, cartridge tape system, paper tape reader,

and "front-end" decommutation equipment. Data base information is transferred between the ground-based data reduction system and the airplane via the cartridge tape. The system is used to verify that the data acquisition system is functioning properly on a measurement-by-measurement basis before each flight. The system also provides a real-time data analysis capability through application programs entered into the computer via the cartridge tape.

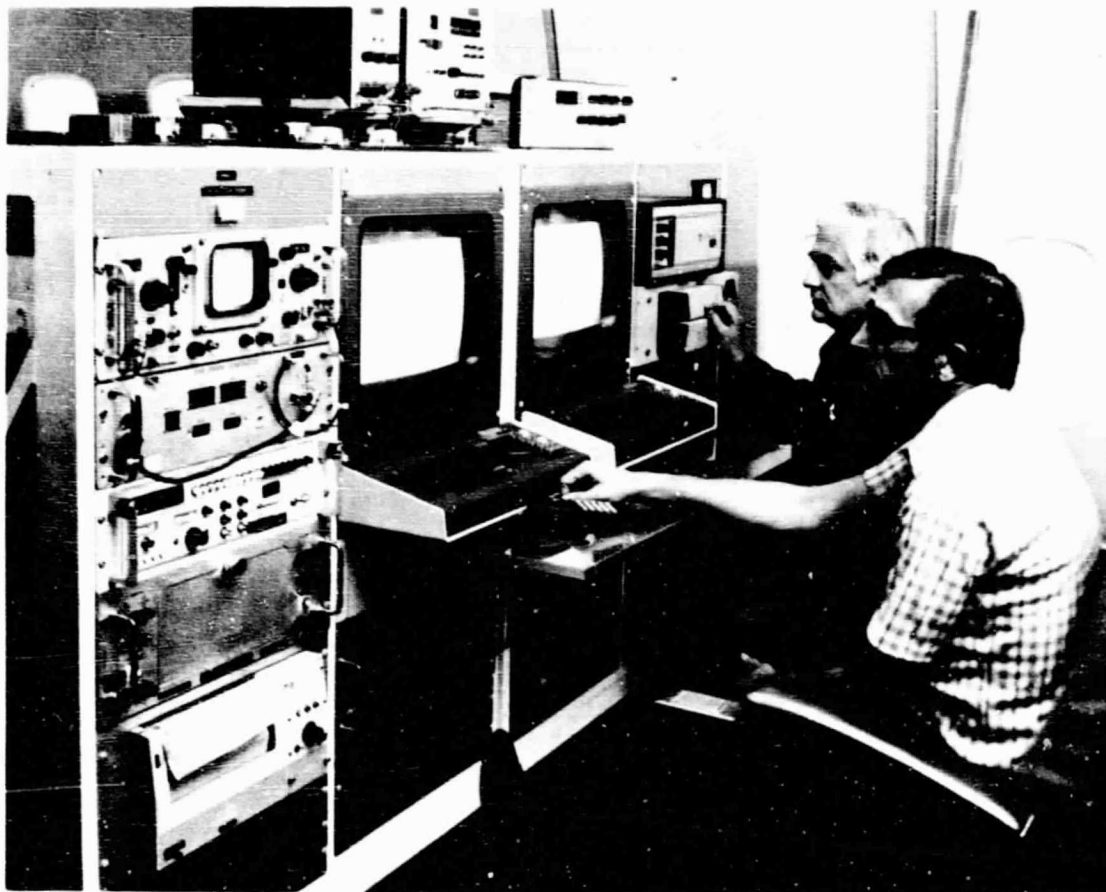


Figure 5.1-2 Airborne Data Analysis and Monitor Systems

There are several methods of real-time data display. The ADAMS system provides a 16 channel digital-to-analog converter (DAC) and a direct write oscillograph to display time history data in strip chart form. This DAC operates under computer control allowing the operator to select preplanned lists of measurements to be displayed. These lists can also be modified or built from "scratch" as the need arises. There

ORIGINAL PAGE IS
OF POOR QUALITY

are a number of digital panel displays on the airplane that may also be controlled by the operator to display in engineering units any parameter being recorded. The CRT/keyboard stations can be used for in-flight monitoring with a maximum of 20 parameters being displayed on each CRT at one time. As before, these lists may be preplanned or built during flight so that any measurement being recorded may be monitored. The ADAMS system may also be used to provide some data processing after a test or flight is complete.

5.1.2 Existing Wiring Quantities

The following table shows the wiring currently installed in RA001 and the provisions for additional wiring.

<u>Engine Number</u>	<u>Currently Installed Four-Conductor Cables</u>	<u>Currently Installed C/A Thermocouples</u>	<u>Provisions for Additions</u>
1	56	20	150
2	16	70	450
3	133	72	450
4	36	12	150

5.1.3 Constraints on Additional Wiring

The limiting factor for wire routing to the engines is the number of wires that can be routed through the engine strut for inboard engines and the number that can be routed through the wing leading edge for outboard engines.

5.1.4 Selection of Engines

To achieve the objectives of the flight load test program, one inboard and one outboard engine must be instrumented for testing. During the time frame considered for this testing, the number 2 position may be used for other engine testing. This dictates that engine number 3 be the inboard engine used. The selection of engine number 1 as opposed to number 4 is due to the larger number of instrumentation wires existing on the number 1 engine. Having it on the opposite side of the airplane from the other engine being tested also allows more wires to be routed to the heavily instrumented inboard engine if necessary due to fuselage penetration hole size limitations.

5.2 PRESSURE LOADS

The results of previous flight test measurements discussed in Section 4.3 indicate that the pressure load on the inlet and fan cowl produce almost the total resultant pressure loading on the nacelle. The pressure loadings on the other nacelle sections (core cowl and primary nozzle) are essentially axisymmetric except for local areas of interference effects close to the struts or pylon. Because of close proximity to the engine support points, the contribution of these loads to engine bending and clearance change is very small. The results of these previous flight test measurements also indicate that the pressure loadings on the inboard nacelle are significantly higher than on the outboard nacelle for a given flight condition, due in part to the strong sidewash over the inboard wing and in part to the lower angle of attack of the outboard wing caused by wing flexibility.

On this basis, the inboard nacelle fan cowl and inlet should be heavily instrumented to provide for detailed measurement of the pressure distribution in both the axial and circumferential directions. In view of the complexity and strong asymmetry of the inlet pressure distribution discussed in Section 4.3.1, it is felt that the minimum number of circumferential pressure stations to ensure confidence of achieving this objective should be as follows:

Lip (hi-lite to throat): 1 station every 30 degrees (12 total)
Fan Cowl (throat to T.E.): 1 station every 60 degrees (6 total)

At each circumferential station, the axial distribution of pressure taps should be located such as to accurately measure the steep pressure gradients that occur between hi-lite and throat (I.S. 12.369)*, as well as the effect of shock waves just down-stream of the throat. The technically preferred arrangement, based on a minimum practical spacing of 0.5 inch between taps, would lead to 24 taps around the lip and 18 taps downstream of the throat, for a total of 396 taps as shown in Figure 5.2-1.

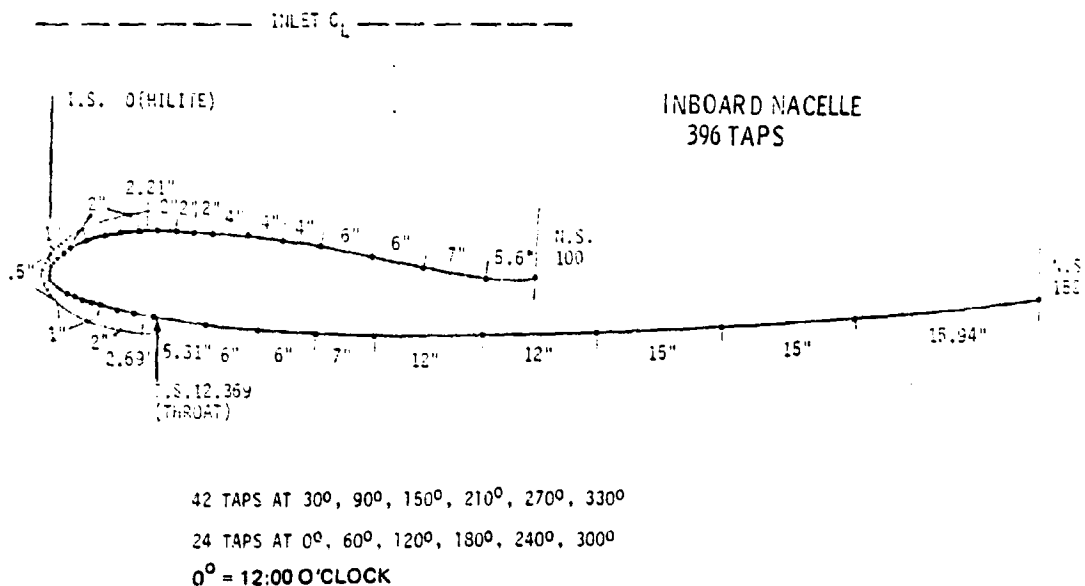
A somewhat more economical, but still technically acceptable arrangement, shown in Figure 5.2-2, would consist of 252 taps on the inboard nacelle. A third arrangement, consisting of 126 pressure taps, was also studied as a lower bound on the pressure instrumentation and is shown in Figure 5.2-3. It is felt that the

* I.S. = Inlet station, 12.369 = distance from hi-lite to throat in inches.

pressure distributions obtained from this third arrangement, which has a maximum of only 15 pressure taps at each circumferential station (versus 12 taps in previous tests) would not lead to a substantial improvement of our knowledge of flight loads. Consequently, this third arrangement should not be given serious consideration.

Either the first or second pressure tap distribution will eliminate the need to apply an arbitrary interpolation formula to obtain total integrated pressure loads, as discussed in Section 4.3.1 and utilized in the studies made to date. Either of these distributions of pressure taps on the inboard nacelle will permit a reduced number of taps on the outboard nacelle. Interpolation between measured pressure data points will be greatly facilitated by the data from the inboard engine. On the outboard nacelle, three circumferential stations (60, 180, and 300 degrees) must be instrumented with 15 static pressure ports per station, for a total of 45 taps, as shown in Figure 5.2-4.

Each pressure port will have an individual pressure transducer so that simultaneous data can be obtained from all taps at any given time. As with all pressure load testing, it is imperative that the flights be performed during relatively dry weather conditions to prevent moisture from collecting in the pressure tubes and invalidating the data as a result of blockage or freezing. The installation of the pressure taps in the quantities and locations discussed above for both inboard and outboard locations has been determined to be feasible.



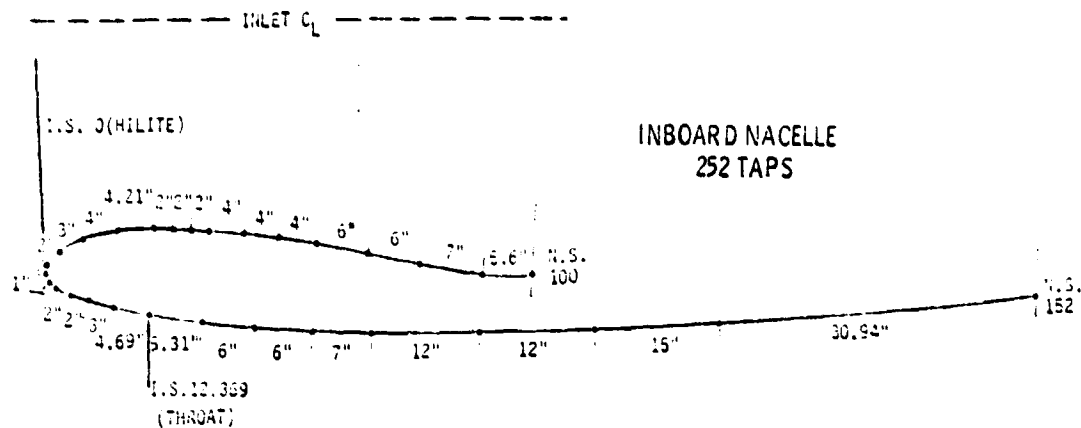


Figure 5.2-2 Alternate Pressure Load Instrumentation Configuration for the Inboard Engine Nacelle.

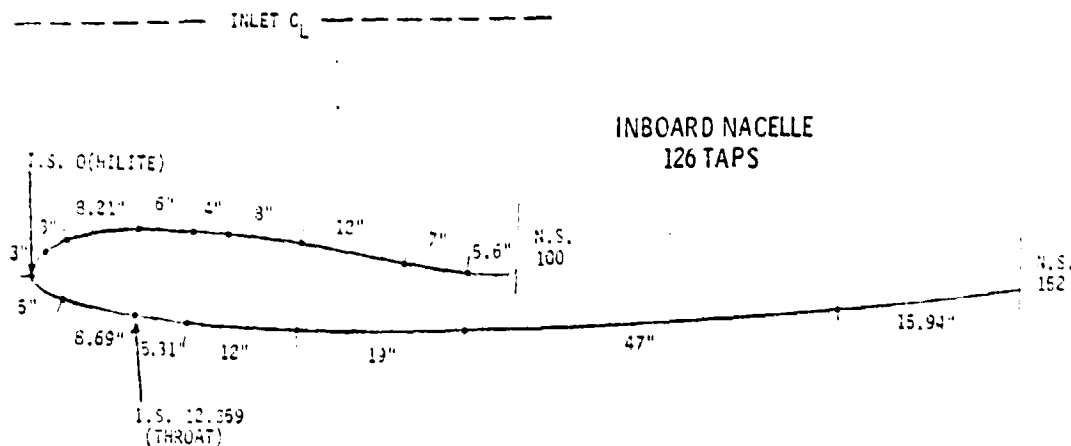


Figure 5.2-3 Lower-Bound Pressure Load Instrumentation for the Inboard Engine.

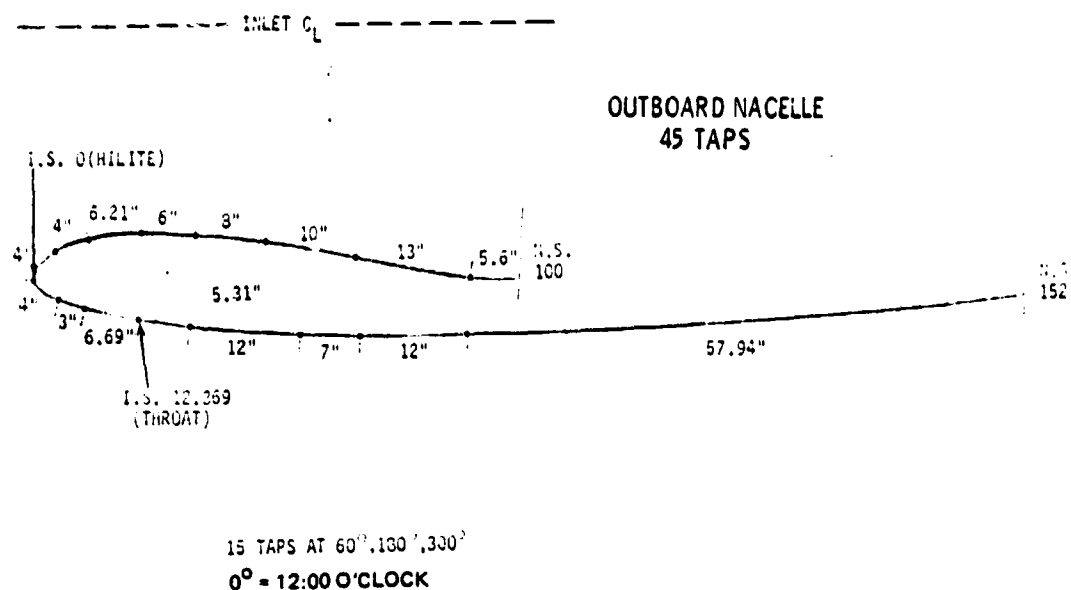


Figure 5.2-4 Pressure Load Instrumentation Configuration for the Outboard Engine Nacelle.

5.3 INERTIA LOADS

As explained previously, the nacelle experiences inertia loads both because of its own vibration about the support points and because of entrainment by the wing. Only the latter effect has been accounted for in previous attempts to evaluate nacelle inertia loads, and even these evaluations were based on airplane C.G. load factors multiplied by theoretical load magnification factors. A requirement exists therefore for a direct measurement of g loads as well as pitch and yaw rates on the nacelle to infer the gyro loads.

Inertia loads on the nacelle are due to gusts, maneuvers, and landing impact, as well as gyroscopic loads from the rotors.

5.3.1 Instrumentation Location and Quantity

The quantity of transducers that can be installed is influenced by physical accessibility, operating environment, and the rigid body equations of motion. To determine the g loads at every point on the nacelle, a knowledge of the linear and angular acceleration vectors at the nacelle c.g. (six components) would be sufficient if the nacelle were a rigid body. If this assumption is not warranted, the distribution of g loads on the nacelle cannot be calculated but must be measured by installing, in principle, one accelerometer at each station of interest.

Based on the analysis conducted for the previous Feasibility Study, it was decided to install 18 accelerometers and a pitch and yaw rate gyros at the locations shown in Figure 5.3-1 and identified in Tables 5.3-I and 5.3-II. This will provide a reasonably adequate description of actual g loads in the nacelle, regardless of any rigid body assumption, and will permit the calculation of nacelle c.g. accelerations if frequencies above 10 Hertz (lowest nacelle bending mode) are filtered out. Pitch and yaw rates for the nacelle c.g. based on the rigid body assumption can also be inferred by filtering out the higher frequencies.

It should be emphasized that the rigid body assumption is introduced only for the purpose of calculating the engine c.g. accelerations and does not imply that engine bending is absent.

In other words, the acceleration measured at any point on the engine is assumed to result from the superposition of rigid body motion about the c.g. plus elastic motion with respect to the c.g. Knowledge of the c.g. acceleration can be used as input for a complete dynamic analysis of the nacelle if the elastic part of the motion is found to contribute significantly to deterioration.

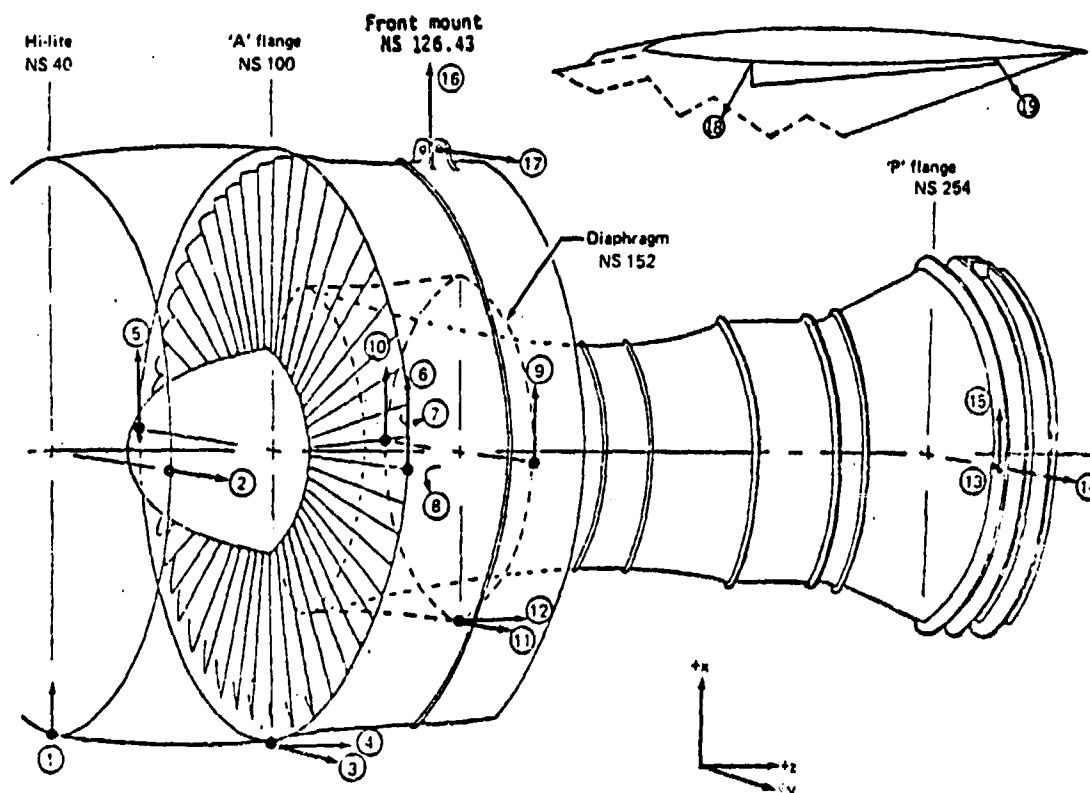


Figure 5.3-1 Inertia Loads Instrumentation Locations - 16 accelerometers, a pitch and yaw rate gyro and a thermocouple are located as shown, see Tables 5.3-I and 5.3-II for identifying code.

TABLE 5.3-I
INERTIA LOADS PRIMARY INSTRUMENTATION

<u>Code</u>	<u>Description</u>	<u>Units</u>	<u>Min</u>	<u>Max</u>	<u>Accuracy</u>	<u>XDCR type</u>	<u>Expected operating temp.</u>
1	Vertical acceleration - NS40 -6 o'clock	g	-4	6	0.1	Q-Flex	150° F
2	Lateral acceleration - NS40 -3 o'clock	g	-2	2	0.04	Q-Flex	150° F
3	Lateral acceleration - NS100 -6 o'clock	g	-2	2	0.04	Q-Flex	150° F
4	Longitudinal acceleration - NS100 -6 o'clock	g	-2	2	0.04	Q-Flex	150° F
5	Vertical acceleration - NS100 -9 o'clock	g	-4	6	0.1	Q-Flex	150° F
6	Vertical acceleration - NS100 -3 o'clock	g	-4	6	0.1	Q-Flex	150° F
7	Yaw rate - NS 100 -3 o'clock	deg/sec	-10	10	0.2	Northrup 3-axis	150° F
8	Pitch rate - NS100 -3 o'clock	deg/sec	-15	15	0.3		

TABLE 5.3-II
INERTIA LOADS REDUNDANT INSTRUMENTATION

<u>Code</u>	<u>Description</u>	<u>Units</u>	<u>Min</u>	<u>Max</u>	<u>Accuracy</u>	<u>XDCR type</u>	<u>Expected operating temp.</u>
9	Vertical acceleration - NS152 -3 o'clock	g	-4	6	0.3	Kaman 1901	350° F
10	Vertical acceleration - NS152 -9 o'clock	g	-4	6	0.3	Kaman 1901	350° F
11	Lateral acceleration - NS152 -6 o'clock	g	-2	2	0.12	Kaman 1901	350° F
12	Longitudinal acceleration - NS152 -6 o'clock	g	-2	2	0.12	Kaman 1901	350° F
13	Temperature - NS254 -3 o'clock	°F	0	1100	11		1050° F
14	Lateral acceleration - NS254 -3 o'clock	g	-2	2	.12	Kaman 1901	1040° F
15	Vertical acceleration - NS254 -3 o'clock	g	-4	6	0.3	Kaman 1901	1040° F
16	Vertical acceleration - NS126.43 front mount	g	-4	6	0.1	Kistler	100° F
17	Lateral acceleration - NS126.43 front mount	g	-2	2	0.04	Kistler	100° F
18	Vertical acceleration - Front Spar wing/strut intersection	g	-4	6	0.1	Kistler	100° F
19	Vertical acceleration - Rear Spar wing/strut intersection	g	-4	6	0.1	Kistler	100° F

A minimum of six accelerometers are needed to calculate the six components of the c.g. accelerations. The remaining ten accelerometers can be considered redundant and used either to confirm the measurements (and the rigid body assumption) by repeating the calculation with different sets of six accelerometers or eliminated completely.

In the latter case, one would need to retain accelerometers 1 through 6 plus accelerometers 18 and 19, mounted on the front and rear spar at the wing/strut intersection, to verify the forcing function imposed by the wing on the nacelle. In addition, the pitch and yaw rates at locations 7 and 8 are required to infer gyro loads.

Highest inertia loads occur on the outboard engine, so that it should have the most complete instrumentation. The feasibility of installing the inertia load instrumentation was previously determined and reconfirmed during this study.

5.4 ENGINE CLEARANCE CHANGES

As discussed in Section 4.2, clearance changes are believed to be the dominant mechanism in short-term performance deterioration. An investigation was made to determine the feasibility of making in-flight clearance measurements in the fan, low-pressure compressor, high-pressure compressor, and high-pressure turbine of a JT9D-7 engine. In previous testing, it was found that electrical and magnetic property changes of materials at high temperatures make clearance measurements with electrical or electromagnetic devices such as eddy current or capacitive probes unreliable. Experience has shown that the most reliable technique for measuring clearances at high temperature and at distances up to 0.350 inch has been with laser proximity probes. The clearance measurement is based on an optical triangulation system, shown in Figure 5.4-1. This clearance measurement system provides a highly stable measurement that is independent of both temperature and pressure.

To assess the feasibility of installing such instrumentation in JT9D engines on the RA001 airplane, meetings were held with BCAC flight test personnel and physical examination of RA001 was undertaken. The findings of the feasibility study are listed below by stage in order of priority.

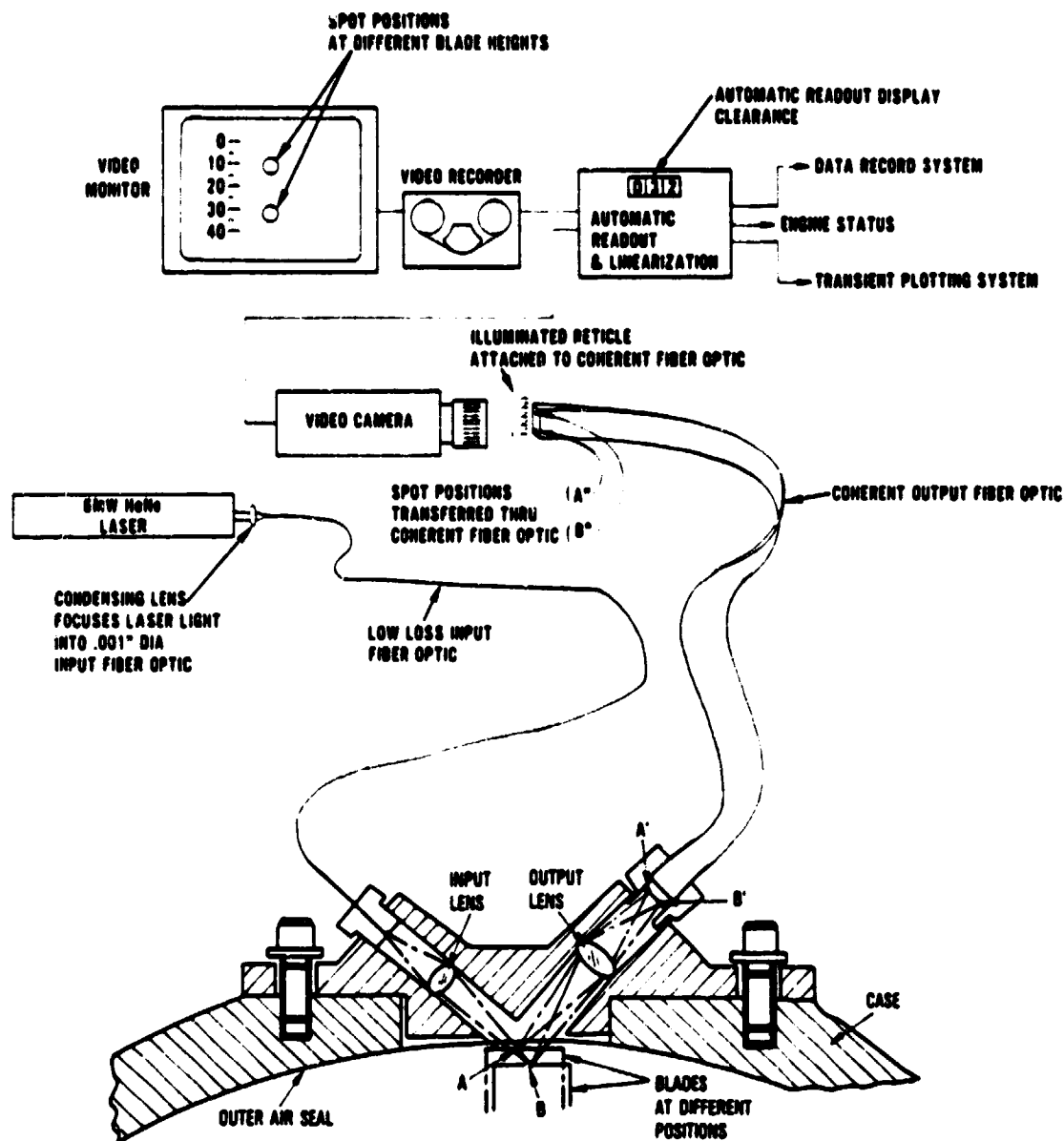


Figure 5.4-1 Compressor-Type Laser Proximity Probe System

5.4.1 Study Results

5.4.1.1 Fan

It is feasible to mount four compressor-type proximity probes, illustrated in Figure 5.4-1, in the fan case on both inboard and outboard engines. During the study, it was an objective that the probe locations coincide with the fan probe locations utilized in the X-Ray Facility Load Test program to permit cross checks of data. The

locations selected for the fan proximity probes are shown in Figure 5.4-2. The probes used for the X-ray program are, however, not suitable for the flight test since their intensity and resolution is not sufficient to use with the long input fiber optics required for the flight test. Both the input and output fiber optics are required to be appreciably longer in the flight test since neither the laser source nor the camera can be mounted in the engine nacelle. Additionally, the X-ray test probes cannot be used due to a lack of clearance for the probe when the fan cowl doors are closed. A new probe must, therefore, be designed. The holes and bosses on the fan case being used in the X-ray test are also not compatible with the required new probe design, and the case must either be reworked, if possible, or another case must be used. The measurement of fan blade tip clearance during the flight test program is desirable for the following reasons:

- o The clearance changes are physically the largest and are more easily correlated to flight aerodynamic or inertia load level and type of flight maneuver.
- o Rub strip wear can be visually observed during the progress of the flight test program.
- o Response of other low spool shaft components, low-pressure compressor and turbine, can be estimated based on correlations developed from the X-Ray Facility Test Program and analytical studies.

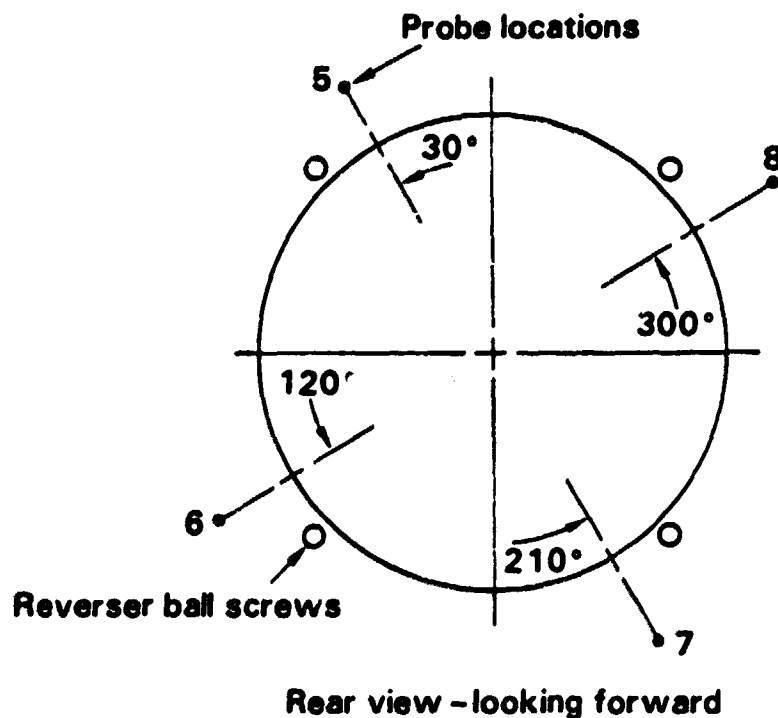


Figure 5.4-2 Angular Location of Fan Blade Proximity Probes

The camera for the fan probes will be mounted in the anti-icing supply ("TAI") duct fairing (Figure 5.4-8) on both the inboard and outboard engines by removing the Boeing inlet anti-icing line. This camera location and the required lengths of the fiber optic leads from probes to the camera are acceptable. The measurement of fan clearance changes during flight is, therefore, judged to be feasible.

5.4.1.2 High-Pressure Turbine, Front

It is feasible to mount four turbine-type proximity probes, shown in Figure 5.4-3, on the high-pressure turbine case on both inboard and outboard engines to monitor the first-stage blade clearances. It will not be possible, however, to locate the probes in the same angular locations as in the X-ray program, nor will it be possible to space the probes exactly 90 degrees apart, see Figure 5.4-4. Coincident location of the probes relative to the X-ray program is not possible because of P&WA and Boeing external plumbing and equipment in this region, see Figures 5.4-5 and 5.4-6. It may be possible to use the existing turbine case from the X-ray test if a structural analysis shows that the addition of more holes for the flight loads testing will not adversely influence the flight-worthiness of the case. The probe design being used on the X-ray test appears to be acceptable for use during the flight test.

The camera for the turbine proximity probes will be mounted in the "knee-cap" region of the strut-pylon-wing assembly (Figure 5.4-8) on both the inboard and outboard engines. Some rerouting of existing aircraft Bill-of-Materials wiring in this region may be needed. Lengths of the required fiber optics from the probes to the camera are acceptable. The measurement of high-pressure turbine first-stage blade clearances during flight is, therefore, judged to be feasible.

5.4.1.3 Low-Pressure Compressor, Rear

It is feasible to mount four proximity probes on the low-pressure compressor case on inboard and outboard engines to monitor clearances in the final stage of the compressor. Lead routing to and from the probes as currently planned for the X-ray test, via the fan anti-icing lines in the intermediate case, is not acceptable for a flight test operation. Lead routing would require some design work and some modification to the fan splitter bulkhead. Once through the bulkhead, the leads would need to be routed through a congested region on the case to reach the pylon.

For the inboard engine, a camera could be housed in the "knee-cap" region of the strut-pylon-wing assembly. However, there is no room for a camera at the outboard engine nacelle or pylon. The required output fiber optic length to reach from the probe to the camera is sufficiently long to be unsatisfactory for two reasons: 1) the output fiber is a high-loss fiber, and the greater lengths result in reduced output intensity; and 2) the manufacturing process for the fiber is limited with respect to fiber length, and splices are not acceptable. For these reasons, the measurement of low-pressure compressor clearances is not judged to be feasible.

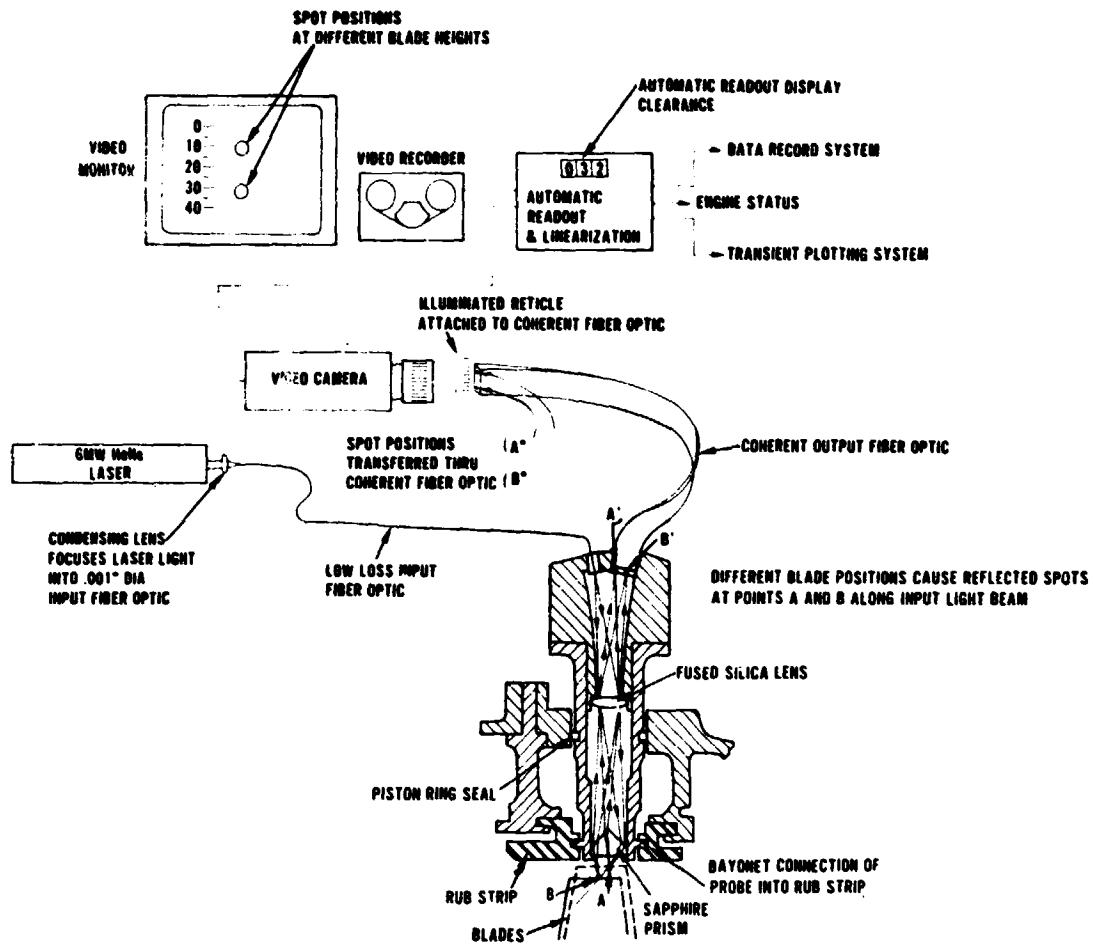


Figure 5.4-3 Laser Proximity Probe System for the Turbine

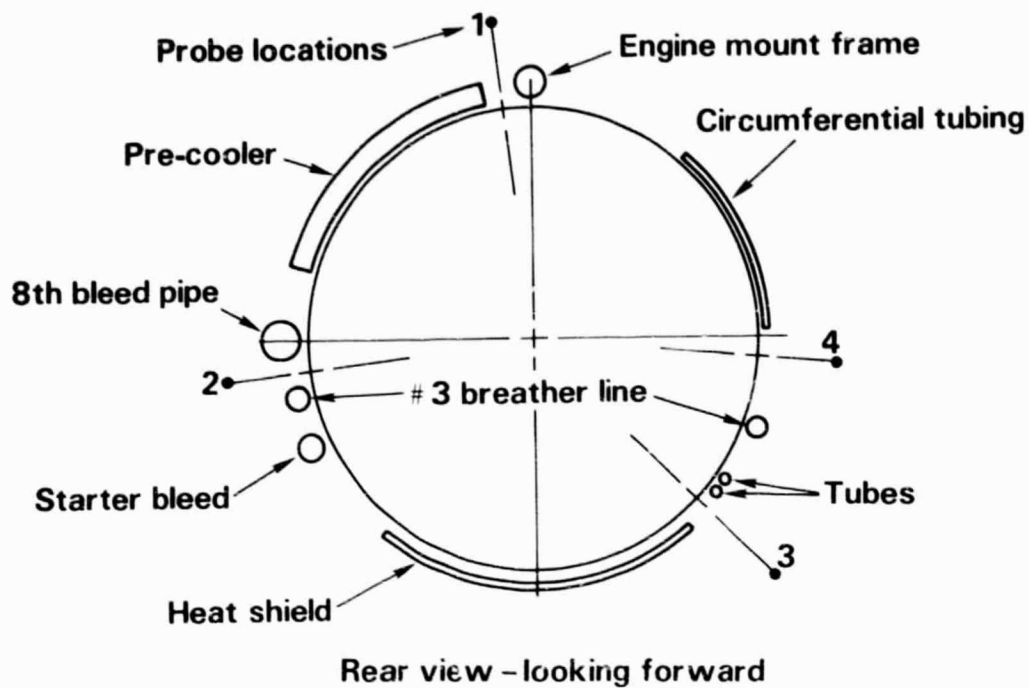


Figure 5.4-4 Angular Location of Turbine Blade Proximity Probes

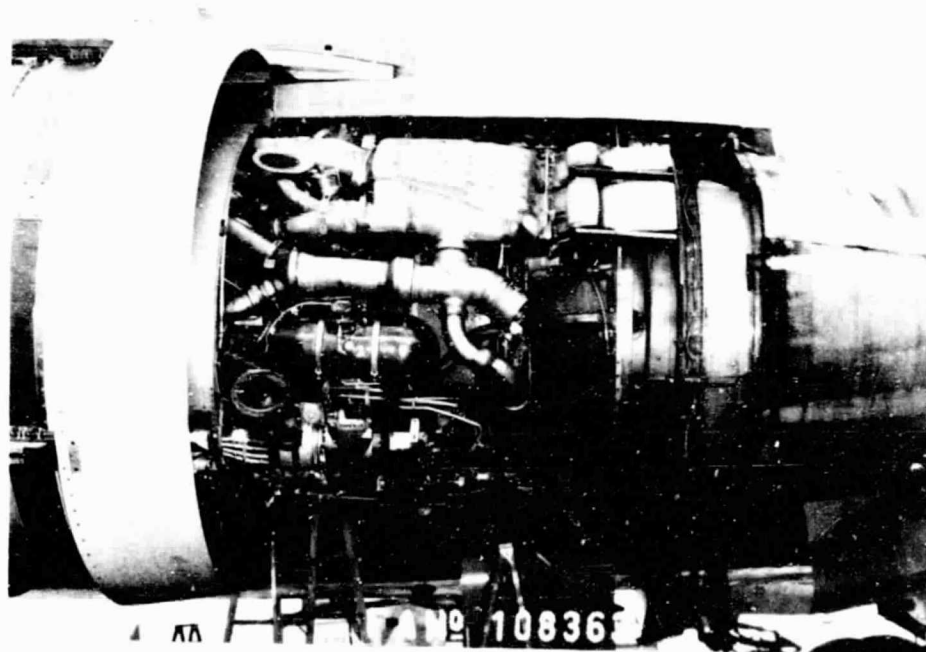


Figure 5.4-5 Left Side of JT9D-7 Flight Engine

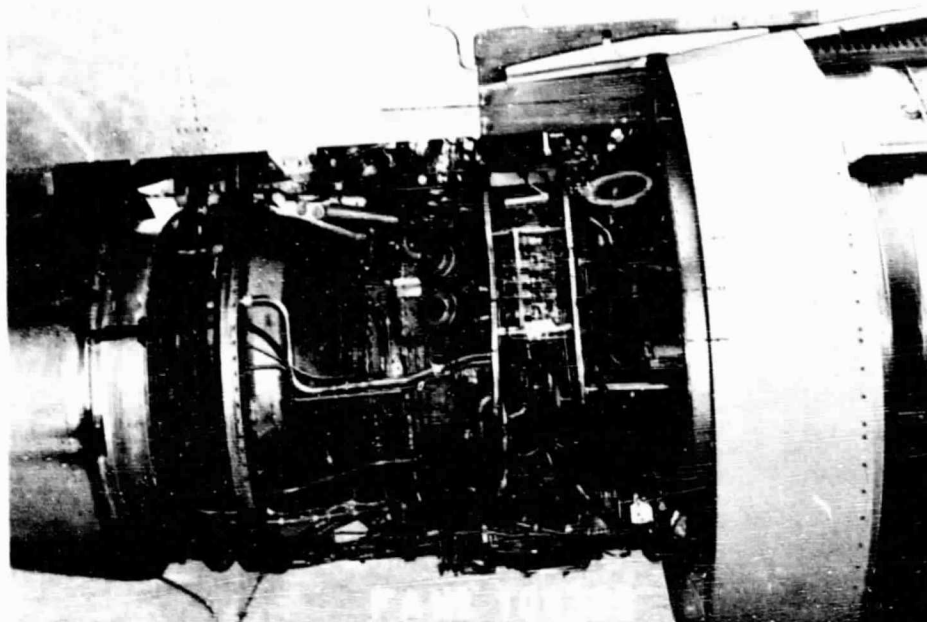


Figure 5.4-6 Right Side of JT9D-7 Flight Engine

5.4.1.4 High-Pressure Compressor, Front

Since no camera space exists in the nacelle or pylon within a reasonable distance for proximity probes in the early stages of the high-pressure compressor, no further effort was undertaken to measure clearances in this region.

In addition to locating space for mounting the probes in the engine cases, space and mounting provisions for the rest of the required equipment were identified as shown in Figures 5.4-7 and 5.4-8.

5.4.2 Proximity Probe Clearance Measuring System

Detailed information of each part of the clearance measuring system is presented in the following subsections.

ORIGINAL PAGE IS
OF POOR QUALITY

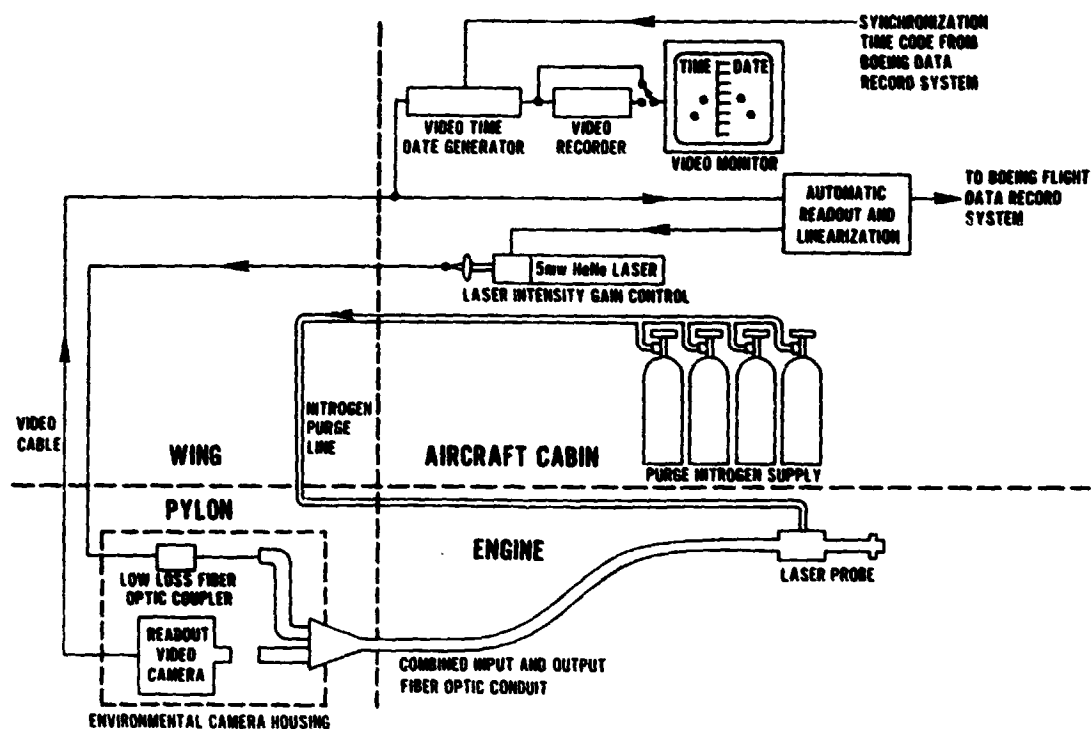


Figure 5.4-7 Laser Proximity Probe In-Flight Data Acquisition System - The schematic shows the location of the various equipment elements of the laser proximity probe system.

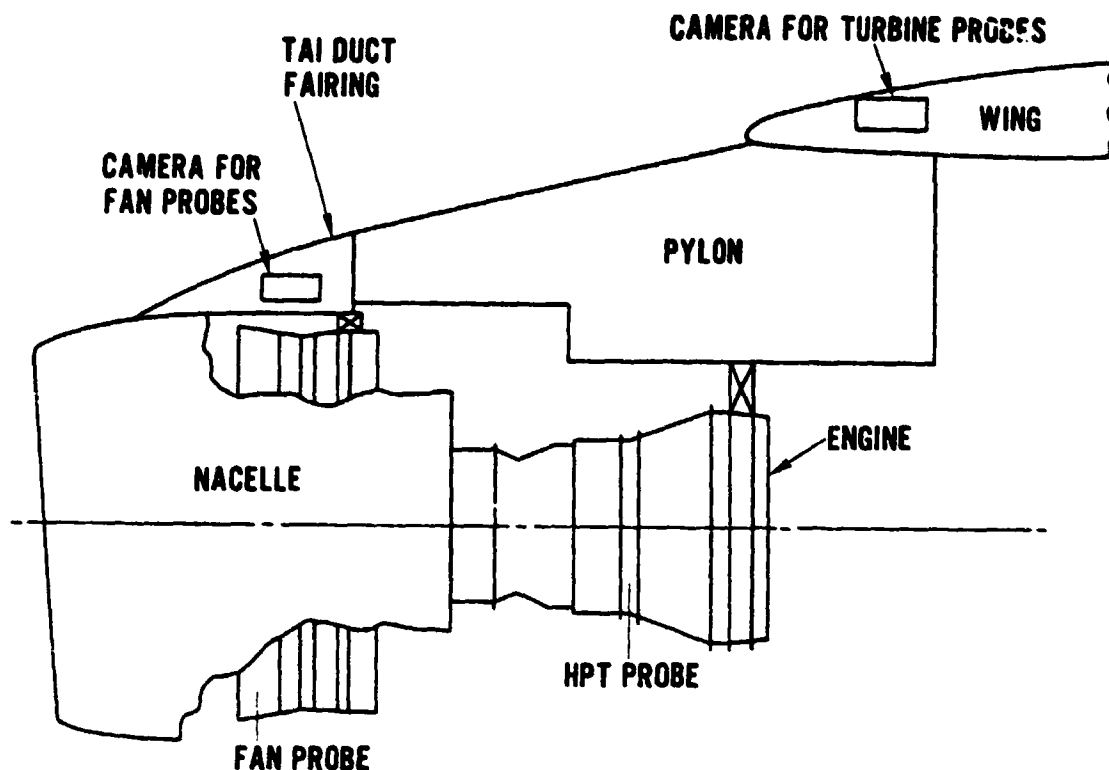


Figure 5.4-8 Axial Location of Proximity Probes and Associated Camera Locations - Allowable length limitations on output fiber optics cable, environmental considerations for the camera, and available space dictate the selected locations for the probe cameras.

5.4.2.1 Lasers and Input Fibers

The 5 mw helium/neon lasers will be mounted in the airplane cabin. This location will allow the lasers to be operated at cabin pressure and temperature and mounted in standard P&WA laser boxes secured to the floor of the cabin. This arrangement will eliminate the necessity of building special environmental housings for mounting on the airplane wing. Low loss fiber optic cables will be used to transmit the light through the wing leading edge to the probe locations. ITT T-202 type fiber optics will be utilized and provide less than 2 dB attenuation in the distance between the cabin and the probes. A fiber optics connector located at the camera box will be used to couple this fiber to a fiber optic connected to the probe. The fiber optic connector will provide an additional 0.5 to 1.5 dB attenuation. A total of less than 4 dB attenuation, which is acceptable for this program, can be expected from this system.

5.4.2.2 Video Cameras and Output Fiber Optics

One video camera is required for each set of four laser proximity probes to read out the probe signal. This camera must be mounted within 20 feet of the probes because of current manufacturing limitations on the interconnecting coherent array output fiber optic bundle. Because these output fibers must currently be made from high loss fiber optics, unacceptably high attenuation of the optical signal would result for bundles longer than 20 feet. As previously mentioned, cameras for the turbine probes will be mounted in the "knee-cap" region, and cameras for the fan probes will be mounted in the "TAI" duct fairing. All probe locations on the fan and turbine can be reached with 20-foot long fiber optics.

The video cameras are specifically designed for instrumentation applications and maintain a geometric stability with both temperature and power variations. The camera draws 11 watts and will need to be mounted in an environmental chamber that will be provided with cooling, resistance heating, and pressurization from a nitrogen supply line. The environmental chamber will be shock mounted to reduce vibration transmitted to the camera.

5.4.2.3 Video Monitor Tape-Recorder, Electronic Readout, and Time-Date Generator

A 17 inch video monitor will be used to view the output from the video camera. A cassette video tape recorder will be used to continuously record the output from the camera. A time-date generator will be used to convert an IRIG B time synchronization signal from the Boeing data recording system into an alpha-numeric time/date signal that will be superimposed on the video signal. In addition to this signal, the IRIG B will be recorded on one audio track of the video tape recorder along with engine speed and voice on the other audio track. The video data will be manually monitored in flight, and the data can be further analyzed after the flight by playing back the tape recorded data.

In addition to the video data, an electronic readout system will be used to read the clearance from the video camera. The readout automatically converts the position of the spot of light into a millivolt signal that is proportional to the engine clearance. The readout functions by counting TV raster lines to find the line number which represents the center of the spot of light. The unit does this by starting at the top of the TV raster and counting each line until a line with sufficient intensity (representing the top of the spot) is found. The number of this line is added to a second number representing the last line with sufficient intensity. The resulting sum is twice the line number at the center of the data spot. This number is scaled to provide a calibrated millivolt output that is proportional to the blade clearance.

The millivolt output from the electronic readout is fed into the Boeing High-Speed Pulse Code Modulated (HSPCM) data recording system. The HSPCM data system will allow direct computer analysis by P&WA of the clearance data and will provide correlation of the clearance data with other data such as g loads and gyroscopic loads.

The video monitor, tape recorder, time-date generator, and electronic readout will all be rack mounted in a standard 4 foot Boeing flight test rack. Each set of four proximity probes will require one rack with the above equipment.

5.4.2.4 Probe Purge and Cooling Requirements

Prior experience during ground test stand testing has shown that the turbine laser proximity probes require purge nitrogen to prevent contamination of the optics and to maintain the fiber optic end tips cool enough to prevent damage of the high temperature epoxy bonds. Several options were considered for providing purge air or nitrogen on the airplane during flight testing, and it was determined that the most appropriate technique would be to provide nitrogen from high pressure storage tanks. A flow rate of 15 pounds per hour is required for each probe. For a 4-hour flight using eight turbine proximity probes plus 50 percent extra capacity, a total of 52 "T"-size gaseous nitrogen bottles will be required. If proximity probes are mounted on the inboard engine only, the required number of nitrogen bottles would be reduced to 26. These bottles will be rack mounted in the cabin of the airplane. A pressure regulator will reduce the nitrogen pressure at the probes to 400 psi. The purge nitrogen will be supplied by 1/2-inch diameter tubing through the wing (one line per four probes).

A summary of the clearance measurement equipment, cabling sizes, and power and cooling requirements are shown on Tables 5.4-I, 5.4-II, and 5.4-III.

5.5 FEASIBILITY OF USING NASA SPACE SHUTTLE CARRIER AIRCRAFT

The NASA space Shuttle Carrier Airplane (SCA), shown in Figure 5.5-1, was inspected by a team of personnel from Boeing, Pratt & Whitney Aircraft, and NASA to determine the requirements to bring that airplane up to an equivalent capability that now exists on the Boeing RA001 airplane. In addition, the flight loads program schedule and requirements were presented to NASA Johnson Space Center and to NASA Dryden Flight Center. It was determined that the following items must be considered:

- o Mach Number Limitations
- o Rotation Angle Limitations
- o Available Instrumentation Wiring
- o Data Acquisition System
- o Lay-Up Time
- o Removal/Reinstallation of Stabilizer Tip Fins and Space Shuttle Support Structure

TABLE 5.4-I

EQUIPMENT REQUIREMENTS FOR LASER PROXIMITY PROBES
DURING FLIGHT TEST

TO BE SUPPLIED BY P&WA:

8 plus 4 spares	Fan Proximity Probes.
8 (4) plus 8 (4) spares	Turbine Proximity Probes.
4 (3)	Environmental Boxes with Heater & Cooling Coils.
4 (3) plus 4 (3) spares	Television Cameras.
4 (3) plus 1 spare	Laser Proximity Readout System Consisting of: Television Monitor, Time-Date Generator, Digital Readout Electronics.
4 (3) plus 1 spare	Video Tape Recorders.
4 (3) plus 4 (3) spares	Laser Boxes with Lenses & Power Supplies; Contains four Lasers per Box.
1 plus 1 spare	Thermocouple (TC) Readout Box with Switch.

TO BE SUPPLIED BY BCAC:

As Required	Rack Mounts for Laser Proximity Readout System, Video Tape Recorder, Laser Boxes, Thermo- couple Readout Box.
52 (26) for 4-hour flight, including 50% extra capacity	Gaseous Nitrogen (GN2) Bottles, "T"-Size.
As Required	Gaseous Nitrogen Fittings & Regulators
As Required	Power Converter/Sola Regulators

Note: Numbers of parts shown based on fan stage and turbine stage both instrumented on two engines. The numbers of parts shown in () are for recommended program with only one turbine stage instrumented.

TABLE 5.4-II

CABLING REQUIREMENTS FOR LASER PROXIMITY PROBES
DURING FLIGHT TEST

<u>Number of Units Required</u>	<u>Part Name</u>	<u>Diameter (inch)</u>	<u>Location *</u>
RESPONSIBILITY OF P&WA:			
8 (6)	Input Fiber Optics Bundle (has internal spares)	0.400	Fus, EB
16 (12) + 4 (3) spares	Input/Output Fiber Optics Bundle	0.400	EB, Pr
2 (1)	GN2 Manifolds (near probes)	---	Nacelle
16 (12)	GN2 Purge Lines, Copper Tubing	0.250	Man, Pr
RESPONSIBILITY OF BCAC:			
4 (3)	AC Power for Camera	---	Fus, EB
4 (3)	AC Power for EB Heater	---	Fus, EB
4 (3)	Video Output RG-302 U, BNC Plugs Both Ends	0.200	Fus, EB
2 (1)	GN2 Purge Master Line, Copper Tubing, No Fitting at Outboard End	0.500	Fus, Man
4 (3)	Pressure/Cooling Line for EB	0.250	Fus, EB
8 (6)	Thermocouple Wires to Cameras	---	Fus, EB
16 (12)	Thermocouple Wires to Probes	---	Fus, Pr
* Abbreviations: Fus = Fuselage			
GN2 = Gaseous Nitrogen			
EB = Environmental Box for TV Camera			
Pr = Probe			
Man = Manifold			

Note: Numbers of parts shown based on fan stage and turbine stage both instrumented on two engines. The numbers of parts shown in () are for recommended program with only one turbine stage instrumented.

TABLE 5.4-III
POWER REQUIREMENTS FOR LASER PROXIMITY PROBE SYSTEM
DURING FLIGHT TEST
BCAC Responsibility

<u>Circuit Number</u>	<u>Equipment</u>	<u>Total Power (watts)</u>
1	Camera Circuit, 15 watts/camera; 115 VAC, 60 Hz, <u>+1%</u> voltage regulation	60 (45)
2	Environmental Box Heater Circuit, 230 watts/box; 115 VAC, 400 Hz, no regulation	920 (690)
3	Rack Mount Circuit: Laser Proximity Readout System, 500 watts/system; Laser Boxes, 50 watts/box; 115 VAC, 400 Hz, <u>+1%</u> voltage regulation	2200 (1550)
4	Tape Recorder Circuit, 150 watts/recorder; 115 VAC, 60 Hz, <u>+1%</u> voltage regulation; <u>±1%</u> frequency regulation	600 (450)

Note: A switch should be provided for each of circuits number 1 and 2 above, located at the rack mount. The total powers shown in () are for the recommended program with only one turbine stage instrumented.

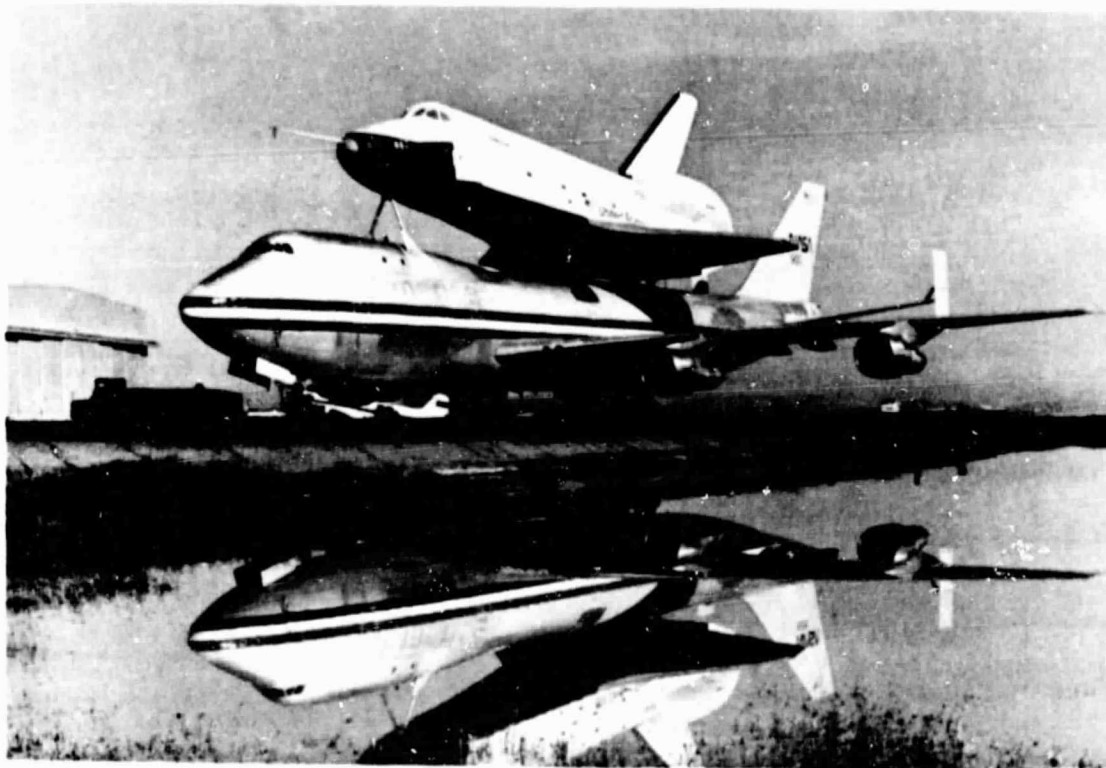


Figure 5.5-1 NASA Space Shuttle Carrier Airplane (SCA).

5.5.1 Performance Limitations

The maximum operating speed (V_{mo}) and design dive speed (V_d) for the NASA 747 are restricted (relative to a production 747-100) with the orbiter support struts and tip fins installed. The speeds are restricted to:

$$V_{mo}/M_{mo} = 250 \text{ knots}^*/\text{Mach } 0.6$$

$$V_d/M_d = 312 \text{ knots}^*/\text{Mach } 0.7$$

These speed restrictions would affect several of the test points of the acceptance flight profile and all of the turbulence test conditions.

The horizontal tail tip fins on the NASA 747 reduces structural ground clearance during take-off. In addition, there are restrictions on roll angles during take-off due to the adverse effect of bank angle on tip fin clearance.

Tip fin clearance during take-off is primarily influenced by rotation speed and pilot technique. The rotation speeds for the NASA 747 were changed relative to a production 747 as a compromise between take-off distance and ground clearance. To provide adequate tip fin clearance,

* knots, corrected air speed.

the rotation pitch rate is reduced prior to lift-off. Therefore, the changes in technique and take-off speeds for the NASA 747 would mean a 2 to 3 degree difference in pitch attitude at take-off relative to a production 747.

5.5.2 Instrumentation Wiring and Data Acquisition Systems

Most of the instrumentation wiring installed for the SCA testing was removed, and over 90 percent of the required wires would have to be purchased and installed.

The data system that was installed during SCA testing was removed and distributed to various NASA groups. The system would either have to be reacquired from the groups now possessing them, or a new system purchased, wired, and checked out.

5.5.3 Aircraft Modification

The lack of a data acquisition system and instrumentation wiring in the SCA would require additional lay-up time. The console build-up of the data acquisition system, check-out, and installation aboard the airplane would require four to six months. Additional aircraft lay-up time would be necessary to route the data wires to the engines and to route the power and control wires necessary for utilizing the data acquisition system.

The stabilizer tip fins and orbiter support struts were designed for quick removal and reinstallation. Because of the operational limitations of the SCA, the tip fins and orbiter support struts would have to be removed to bring the SCA up to the performance capability of the production 747 airplane.

5.5.4 Feasibility

It was determined that the NASA Shuttle Carrier Airplane would be unavailable to NASA for any shuttle activity and would be required at Boeing for a minimum time period of five to six months to accommodate the flight loads test program. This time period is necessary for required hardware modifications, up-dating the instrumentation and data acquisition system, removal and reinstallation of the stabilizer tip fins and space shuttle supports, flight test time, and refurbishment of the airplane.

At the conclusion of the meeting at Dryden, the NASA Johnson representatives indicated that the NASA airplane could not be taken out-of-service for the time necessary to conduct the flight loads test and would, therefore, be unavailable for the program. In addition, it is estimated that the added cost to the program to bring the NASA airplane to an equivalent capability of the Boeing RA001 airplane would approximately double the cost of the recommended program option. It is, therefore, judged unfeasible to consider the use of the NASA airplane for the flight loads test program.

SECTION 6.0

INSTRUMENTATION SELECTION AND MEASUREMENT ACCURACY

6.1 AERODYNAMIC PRESSURE LOAD INSTRUMENTATION SYSTEM

6.1.1 Sensor Type and Accuracy

The technique presently used to measure pressures such as will be encountered in the flight loads test program is to very accurately measure a reference pressure with an absolute pressure encoder. The encoder is an AiResearch model 2100776, modified to Boeing part number 65Y10787. This encoder has a range of 3 to 31 inches Hg with an accuracy of ± 0.006 inch Hg and a resolution of 0.00007629 inch Hg. These encoders have been used for the 747SP certification program and have proven to be reliable and accurate.

The pressure of interest is then measured differentially with the reference pressure and then mathematically combined using the Final Data System and the onboard ADAMS (for realtime evaluation).

Currently, Statham Model PL722TC pressure transducers (Figure 6.1-1) are being used for this type of differential pressures. Investigations are underway to replace the Statham with Endevco 85XX series transducers (Figure 6.1-2) due to the comparative size of the Statham. Either transducer is capable of accomplishing the required job. If the investigations show the small size of the Endevco will be advantageous, and they meet the required specifications, they will be used. Preliminary results indicate that the Endevco transducer will be chosen.

6.1.2 Data Recording Frequency

The frequency of the pressures to be measured is 2 Hertz. Using the Boeing criteria of ten samples per cycle to describe the amplitude of a wave form gives a data sample rate of 20 samples per second.

6.2 INERTIA LOAD INSTRUMENTATION

6.2.1 Transducer Selection

The estimated requirement for measurement accuracy in the range of 1 to 2 percent of full scale dictated the use of highly accurate linear accelerometers on the powerplant. To obtain angular as well as linear accelerations at the powerplant center-of-gravity (c.g.), a system of equations based on rigid body motion was derived. The installation locations were then determined based on these equations and other requirements such as operating environment, accessibility, and structural rigidity.

1.2 Positive Pressure Media	Fluids compatible with stainless steel
1.3 Reference Pressure Media	Dry, non-corrosive gases
1.4 Internal Case (line) Pressure	1 to 1,000 psia
1.5 Transduction	Resistive, balanced, fully active strain gage bridge
1.6 Nominal Bridge Resistance	350Ω
1.7 Excitation	5V DC or AC (rms) through carrier frequencies
1.8 Full-scale Output (open circuit)	5 mV/V nominal
1.9 Resolution	Infinitesimal
1.10 Combined Non-linearity, and Hysteresis	Less than ±0.75%FS
1.11 Temperature Range	-65 to +250°F
1.12 Thermal Sensitivity Shift	Less than 0.01%/°F from -65 to +250°F
1.13 Thermal Zero Shift	Less than 0.01%FS/°F from -65 to +250°F
1.14 Positive Pressure Connection	7/16-20 UNF-3A external thread per MS33656E4
1.15 Reference Pressure Connection	
1.16 Electrical Connection	Four-pin receptacle and mating Bendix PC06W-8-4S plug or equivalent
1.17 Weight	Approximately 7 oz
1.18 Identification	The model designation, serial number, range, maximum excitation, and manufacturer are engraved on each unit.
1.19 Dimensions	See Outline Drawing Number 21070.
1.20 Calibration	Statham pressure transducers are calibrated individually by qualified technicians using specialized equipment of laboratory accuracy. Interim data are furnished at time of shipment.

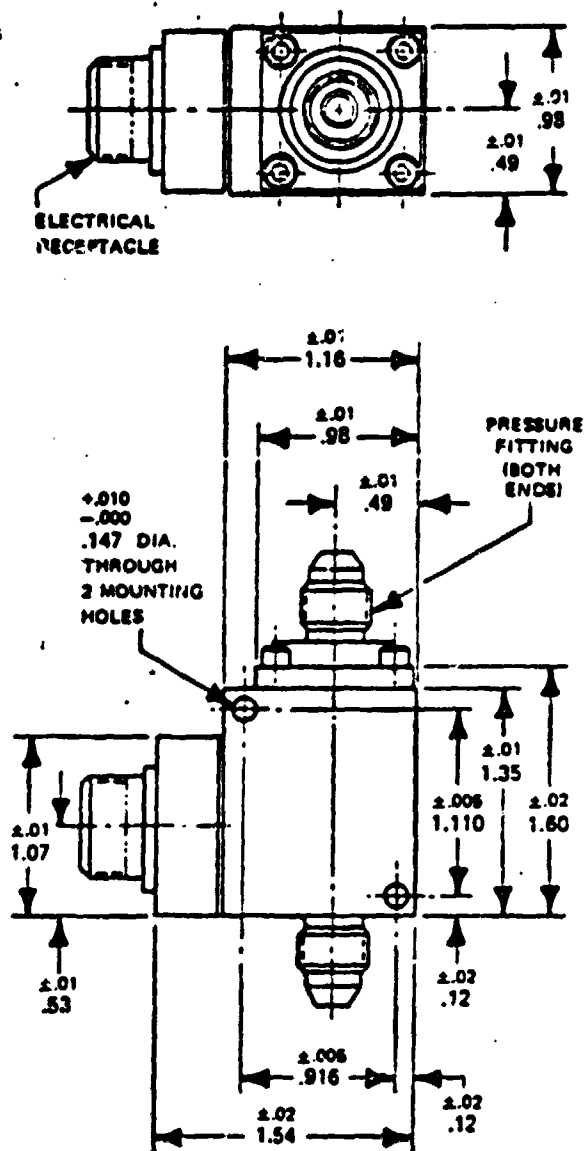
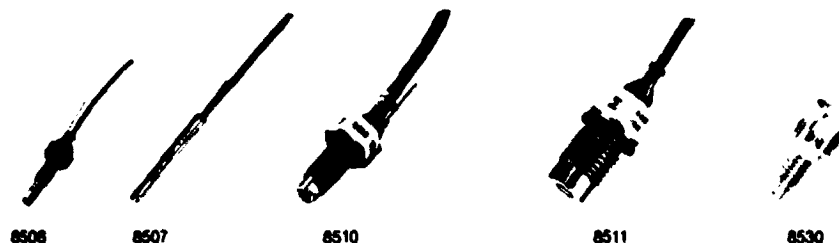


Figure 6.1-1 Stratham Model AL722 TC Transducer



DIFFUSED SILICON DIAPHRAGM SERIES

MODEL NUMBER	8506-2, -5, -15, -50	8507-2, -5, -15, -50	8510-2, -5, -15, -50, -100, -200, -500, -1000, -2000	8511-5K, -10K, -20K, -50K	8530-15, -50
Range, psig FS	2 to 50	2 to 50	2 to 2 000	5 000 to 50 000	15 to 50 psia
Sensitivity, mV/psi	150 to 6	150 to 6	150 to 0.15	0.10 to 0.01	20 to 6
Resonance, Hz	45 000 to 180 000	45 000 to 180 000	45 000 to 900 000	> 500 000	120 000 to 240 000
Linearity, % FSO	1.0 to 0.25	1.0 to 0.25	1.0 to 0.25	0.3 to 0.6	0.25
Temperature, °C	-54 to +107	-54 to +107	-54 to +107	-54 to +107	-54 to +121
Differential Burst Pressure, psi	40 to 300	40 to 200	40 to 10 000	20 000 to 75 000	90 to 300
Vent Tube Burst Pressure, psi	200	50	300	—	—
Shock Limits, g	10 000	10 000	20 000	20 000	20 000
Face Diameter, inches (mm)	09 (2.31)	09 (2.34)	15 (3.84)	32 (8.1)	15 (3.86)
Mounting Thread	6-32	—	10-32	4-24	10-32
Weight, grams	3	1	10	11	10

Figure 6.1-2 Endevco 85XX Series Differential Pressure Transducers

6.2.2 Data Recording Frequency

The frequency range of interest for the inertia data is from DC to 40 Hertz. Using the Boeing criteria of ten data samples per cycle, to describe the amplitude of a waveform, gives a data sample rate of 400 samples per second. This sample rate would provide the capability to compute frequency response data to 200 Hertz, if necessary.

6.2.3 Powerplant Primary Transducers

Most flight test experience with accelerometers designed for DC to low frequency response in the past ten years has been with servo-type accelerometers in temperature environments not exceeding 240°F. A highly accurate servo accelerometer, the Sunstrand Q-Flex Model QA-1200 (Figure 6.2-1), is available in ranges to +60 g's for operation in environments up to 240°F. It was decided that this instrument would be the primary sensor if a low temperature location could be found for installation.

Pratt & Whitney Aircraft engine case temperature data (Figure 6.2-2) was then reviewed to determine instrumentation locations that were below 160°F. To be conservative, the worst case of 120°F take-off at sea level with eighth-stage bleed was selected, during which the only region cooler than 240°F is forward of Nacelle Station 110, as shown in Figure 6.2-2. To solve the equations of motion for all c.g. acceleration components, at least six accelerometers would be required in this region (see Locations 1 through 6, Figure 5.3-1).

Q-FLEX QA-1200



SPECIFICATIONS

RANGE _____ TO ± 60 g MAXIMUM

LINEARITY _____ .03% OF READING

HYSTERESIS _____ < 0.001% OF FULL SCALE

TEMPERATURE RANGE _____ -67 TO $+239^{\circ}\text{F}$

ZERO SHIFT WITH TEMPERATURE _____ ± 90 mg/ $^{\circ}\text{C}$ MAXIMUM

SENSITIVITY SHIFT WITH TEMPERATURE _____ $\pm 0.018\%$ / $^{\circ}\text{C}$ MAXIMUM

Figure 6.2-1 Q-Flex Model QA-1200 Accelerometer

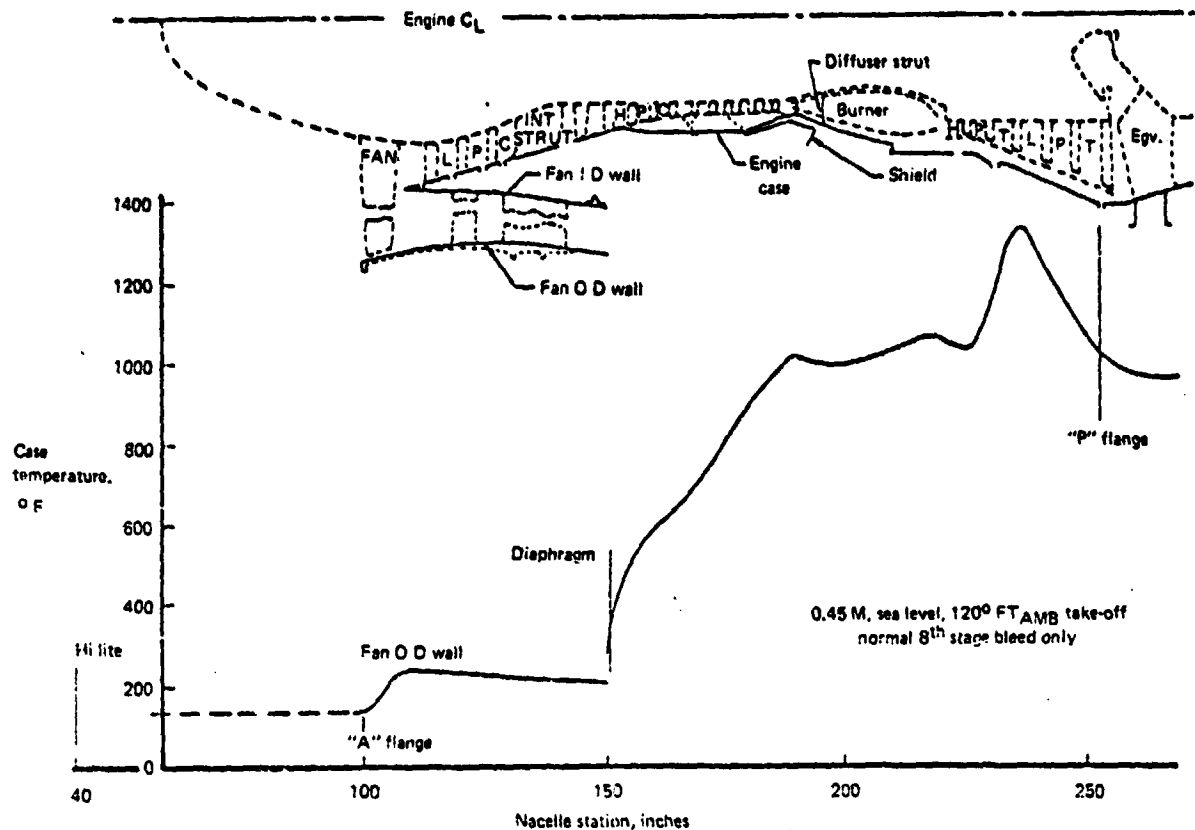
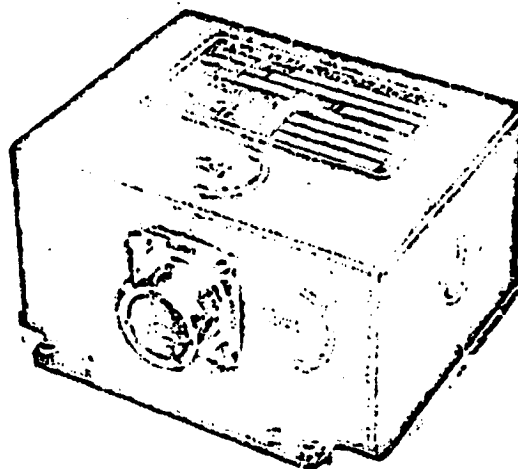


Figure 6.2-2 JT9D Engine Case Temperature Profile

Primary instrumentation includes a vertical and lateral accelerometer on the hi-lite at NS 40 and two vertical, one lateral, and one longitudinal accelerometer on the "A" flange at NS 100. All of these accelerometers will be +60 g models to preclude loss of data due to high g levels at frequencies out of the range of interest. Additionally, these unwanted frequencies (above 40 Hertz) will be removed from the transducer output before digitization through the use of four-pole Butterworth low-pass filters. To measure engine angular rates in pitch and yaw, a Northrup three-axis DC gyro (Figure 6.2-3) will be installed at the 3 o'clock position (looking aft) at NS 100. This gyro has been used extensively on flight test programs in the past seven to eight years and is highly reliable.

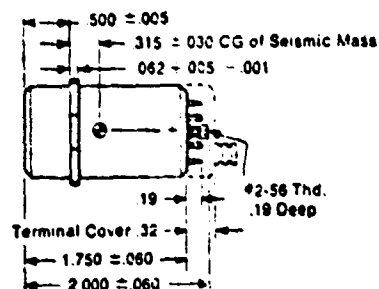
Additional powerplant instrumentation includes vertical accelerometers at the wing/strut intersection. These installations will employ the Kistler, Model 303TF20 (Figure 6.2-4), a low temperature servo accelerometer already existing and proven in flight test.



Specifications

Range	Pitch	± 15 deg/sec
	Roll	± 60 deg/sec
	Yaw	± 10 deg/sec
Linearity		$\pm 0.5\%$ full scale
Hysteresis		$\pm 0.2\%$ full scale
Threshold and resolution		± 0.01 deg/sec
Damping ratio		0.7 ± 0.07 critical
Frequency response		Flat to 0.5% full scale from 0-15 hz
Phase shift		Output lagging no greater than 18° from 0-5 hz
Acceleration sensitivity	Linear	< 0.05 deg/sec/g
	Angular	< 0.04 deg/sec/radian/sec ²
Non-repeatability		$< 0.04\%$ full scale
Thermal zero shift		$\pm 0.01\%$ full scale/ $^\circ$ F
Thermal sensitivity shift		$\pm 0.03\%$ full scale/ $^\circ$ F
Output voltage		± 2.5 V full scale
Output impedance		< 5000 ohms
Output ripple		< 40 MV p-p
Overrange capability		To ± 500 deg/sec in any axis
Operating temperature		20 to 135° F

Figure 6.2-3 Northrup 3-Axis Angular Rate Gyro



303T/TF PIN CONFIGURATION

- PIN 1. +28 VDC
- 2. POWER GROUND
- 3. LOW IMPEDANCE SIGNAL
- 4. SIGNAL GROUND
- 5. GAIN
- 6. SIGNAL
- 7. +TEST
- 8. -TEST

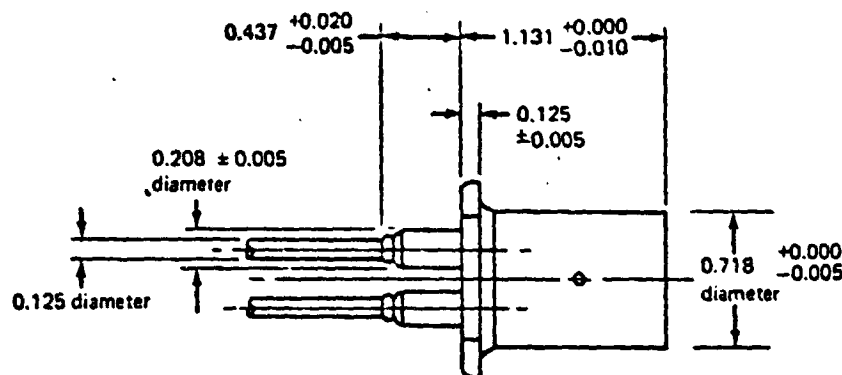
Specifications

Range (full scale)	±40g
Voltage sensitivity (adjustable)	0.1 V/g
Current sensitivity (nominal)	0.24 ma/g
Output voltage	to ±5.0 V
Noise: 1 MHz to 8 MHz (less than)	5 mV, rms
Below 1 MHz (less than)	1 mV, rms
DC to 1 Hz (resolution)	5 micro-g
Supply voltage and current	±28 VDC ±10%; 40 ma, max
Electrical isolation at 50 VDC, pins to case	50 megohms
input to output at 50 VDC	50 megohms
Linearity (to 50 volts any range)	±0.05% full scale
Hysteresis and repeatability	0.0005 g
Output at 0 g (max)	±500 mg (303TF)
Zero shift with line voltage (max)	0.005 g/V
Sensitivity shift with line voltage (max)	0.05%/V
Temperature range	-65° F to +185° F
Zero shift with temperature variation	0.150 g/100° F
Sensitivity shift with temperature variation	0.01%/° F
Transverse acceleration -DC to 5 HZ	±100 g
-5 HZ to 2000 HZ	40 g peak
Cross coupling coefficient (pendulosity error)	none
Case alignment (to true sensitivity axis)	0.002 g/g
Acceleration limit (non-operating sensitive axis)	200 g
Shock limit (5 msec pulse)	200 g
Weight (with terminal cover)	3.4 oz.

Figure 6.2-4 Kistler Low Temperature Accelerometer

6.2.4 Powerplant Redundant Instrumentation

To support the primary instrumentation, a total of eight additional accelerometers will be used. Six of these are located in the higher temperature regions of the engine (Figure 6.2-2) at two locations -- the diaphragm at NS 152 and the "P" flange at the aft end of the low-pressure turbine, NS 254. These locations will employ a yet-to-be-proven accelerometer, the Kaman 1901 (Figure 6.2-5). This transducer provides very high accuracy with low hysteresis in environments up to 1050°F. The transducer will, of course, be subjected to a thorough check-out at the BCAC Flight Test Instrumentation Technology Laboratory prior to inclusion on any test flight. The remaining accelerometers are located at the front mount, NS 126.43, and will employ the Kistler, Model 303TF20 (Figure 6.2.4). A thermocouple (at Location 13, Figure 5.3-1) is also needed to provide temperature corrections for the high temperature accelerometers. A complete tabulation of all powerplant transducers and their specifications is included in Table 6.2-I.



Specifications

Range	±1.0 g to ±100 g
Input	28V DC, 110 VAC, 60~
Output	+5V DC
Dynamic resolution	0.1% full scale
Operating temperature	-100° F to 1050° F continuous
Non-linearity	< ±1% full scale
Sensitivity shift w/temp	< 0.01% full scale/ °F
Zero shift w/temp	< 0.01% full scale/ °F
Frequency response range	Dependent on range i.e., for ±5g the response is DC to 150 hz (down 3dB @ 150 hz)
Overload capability	300% full scale
Humidity effect	None
Operating pressure	500 PSI

Figure 6.2-5 Kaman 1901 High Temperature Accelerometer

6.2.5 Airplane Basic Instrumentation

To obtain airplane air speed, altitude, and Mach number, the copilot's total and static pressures will be recorded along with airplane total temperature. The six components of acceleration at the airplane C.G. will also be recorded. The airplane basic measured parameters are listed in Table 6.2-I.

TABLE 6.2-I
AIRPLANE BASIC INSTRUMENTATION

<u>Description</u>	<u>Units</u>	<u>Min</u>	<u>Max</u>	<u>Accuracy</u>
Co-pilot's total pressure	In. HG	.1	12	.003
Co-pilot's static pressure	In. HG	3	31	.006
Total air temperature	Deg. C	-60	60	0.6
C.G. lateral acceleration	G	-2	2	0.04
C.G. longitudinal acceleration	G	-1	1	0.02
C.G. normal acceleration	G	-1	3	0.04
C.G. pitch acceleration	Deg/sec ²	-35	35	1.4
C.G. roll acceleration	Deg/sec ²	-40	40	1.6
C.G. yaw acceleration	Deg/sec ²	-15	15	0.6
Irig time	Hr:min:sec			0.001 sec

6.3 CLEARANCE MEASUREMENT INSTRUMENTATION

Laser proximity probes will be used to measure the changes in running clearances in the fan and high-pressure turbine due to flight loads. Four probes will be mounted around the fan containment case and around the first-stage high-pressure turbine case in both the outboard Position No. 1 and inboard Position No. 3 engines. The position of each probe is shown in Figures 5.4-2 and 5.4-4 (of Section 5.4).

Laser proximity probes offer a highly accurate means of measuring blade tip clearances during the flight test. The laser probes supply clearance measurement changes at accuracies up to ± 0.003 inch.

These probes have an additional advantage because they actually view the blades. This function provides the ability of visual detection of rubbing anywhere in the stage because the rub is accompanied by local heating and appears to the proximity probe as a glow. Whirl is also detected because the blades are viewed directly. If off-axis rotation of the stage occurs, an indication of two different clearances will be indicated by the proximity probe.

The proximity probes which are to be used for these tests utilize a laser source and are commonly called laser blade tip clearance probes. Operation of this type of probe is based on an optical triangulation system. Illustrations of the two basic configurations, single-case and multiple-case probes, are shown in Figures 5.4-1 and 5.4-3.

In both configurations, light from a helium-neon laser is focused onto a single 0.001-inch diameter fiber optic. The light is carried along this fiber and emitted from the end of the fiber in the probe, acting as a point source of light. This point source of light is focused on the blades by the input lens. If the blades are at Position A, shown on the figures, the reflected spot of light will be focused by the output lens onto a coherent fiber optic at point A'; similarly, if the blades are at Position B, the reflected spot will be focused onto the coherent output fiber at Point B'. It should be noted that the imaged spot positions at A' and B' do not depend on the reflectivity of the blades (specular or diffuse, absorptive or reflective) or on the angle of tilt of the blade with respect to the probe. It is a function of only the distance of the blade from the probe. The coherent fiber optic bundle transfers the imaged spot positions from the probe end to the other end where the spot position is viewed through a lens system by a video camera. The video camera image is displayed on a TV monitor, so that the position of the light spot on the raster of the TV is a measure of the position of the blade clearance. An illuminated reticle is attached to the output fiber optic and serves as a calibration reference for the system. The system is calibrated so that any given position along the scale corresponds to a given blade clearance between the blades and the outer air-seal surface.

The TV image is video-tape recorded for permanent record and further analysis of transients. Time and date are superimposed on the video signal for reference. The fact that the clearance data are viewed by a video system limits the data acquisition rate to 30 inputs per second.

The video data is also processed by a laser proximity probe electronic readout. The readout unit functions by counting TV raster lines to find the line number which represents the center of the spot of light. The unit does this by starting at the top of the TV raster and counting each line until a line with sufficient intensity (representing the top of the spot) is found. The number of this line is added to a second number representing the last line with sufficient intensity. The resulting sum is twice the line number at the center of the data spot. This number is scaled to provide the calibrated millivolt output proportional to the engine clearance. This clearance signal is then fed into the RA001 airplane onboard data acquisition system. Depending upon the clearance range spanned for specific stages, average accuracy is ± 2 to ± 3 mils (two standard deviations, 95 percent confidence).

The probe in Figure 5.4-1 is intended for making blade tip clearance measurements through single case structures. It is low in profile and, therefore, can fit between the fan cowl and the fan case. The current probes have high-temperature epoxied fiber optics which limit the operating temperature of the fiber optics portion of the probe to 600°F.

Turbine probes, as in Figure 5.4-3, have to operate in a significantly more hostile environment, requiring nitrogen cooling and high pressure seals. Due to the high temperature environment, the blade tips emit radiation which can be picked up by the video system. This "background radiation" is eliminated by using an optical band-pass interference filter which blocks out all light except for the reflected laser beam light. A folded optical system utilizing a prism at the base of the probe provides a system that is analogous to the compressor type probe built into a cylindrical form. The probe is cylindrical so that it can be effectively sealed at the outer case with a piston-ring type seal. The probe is bayonetted into the rub strip so that the probe moves with the rub strip, resulting in measurements relative to the rub strip.

The probe is purged with nitrogen to prevent the accumulation of contaminants on the probe optics. The temperature vulnerable portion of the probe is the fiber optics which is the part of the probe farthest from the engine flow path. These probes have been operated in the JT9D first- and second-stage turbines with no adverse temperature effect. These probes are currently capable of making clearance-change measurements from the face of the probe out to 0.20 inch from the face of the probe. A change of optics would provide other ranges.

To make these probes capable of functioning in a flight engine, the proximity probe system must be set up as shown in Figure 5.4-7. This arrangement will require operating the laser light source in the airplane cabin and focusing the laser beam into a low loss fiber optic. The low loss fiber optic passes through the wing to an environmental camera housing mounted in the pylon. Here the fiber is coupled to another section of low loss fiber routed through a conduit to the laser probe. The output fiber optic is brought back out through the same conduit to the readout video camera in the pylon. The output from the camera is brought through a video cable back to the airplane cabin where it is recorded on video tape, viewed on the video monitor, and read on the electronic readout. A supply of bottled high pressure purge nitrogen is also mounted in the cabin and piped through the wing and pylon to the laser probe.

A summary of the equipment, cooling, cable sizes, and power requirements is set forth in Section 5.4, Tables 5.4-I, 5.4-II, and 5.4-III.

6.4 ENGINE PERFORMANCE AND CASE TEMPERATURE INSTRUMENTATION

Various program options in the flight test program could involve performance testing of one or more of the following types: 1) bare engine tests, 2) installed ground tests, and 3) flight monitoring on one or two instrumented engines. The performance testing and types of data envisioned to be recorded are summarized in Table 6.4-I.

TABLE 6.4-I
PERFORMANCE TESTS AND TYPES OF DATA

	<u>Engine Perform- ance</u>	<u>Running Clear- ances</u>	<u>Thermal Loads</u>	<u>Thrust</u>
Engine Calibration at Middletown	X	X		X
Initial Installed Ground Run	X	X	X	
Simulated Flight Acceptance Test	X	X	X	
Installed Ground Run	X	X	X	
Multiple Take-Off and Landing Tests	X	X	X	
Installed Ground Run	X	X	X	
Flight Maneuver Tests (Wind-Up Turns)	X	X	X	
Installed Ground Run	X	X	X	
Flight Gust Loads Tests	X	X	X	
Installed Ground Run	X	X	X	
Engine Calibration at Middletown	X	X		X

Engine installed instrumentation associated with the flight loads program will be used to measure essentially two classes of data; (a) engine performance, (b) engine thermal loads. The primary objective of the program is the determination of changes in engine performance, more specifically, performance deterioration, which results from initial aircraft flight and various flight maneuvers, and to relate this performance deterioration to changes in the physical configuration of the engine such as seal and blade tip clearance. Engine surface temperature and thermal load data are acquired to determine the extent to which various seal clearances and blade tip clearances are influenced by both spacewise and timewise surface temperature gradients. Both the performance data and the thermal load data will be correlated with proximity probe data simultaneously acquired.

It will also be a requirement to compare and correlate data acquired during this flight loads test program with similar data acquired earlier in the NASA JT9D Diagnostic Programs.

Success in correlating and comparing data acquired from different test programs is dependent upon similarities in the physical characteristics of the various data systems involved and similarities in the methods of acquiring the data. The technical feasibility of the successful completion of this program thus rests with our ability to employ data systems as nearly alike as possible and to acquire data in as nearly a similar fashion as possible throughout the program.

6.4.1 Description of the P&WA Data Systems

Initial performance calibration testing of the engines will take place in a production test cell at Pratt & Whitney Aircraft's Middletown, Connecticut facility. The flight test program will be followed by the return of the engines to the Middletown facility for postflight calibration testing. Engine performance will be acquired by test systems in the Middletown facility, the APTDAC system and the HAPTS system, each of which are described below.

6.4.1.1 The APTDAC Data System

The Automatic Production Test Data Acquisition and Control System (APTDAC) replaces all visual instrument readout devices with computerized display and control modules. Measurements acquired by the system are converted to engineering units, the converted data are used to calculate the required performance parameters, and the results are checked to determine out-of-limits conditions.

Computer System

The basic computer is a 16-bit digital computer with a 1.1 microsecond cycle time. The computer also employs a disk storage drive for additional storage capacity. The test stand has peripheral devices (line printer, cathode ray tube (CRT) display) for interfacing with the system. The computer also has a teletype writer, card reader, and magnetic tape transports for programmer communications with the computer, rapid storage of bulk data, and as a back up for operating system programs.

The ADTDAC system acquires measurements from the following subsystems and provides the indicated number of channels:

o temperatures	(35)
o pressures	(31)
o thrust	(4)
o position measurements	(3)
o fuel flow	(2)
o mass oil flow*	(1)
o speeds	(2)
o vibration*	(4)
o barometric pressure	(1)
o fuel density	(1)
o oil level*	(1)
Total	85

*not required for performance measurements

Electrical signals from these subsystems are fed into the computer which converts them into the appropriate engineering units and outputs the results to the CRT display or line printer.

Temperatures

The 35 temperature channels are routed to two Pace 150°F thermocouple reference ovens. The output of the ovens are routed through a 36-pin connector to the input of the data system. All wiring and connector pins between the thermocouples and the ovens are chromel-alumel. The output wiring from the reference ovens is copper. The millivolt output from the reference oven is referenced such that zero millivolts corresponds to 150°F. The data reduction portion of the system converts the millivolts to temperature from tables published by the National Bureau of Standards (NBS) via polynomial curve fits. Five

millivolt ranges and the corresponding curve fits are utilized with a total curve range of -190°F to +2334°F.

The 150°F reference ovens are calibrated using a mercury glass thermometer traceable to the National Bureau of Standards (NBS). The thermometer is inserted into a calibration port on the oven and readings taken after a 15 minute stabilization period. The oven can be adjusted for deviations of $\pm 0.5^\circ\text{F}$ from 150°F.

Pressures

All performance pressure measurements on the APTDAC systems are acquired from linear-variable differential transducers (LVDT's). The transducers are located in a controlled environment together with the associated calibration instruments. The transducers' ranges are:

<u>Range (psi)</u>	<u>No. of Transducers</u>
1	10
3	8
10	3
25	2
50	2
100	3
400	3

$$\text{Total} = \overline{31} + \text{TI} = 32$$

In addition, the barometric pressure in the transducer environment is monitored with a 16-psia precision gage.

The computer system receives the millivolt outputs of the transducers and converts these data to engineering units based upon the preinput slope and intercept (zero value) primary calibrations. The system also converts the output of the TI barometric gage to pressure units via the preinput calibration data. All pressures are output by the computer in gauge units.

Thrust

Thrust is measured with two 50,000 pound, double bridge, strain gauge load cells which are mounted in parallel on each side of the thrust bed. A calibration load cell is mounted on the thrust bed centerline and is hydraulically loaded. The working load cells are thus calibrated in place in the thrust stand.

Fuel Flow

The test stand utilizes two turbine-type flowmeters mounted in series in the fuel line. The fuel flow meters are calibrated in the Production Metrology Laboratory utilizing a weight/time calibrator.

Rotor Speeds

N1 speed is sensed by a proximity type pickup, and N2 speed is sensed by a tachometer mounted on the engine. Frequency-to-voltage converters and event counters are employed in the speed system. The counter frequencies are calibrated to within ± 1 Hz of the theoretical frequency.

Barometric Pressure

The reference pressure of the transducer environment is monitored by a precision gage. The pressures are utilized by the computer to convert transducer measurements to absolute units on the data reduction printout. The gage is calibrated versus a traceable dead weight tester in the Middletown Metrology Laboratory.

Fuel Density

Fuel density is measured with a density measuring system. The density measurement source is checked and calibrated in two ways:

- o Fuel samples are acquired three times per week and the density determined by a hydrometer, and
- o A fluid with a known density is input to the stand pipe and the density recorded (six month intervals).

Position Measurements

Three rotary position potentiometers measure Power Lever Angle (PLA), Condition Lever Angle (CDLA) (fuel selector and enrichment), and Stator Vane Angle (β). The potentiometers receive excitation from an adjustable power supply (approximately 4.5 volts) which is monitored by a digital voltmeter. The output of each potentiometer is

converted to degrees via experimentally determined slopes for the PLA, CDLA, and stator vane potentiometers. The position potentiometers are calibrated using a traceable digital voltmeter.

6.4.1.2 The HAPTS Data System

A portable, High Accuracy Pressure and Temperature Data Acquisition Systems (HAPTS) will also be used to acquire data in the Middletown Test Facility. The HAPTS has the capacity to record up to 609 bipolar millivolt inputs and 192 pressure inputs on four 48-port scanivalved transducers. Data are recorded at a rate of 20 channels per second. The data are scanned, digitized by an integrating digital volt-meter, and recorded on magnetic tape. If required, the raw millivolt data can also be printed simultaneously as a grocery tape output.

Temperatures

All chromel-alumel thermocouple inputs will be routed through Uniform Temperature Reference (UTR) units. Each unit has 30 input channels, which includes an ice point reference (32°F) supplied by an ice point cell.

Pressures

All pressure measurements will be recorded on 48-port scanivalved transducers. The pressure transducer ranges follow:

3	25 psig transducers
3	50 psig transducers
4	400 psig transducers
3	100 psig transducers
1	20 psia transducers

The pressure transducers and the ranges required will be selected based upon the final design for the data system measurement requirements.

Data Reduction for HAPTS

All data recorded on the HAPTS magnetic tape unit will be processed off-line (after the engine tests) on the Sigma 8 computer system in the Pratt & Whitney Aircraft Engineering Building in East Hartford. Processed data will be generated in engineering units. In addition, computer data cards and/or a magnetic tape can be produced for additional downstream processing or for generating computer plots.

6.4.2 Measurements Made on the P&WA Data Systems

The APTDAC System

Thrust
Fuel Flow
Fuel Density
N1
N2
PA (ambient) 1 port
Pt2 (free stream total) 1 port
Pt2.5 (manifolded) 1 port
Pt3 1 port or sensor
Ps3 1 port or sensor
Ps4 1 port or sensor
Pt7 (manifolded) 1 port
Tt2 single probe
Tt3 single probe
Tt4.5 single probe
Tt6 Average and
Tt7 individual readings.
T fuel single probe
PLA
EVC (bell-crank angle)
5th IGV position
Bleed Valve Position

The HAPTS System

PA (ambient) 1 port
Pt1 (free stream total) 1 port
Pt 2.5 (manifolded) 1 port
Pt3 1 port or sensor
Ps3 1 port or sensor
Ps4 1 port or sensor
Pt7 (manifolded) 1 port
Tt1 single probe
Tt3 single probe
Tt4.5 single probe
Tt6 averaged
Tt7 averaged
T fuel single probe
Engine surface temperatures 17 (No. 3 engine)
Engine air temperatures 3 (No. 3 engine)

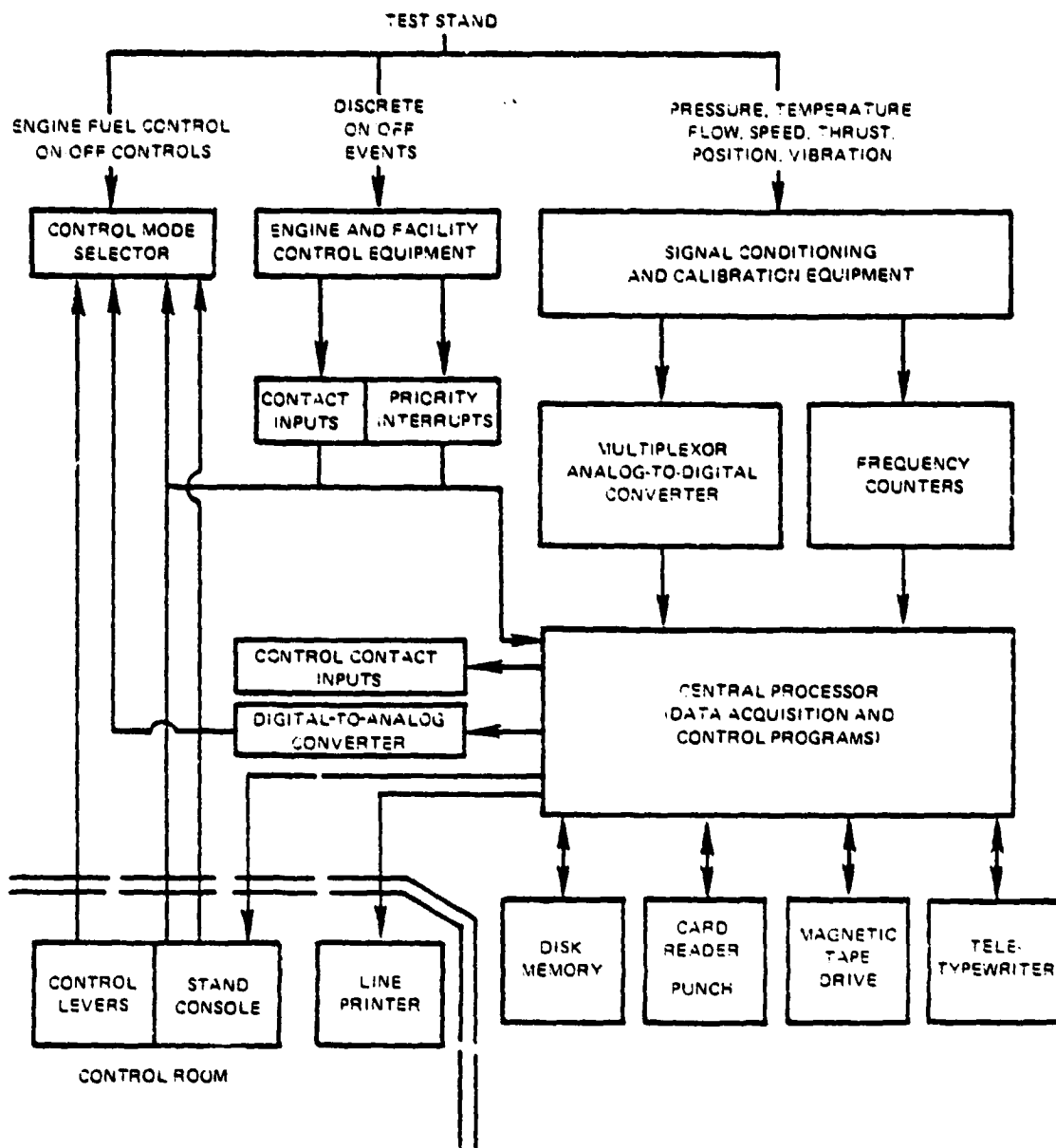


Figure 6.4-1 APTDAC System Functional Block Diagram - The System is designed to perform real time data acquisition and display.

6.4.3 Methods of Data Acquisition on the P&WA Data Acquisition Systems

6.4.3.1 The APTDAC System

The APTDAC system is designed to perform real-time data acquisition and display. The data system samples all direct current (DC) inputs (thrust, pressures, and temperatures) at a scanning rate of 200 channels/second via a low-speed multiplexor which has the capability for on-line checks of the four millivolt ranges (+10, +20, +50, and 500 mv) compared to standard millivolt inputs from the data system. The channels are scanned four times and averaged. The frequency channels (fuel flow and speeds) are totalized by eight counters for a 3- to 4-second gate time and averaged. The total acquisition time for one data scan is approximately 5 seconds, and the total computer conversion and data reduction time is approximately 20 seconds. Figure 6.4-1 is a functional block diagram of the APTDAC system.

6.4.3.1 The HAPTS System

Data are acquired at the rate of 20 channels/sec. It will be the practice to take several complete data scans during the latter portion of steady state runs. Averages of the scans will then be calculated.

6.4.4 Pratt & Whitney Aircraft Data System Accuracies

APTDAC DATA SYSTEM ACCURACY

<u>Parameter</u>	<u>Accuracy</u>
P amb	+0.01 psi
Pt2.5	±0.05 psi
Pt3	±0.06 psi
Ps3	±0.06 psi
Ps4	±1.2 psi
Pt7	±0.02 psi
Tt amb	±1.0°F
Tt4.5	±2.0°F
Tt6	±3.0°F
Tt3	±2.0°F
Tt7	±3.0°F
Tt fuel	±1.4°F
Wf (fuel flow)	±0.45% of rdg
Fn (thrust)	±0.5% ++
N1	+0.1% of rdg
N2	±0.1% of rdg
	++ = 85 lbf

HAPTS DATA SYSTEM ACCURACY

<u>Parameter</u>	<u>Accuracy</u>
Pt1	+0.025 psi
Pt2.5	± 0.025 psi
Pt3.0	± 0.050 psi
Pt4.0	± 0.40 psi
Pt6.0	± 0.10 psi
Tt4	+0.40°F
Tt2.6	$\pm 0.250^\circ\text{F}$
Tt3	$\pm 0.250^\circ\text{F}$
Barometer (HSD)	± 0.025 % of full range
Case temperatures	$\pm 0.250^\circ\text{F}$
Flange temperatures	$\pm 0.250^\circ\text{F}$

6.4.5 General Feasibility and Adequacy of the P&WA Data Acquisition System

6.4.5.1 Accuracy

The above quoted accuracies for the APTDAC data system are estimates of the total uncertainty (bias + precision). The accuracies of the portable HAPTS are estimated precision values. Both accuracy estimates are based on engine tests conducted three months apart. These accuracies are adequate to meet the requirements of the program.

6.4.5.2 Data Acquisition Techniques

In order to eliminate, or to minimize as much as possible, engine performance variations that may deviate from a supposedly steady-state condition, it is planned to acquire performance data for some extended period of time during the last 1-1/2 minutes of each stabilized 7-minute steady state calibration point. All performance data will then be averaged over the total period. Acquisition of data by both the APTDAC and HAPTS systems simultaneously will further maximize the probability that data truly representative of steady state conditions are being acquired.

6.4.6 The Flight Program

Performance data acquisition during installed ground and flight tests will be achieved with the airplane-installed data acquisition system which is a permanent part of the Boeing RA001 experimental 747 airplane.

The program will involve several flights of the aircraft which will be preceded by and followed by ground runs. Additional ground runs will be made when determined to be appropriate.

It will be necessary to compare performance, temperature, and proximity probe measurements acquired during each ground run with measurements acquired during the preceeding run in order to determine the influence of the flight conditions imposed during the intervening flight between the ground runs. In order to maximize the information so gained, repeatability of measurements and precision are of far more importance than absolute measurement accuracy. Thus, a nominal degree of bias in the aircraft measuring system can be tolerated. In order to compare data acquired by the aircraft data system with data acquired by the Pratt & Whitney Aircraft HAPTS and APTDAC systems, any bias in either or both systems must be accounted for. Precision and bias of both systems are, therefore, of importance in establishing the feasibility of the proposed program.

6.4.7 Description of the Boeing RA001 Airplane Flight Test Data Acquisition System

The capabilities of the RA001 data acquisition system are set forth in Section 5.1.1.

6.4.8 Engine Performance Measurements Made on the Boeing RA001 Aircraft

The following engine performance measurement will be recorded on the Boeing RA001 airplane during the proposed flight test program for each engine whose performance is being monitored.

- N2
- N1
- Tt7
- Tt4.5
- Tt3
- Tt6
- Pt7
- Pt3
- Pt136
- Pt2.5
- Ps3
- Ps4
- 5th IGV Position
- Power Lever Angle
- Bleed Valve Position
- Pylon Valve Position
- Air Control Valve, HPC
- Totalizer, Qty
- Fuel Temp
- Elapsed Fuel

Thrust will not be measured in the aircraft. The measured parameters will be used as input to the computer simulation of the JT9D with thrust determined as an output (calculated) value.

6.4.9 Thermal Loads Temperature Instrumentation in the Aircraft

In order to assess the effects of thermal gradients on the changes in engine clearances, it is desirable to install surface thermocouples on one or both of the two test engines to record the thermal gradients encountered during flight.

The Boeing Commercial Airplane Company's 747 test airplane, RA001, is currently provided with 72 thermocouple wires at the inboard No. 3 engine location and 20 thermocouple wires at the outboard No. 1 engine location. It would be advantageous to increase this number to at least that of the X-Ray Facility Load Test program (400 thermocouples) in order to obtain a direct correspondence with the data from that program. However, the expense of related engine case modifications and airframe rewiring to increase the number of lead wires is not considered to be cost effective at this time.

Thermocouples were not planned within the engine's internal cavities because of the difficulty in routing wires out of the engine without the design of special case penetrations.

The study effort was directed toward the definition of thermocouple locations that would provide the optimum thermal load information. Three combinations of thermocouple arrangement were defined as follows:

1. 72 thermocouples on the No. 3 engine; the locations are shown on Figure 6.4-2.
20 thermocouples on the No. 1 engine; the locations are shown on Figure 6.4-3.
2. 72 thermocouples on the No. 3 engine, assuming that only engine No. 3 was instrumented; the locations are shown on Figure 6.4-4
3. 20 thermocouples on the No. 3 engine, assuming that only engine No. 3 was instrumented; the locations are shown on Figure 6.4-3.

The first thermocouple combination would be utilized if both engines were prepared for test by Pratt & Whitney Aircraft. The second thermocouple arrangement was established if only the inboard engine was prepared as an analytical engine. The third thermocouple arrangement was established if only the high-pressure turbine module was prepared and utilized in exchanging the existing module in a spare engine.

KEY:

● THERMOCOUPLE METAL TEMPERATURE MEASUREMENT LOCATION
CASE OR FLANGE LOCATIONS

▲ THERMOCOUPLE (T/C) AIR TEMPERATURE MEASUREMENT LOCATION.
ALL AIR T/C'S MUST BE RADIATION AND HIGH VELOCITY AIR SHIELDED

ALL AIR T/C'S SHOULD BE PLACED MIDWAY BETWEEN THE CASE O.D. AND THE NACELLE I.D.

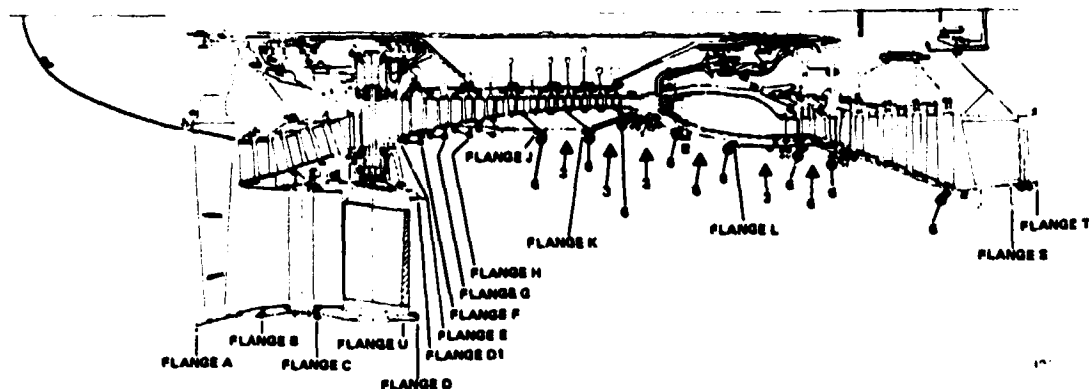


Figure 6.4-2 Configuration 1 with 72 Thermocouples on the Inboard (No. 3) Engine.

KEY:

● THERMOCOUPLE METAL TEMPERATURE MEASUREMENT LOCATION
CASE OR FLANGE LOCATIONS

▲ THERMOCOUPLE (T/C) AIR TEMPERATURE MEASUREMENT LOCATION.
ALL AIR T/C'S MUST BE RADIATION AND HIGH VELOCITY AIR SHIELDED

ALL AIR T/C'S SHOULD BE PLACED MIDWAY BETWEEN THE CASE O.D. AND THE NACELLE I.D.

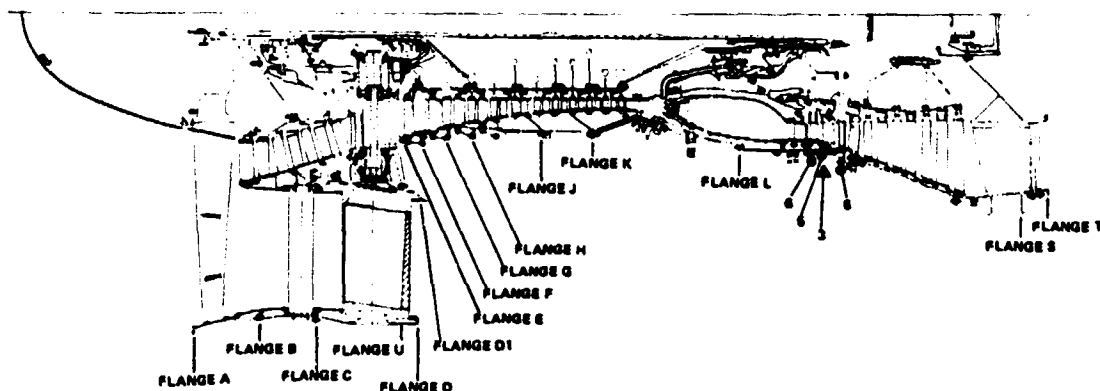


Figure 6.4-3 Configurations No. 1 and No. 3 with 20 Thermocouples on the Outboard (No. 1) Engine.

KEY:

● THERMOCOUPLE METAL TEMPERATURE MEASUREMENT LOCATION
CASE OR FLANGE LOCATIONS

▲ THERMOCOUPLE (T/C) AIR TEMPERATURE MEASUREMENT LOCATION
ALL AIR T/C'S MUST BE RADIATION AND HIGH VELOCITY AIR SHIELDED

ALL AIR T/C'S SHOULD BE PLACED MIDWAY BETWEEN THE CASE O.D. AND THE NACELLE I.D.

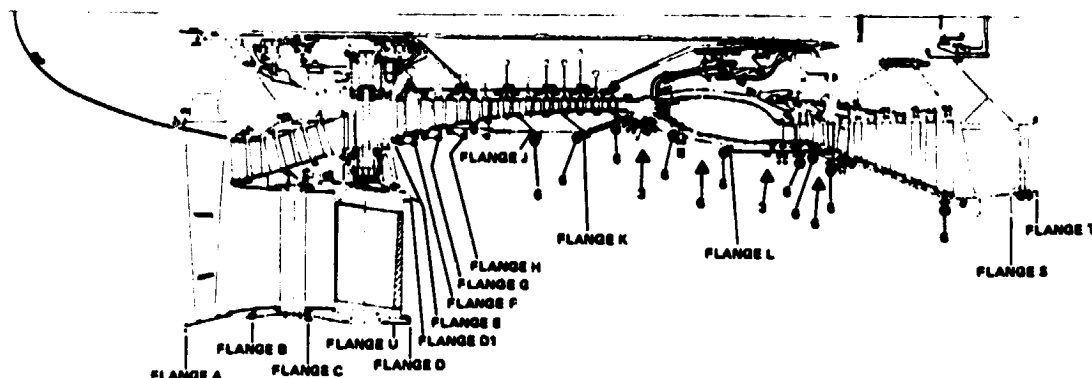


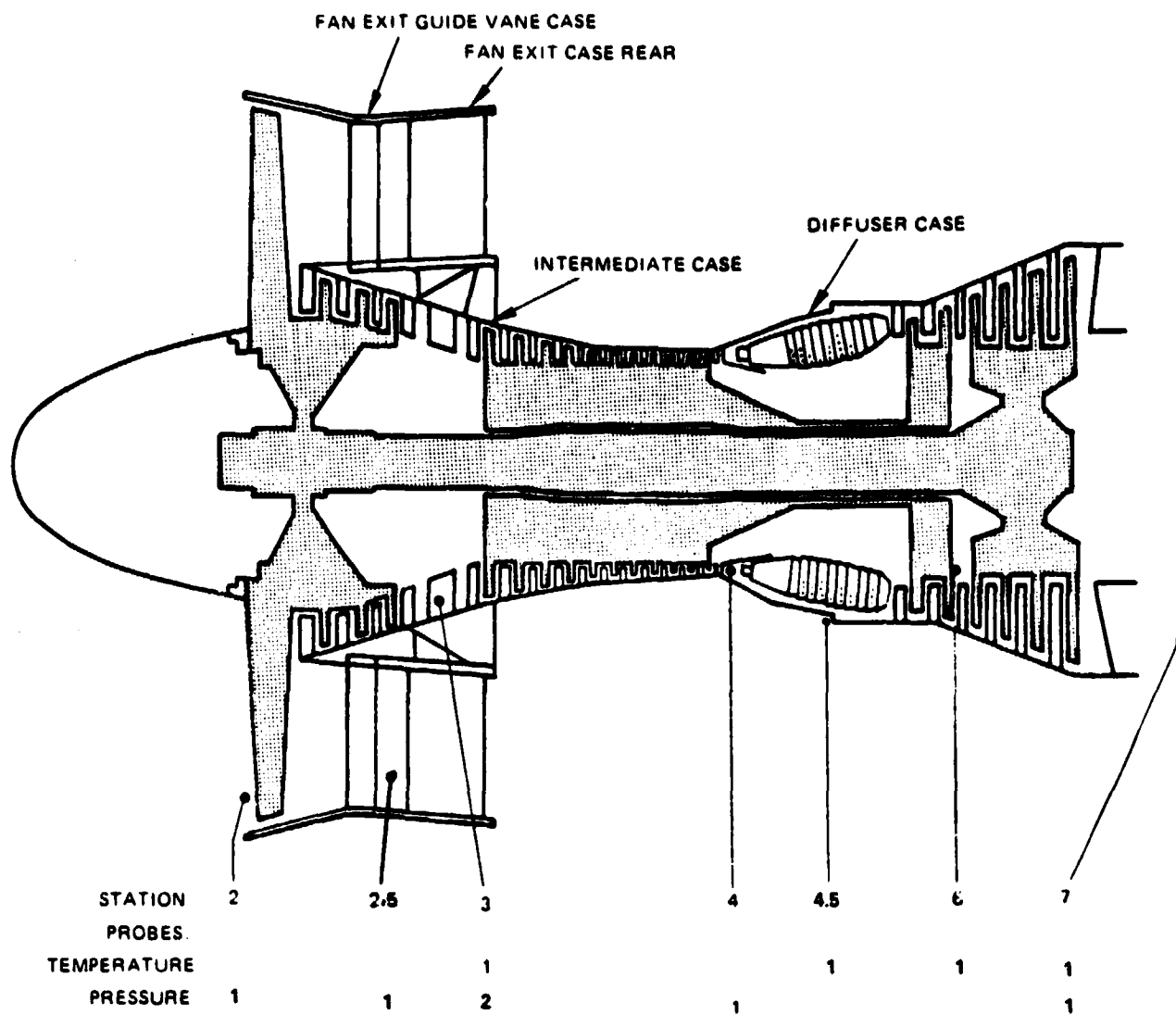
Figure 6.4-4 Configuration No 2 with 72 Thermocouples on the Inboard Engine if the Outboard Engine is Not Instrumented.

6.4.10 Method of Data Acquisition in the Aircraft

Several scans of data will be taken during each steady state ground run point and each stabilized aircraft flight point of interest. Averaging of these scans will ensure that all instabilities are minimized and that small differences in performance are truly representative of actual changes caused by flight loads and clearance changes.

6.4.11 Performance Instrumentation on the Engine

Figure 6.4-5 shows the locations of the performance instrumentation stations on the No. 1 and No. 3 engines.



ADDITIONAL DATA READINGS - N_1 , N_2 , W_1 , VANE ANGLE, T_T , P_{AM}

Figure 6.4-5 Engine Performance Instrumentation Locations.

6.4.12 Aircraft Data Acquisition System Accuracy

Item Number	Description of Parameter	Range		Estimated Accuracy
		Min.	Max.	
1	Free Stream Total Pressure	0.3 to 1.8"Hg Gage	11"Hg Gage	0.009"Hg 0.027"Hg
2	Ambient Pressure (from trailing cone)	5 to 7"Hg Gage	31"HgA	0.015"Hg 0.0275"Hg
3	Free Stream Total Temperature	60°C		0.5°C
4	Low-Pressure Turbine Discharge Total Pressure	0 to 80"HgA		0.12% Full Scale
5	Fan Discharge Total Pressure Measured at Nacelle Station 132	0 to 80"HgA		0.12% Full Scale
6	Low-Pressure Turbine Discharge Total Temperature	100 to 800°C		6°C
7	Low-Pressure Rotor Speed	Idle to 4000 rpm		4 rpm
8	High-Pressure Rotor Speed	Idle to 8000 rpm		8 rpm
9	Fuel Flow Rate	0 to 25,000 pph		0.25% Full Scale
10	Fuel Temperature at Flowmeter	0 to 160°C		1 1/2°C
11	High-Pressure Compressor Discharge Static Pressure	4 to 800" HgA		0.16% Full Scale
12	Low-Pressure Compressor Discharge Static Pressure	4 to 200" HgA		0.14% Full Scale
13	Fuel Control Cross Shaft Angle	0 to 90 deg		2.0% Full Scale
14	EVC Bell-Crank Angle	-40 to +10 deg		1 deg Rotation
15	Low-Pressure Compressor Discharge Total Pressure	0-400" HgA		0.16% Full Scale
16	High-Pressure Turbine Discharge Total Temperature	100-1000°C		8°C

SECTION 7.0

PROGRAM OPTIONS

The objective of this study was to examine combinations of: 1) nacelle load instrumentation, 2) engine clearance and performance instrumentation, 3) flight test program approaches, and 4) flight test aircraft. Contract requirements were to develop several alternate recommendations meeting different total flight test program relative costs levels with varying levels of technical value.

7.1 USE OF NASA 747 AS FLIGHT TEST VEHICLE

As discussed in Section 5.5, a considerable effort would be required to bring the NASA airplane up to an equivalent capability of that currently existing on the Boeing RA001 airplane. The modifications, test, and refurbishment schedule would make the NASA airplane unavailable to the space shuttle program for a minimum time period of five to six months. In addition, the cost to do this work on the NASA airplane is estimated to approximately double the cost of the recommended program on the RA001 airplane.

NASA Johnson has indicated that the airplane could not be out-of-service to them for the required time. On this basis alone, it was judged to be unavailable to the flight loads test program. Due to the unavailability of the airplane and in consideration of the substantial added costs to the flight loads test program, it was concluded that the use of the NASA airplane should be excluded from any further considerations.

7.2 RA001 POTENTIAL PROGRAM CONFIGURATION MATRIX

A matrix of six different instrumentation configuration options were evaluated separately for both determining flight loads and the engine response to these loads. These separate options were developed in a manner to provide options, in descending order, from the highest technical value to the lowest value. The option with the lowest technical value that was considered was compatible with the existing wiring capability of the RA001 airplane. These options considered an inboard position engine (No. 3) and an outboard position engine (No. 1).

PRECEDING PAGE BLANK NOT FILMED

7.2.1 Flight Loads Instrumentation Options

7.2.1.1 Aerodynamic Loads

Due to the importance of the inboard position for aerodynamic loads, it was considered that the inboard position should always be instrumented the heaviest and the outboard position light for correlation of the aerodynamic loads with the inertia loads. The inboard distribution of pressure taps is shown on Figures 5.2-1 through 5.2-3 for the configurations studied. Figure 5.2-4 shows the distribution of the pressure tap locations for the outboard nacelle. The matrix of instrumentation configurations studied for the aerodynamic loads is shown on Table 7.2.1-I.

In the above study, the 396 pressure tap locations represent the desired level for 100 percent technical value on the inboard position, and the 126 pressure taps result from the current instrumentation wiring limitations on the airplane and is considered to provide a technical value in the order of 30 percent. The above combinations of pressure taps were selected to coincide with the selection of instrumentation covering the inertia loads so as to provide the optimum combinations in a descending order of technical value.

7.2.1.2 Inertia (g) and Gyro Loads

The previous feasibility study, NASA CR-135395, reflects the desired inboard and outboard instrumentation for inertia loads to provide 100 percent technical value. These locations are shown on Figure 5.3-1 and Tables 5.3-I and 5.3-II. Again, like the aerodynamic loads instrumentation, configuration options were selected in order to provide descending levels of technical value and are shown in Table 7.2.1-I.

For those configurations in Table 7.2.1-I that call for a total of only ten accelerometers and gyros, it was considered that these should be the primary instrumentation shown on Table 5.3-I plus two accelerometers at the wing/strut intersection, which is considered to be the minimum acceptable.

TABLE 7.2.1-1

AERODYNAMIC AND INERTIA LOAD INSTRUMENTATION OPTIONS

Option	Inboard (No. 3) Engine		Outboard (No. 1) Engine	
	Number of Pressure Taps	Number of Accelerometers and Gyros	Number of Pressure Taps	Number of Accelerometers and Gyros
1	396	18	45	18
2	396	0	0	18
3	396	0	45	10
4	396	0	0	10
5	252	0	0	10
6	126	0	0	10

7.2.2 Engine Preparation and Instrumentation

The objective of engine preparation and instrumentation efforts in the flight loads flight test program is to measure the effect of discrete flight load events on engine clearances and performance. A number of technical options were examined covering: 1) the amount of test engine preparation, and 2) the level of instrumentation related to clearances, performance, and case temperature.

The highest potential for successful correlation of flight load levels with engine performance losses and clearance changes, including identification of the differences between outboard and inboard engine installation locations, would be by analytically preparing both inboard and outboard engines. Performance testing of both engines with expanded instrumentation in sea level test stands, installed prior to each flight, and continuous monitoring during flight would permit direct correlation of performance loss to specific flight events. Installation of fan and high-pressure turbine proximity probes would permit direct correlation of flight load level to clearance changes under both steady and dynamic flight load situations. Postflight test performance calibrations and analytical engine disassembly would permit the changes in clearances and other part conditions throughout the engine to be documented as well as the correlation of measured module performance losses with specific causative factors. The installation of case thermocouples would permit correlation between actual measured case temperatures in flight with those measured during the X-ray Facility Load Test program to facilitate definition of the role of engine case environmental temperatures and leakages in permanent clearance changes and performance losses. This approach represents the first engine program option examined and would involve the lease of two engines from those available in P&WA's lease pool.

As a second engine program option to reduce overall program costs, without sacrificing a significant level of confidence in achieving the desired program objectives, the use of an analytically prepared engine for the inboard location and a partially prepared outboard engine was examined. The spare engine which supports the RA001 airplane test program would be returned to P&WA's Service Center for swap of the fan containment case and high-pressure turbine module with previously analytically prepared units for evaluation in the outboard engine location. This swap could be accomplished in a short period of time and limits the risk of an RA001 airplane out-of-service condition for lack of spare engine support. This second option would require lease of only one engine and one high-pressure turbine module. At the conclusion of the flight test program, both engines would be returned to P&WA and performance tested. The inboard engine and the high-pressure turbine of the outboard engine would be analytically disassembled. The original fan case and high-pressure turbine module would be reinstalled in the spare engine and the engine returned to Boeing in ten days elapsed time to support RA001 continued flight testing.

The third engine program option examined sacrifice of the analytically prepared lease engine for the inboard location. The spare engine with an analytically prepared high-pressure turbine module and fan containment case would be utilized in the inboard location. Twenty case thermocouples and expanded instrumentation would be installed on the inboard engine. The outboard engine would have the fan containment ring exchanged to permit fan clearance measurement. The exchange of fan cases would be accomplished by a Pratt & Whitney Aircraft crew with the outboard engine still installed. Minimum performance and no thermocouple case temperature data would be available on the outboard engine. Under this option, installed performance calibrations would be omitted as the performance change data would be significantly less meaningful than in option one or two. Option three sacrifices confidence in achieving all of the program objectives, however, it retains a portion of all the types of data and the more significant ability to correlate clearance change with specific flight events and load levels. Under this option, lease of only a high-pressure turbine module would be required.

Engine program option four is identical in terms of the engine preparation to option three, however, the engine expanded performance and case temperature instrumentation are deleted in favor of maintaining the clearance change instrumentation. This option completes the sacrifice of the objective of direct correlation of performance changes with flight load levels/events.

Engine program option five retains the inboard engine clearance change instrumentation and preparation as described in option three but deletes the fan case swap and fan clearance instrumentation on the outboard engine. This option would additionally sacrifice the ability to discern differences in engine response to loads between inboard and outboard installation locations as well as data concerning engine response to the higher relative inertia load levels with respect to aerodynamic load expected in the outboard location.

Engine program option six would reduce the clearance instrumentation to the fan only on the inboard engine. The change of the fan containment ring would occur as described for the outboard engine in options four and five. The technical integrity of the program with respect to defining the effect of flight load on the engine has been so compromised as to make this option a waste of technical resources. This option, however, was examined and costed to define a lower boundary of program cost. To reiterate, this option deletes expanded performance instrumentation, all case temperatures, all outboard engine clearance and the inboard high-pressure turbine clearance instrumentation. All performance testing would be deleted and no lease hardware would be needed.

7.2.3 Flight Program Scenario Elements

It is desirable to include in the flight test program every condition and maneuver that occurs during typical revenue flights and that may have a significant impact on engine performance deterioration. The acceptance flight test, which every airplane goes through before delivery, contains many elements of a typical revenue flight, but not all of them.

Take-offs at various gross weights impose different loads on the inlet, and landings affect inertia and gyro loads.

Refueled landings (go-around) lead to particular temperature transients in the engine.

High g, steady state maneuvers impose a combination of air loads and inertia loads on the engine that can be simulated through wind-up turns.

Gusts produce transient inertia loads on the nacelles, as well as special patterns of air load distributions.

Other maneuvers that may cause unusual temperature transients include noise abatement maneuvers, step climbs and descents, variation in climb profile for very long range flights, reduced-thrust take-off effects, and thrust reverser operation.

To run specific flight tests for each one of these conditions would, however, exceed the time and funding limitations imposed on this program. It was decided therefore to limit the test to those conditions that are most representative of typical revenue flights and whose frequency of occurrence is such as to have a major impact on performance deterioration. The selected conditions are:

Take-Offs and Landings at Different Gross Weights

The typical flight acceptance test airplane weighs about 500,000 pounds at take-off. Revenue flights at 650,000 and 820,000 pounds will be simulated because inlet loads during take-off rotation vary considerably with gross weight (speed and angle of attack effect).

Landings at the appropriate maximum permissible gross weight and go-arounds shall follow these take-offs in order to measure landing loads on the engine as well as temperature transients in the engine.

Wind-Up Turns

Wind-up turns, that is, coordinated turns at constant speed and altitude, will be carried out to induce inertia loads on the nacelle. Wind-up turns at 1.3, 1.5, and 2 g's shall be flown to simulate the effects of gusts, avoidance maneuvers, and other flight conditions not occurring during the acceptance flight.

Gust Flying

It is desirable to measure the inertia loads induced by turbulence. These measurements may be accomplished during the above mentioned missions if a sufficient level of turbulence is encountered. If not, flying time could be devoted to seek gust fields.

Flight Hours

First Option

Acceptance Test Flight	7 hours
Gross Weight Variations, Wind-Up Turns, and Maneuvers	8 hours
Ferry Flights	3 hours
Gust Search	15 hours
Total	33 hours

Second Option

Acceptance Test Flight	7 hours
Gross Weight Variations, Wind-Up Turns, and Maneuvers	8 hours
Total	15 hours

Third Option

Acceptance Test Flight	7 hours
------------------------	---------

These flight durations allow for a repetition of missions where unsatisfactory measurements were obtained.

7.3 SELECTED OPTIONS

The various flight load instrumentation, engine instrumentation, and flight program scenario options discussed in Section 7.2 were combined into the seven basic Flight Loads Test Program Options shown in Table 7.3-I.

Program Option I combines the first option for each of the elements (aircraft option and engine option) and has the maximum probability of successfully achieving all of the program objectives. Program Option II represents a small sacrifice in probability of achieving the technical objectives, while each successive option to Option VII reduces the amount of instrumentation for determination of either loads, engine response, or flight coverage. Option VII represents, in the judgement of BCAC and P&WA, a program of such low technical value that the sole purpose in defining it was to bound the potential programs on the minimum side.

In the course of examining the seven basic options and the related costs, two additional options were defined. Option VIII represents an increase of loads instrumentation of Option VI to include outboard nacelle pressure load instrumentation. Option IX incorporates a further refinement of Option VIII to include basic inboard inertia loads instrumentation and engine option 3, which adds fan clearance instrumentation to the outboard engine, and expanded performance and case thermocouples to the inboard engine.

TABLE 7.3-I
FLIGHT TEST PROGRAM OPTIONS INVESTIGATED

Program Option No.	Basic							Added	
	I	II	III	IV	V	VI	VII	VIII	IX
Aircraft Option (BCAC)	1	1	2	3	4	5	6	5+	5++
Engine Option (P&WA)	1	2	3	4	4	5	6	5	3
Flight Hours	33	33	15	15	15	15	7	15	15
Acceptance Flight	X	X	X	X	X	X	X	X	X
Take-Off/Landings	X	X	X	X	X	X		X	X
Wind-Up Turns	X	X	X	X	X	X		X	X
Gust Loads	X	X							

+ and ++; Modifications of Aircraft Option 5 (Table 7.2.1-I).

7.4 PROGRAM RELATIVE COST

Since actual program cost estimates are proprietary, an arbitrary value of program cost was selected, and the ratio of the estimated cost of each program to the base value was determined. Table 7.4-I shows the relative cost of each of the nine Program Options examined. The estimated cost for preparing and refurbishing the NASA space shuttle carrier 747 airplane would essentially double the cost of conducting the recommended or alternate programs as discussed in Section 7.1.

TABLE 7.4-I

RELATIVE COST FOR PROGRAM OPTIONS EVALUATED

Program Option No.	I	II	III	IV	V	VI	VII	VIII	IX
Relative Program Cost	1.544	1.472	1.104	1.12	1.092	0.968	0.664	0.996	1.058

7.5 COST EFFECTIVENESS

A means of evaluating the relative technical merits of each potential program option was developed to facilitate evaluation of the cost effectiveness of each program option. The technique also aided in the assessment of the effectiveness of additional combinations of instrumentation on both inboard and outboard engines and/or flight program scenarios not covered in the original seven options examined.

The basis of the evaluation procedure was the distribution of the program value between determination of load level (cause), engine response (effect), and the flight load event coverage permitted by various amounts of flight time (data quantity). Based on detailed discussions, the consensus favored a distribution of the total program value (100 percent) as follows: 1) 30 percent to load level determination, 2) 30 percent to engine response determination, and 3) 40 percent to data quantity (coverage of specific flight load events).

It was further determined that a value should be given to each type of data (i.e., inboard pressure loads, case temperature, etc.) and flight type (acceptance, gust, etc.) which ranked that particular element importance with respect to other elements of either data or flight type. Additionally, if the amount of instrumentation for a particular element could be reduced, a reduction in value would be assigned that would relate to the change in confidence of achieving the technical goal for that specific data element. The arbitrary scale for data and flight elements of from 1 to 10 was assigned to each element. A value of 10 signifies the highest level of importance and 0 the lowest where no provisions for a particular item have been made.

Table 7.5-I shows the values assigned to each data element and flight type/load type. The total value score for flight load instrumentation/data is 23, engine response is 23, and flight test elements is 30. This scoring provides 23/76 or approximately 30 percent to cause and effect data elements and 30/76 or 40 percent to the flight test program and meets the distribution of program value established.

A reduction in value was assigned when the quantity of instrumentation for any data element was reduced. These values are also shown in Table 7.5-I.

The values assigned are based on a relative ranking of:

- o The technical value of each type of data based on engineering judgment of the significance of the data element in understanding and quantifying the causes for short-term engine performance deterioration.

- o The completeness and quantity of similar existing data from other parts of the NASA JT9D Jet Engine Diagnostics Program or previous contractor/subcontractor testing.
- o The overall importance of specific types of flights or flight maneuver events and relative frequency of occurrence in typical airline service.

As a specific example of the rationale used for assigning the value of 10 to instrumentation to determine pressure loads on the inboard engine, the following factors were considered:

- o Analytical studies predict that 87 percent of the short-term engine performance loss is caused by aerodynamic pressure loads, and these studies are based on estimates of inboard nacelle loads.
- o Previous flight test pressure load information exists for the inboard engine location of the 747/JT9D even though the data are insufficient.
- o The current X-Ray Facility Load Test program is measuring the impact of simulated inboard engine pressure loads on engine clearances.

The rationale for assigning the next highest value of technical merit(s) to instrumentation to determine inboard engine clearances is the same.

While the estimated effects of inertia loads on engine performance are small, there is uncertainty about the normal levels of these flight loads. The inertia load levels are anticipated, based on airplane structural analysis and limited data, to be highest in the outboard engine location. This data element was considered to rank next in overall technical importance.

Provided the test engines are analytically prepared and expanded instrumentation is used, determination of engine and module performance changes can be undertaken and specific causes documented through analytical teardown and examination. This data element is considered next in value or merit. However deletion of the full analytical build and/or expanded performance instrumentation would seriously detract from the value of obtaining such data.

Analysis of performance data from short-term service engines and monitoring of engines just entering service suggests a significant loss of performance during the acceptance flight of the aircraft. The relative ranking of 10 for measuring the loads and engine response during this flight test is therefore obvious.

Rankings or values were established for each data element and flight type by identical methods, based on previous studies conducted under the NASA JT9D Jet Engine Diagnostics Program.

Table 7.5-II shows the Technical Value for the seven options initially examined both in terms of numerical score and relative value in percent.

Two additional options were examined (VIII and IX) which reintroduced the outboard nacelle pressure instrumentation (Option VII), the outboard fan proximity probes, and inboard primary inertia loads instrumentation. The technical score and relative value are shown in Table 7.5-III.

The relative cost for each of the programs is shown in Table 7.4-I.

The relative program costs from Table 7.4-I and technical values were cross plotted, and a line was drawn from the origin to the point of tangency with the curve to determine the optimum program cost and technical value. This curve and tangent line are shown in Figure 7.5-1. Program option IX is the closest to the optimum program, followed in descending order by Program Options VIII and VI.

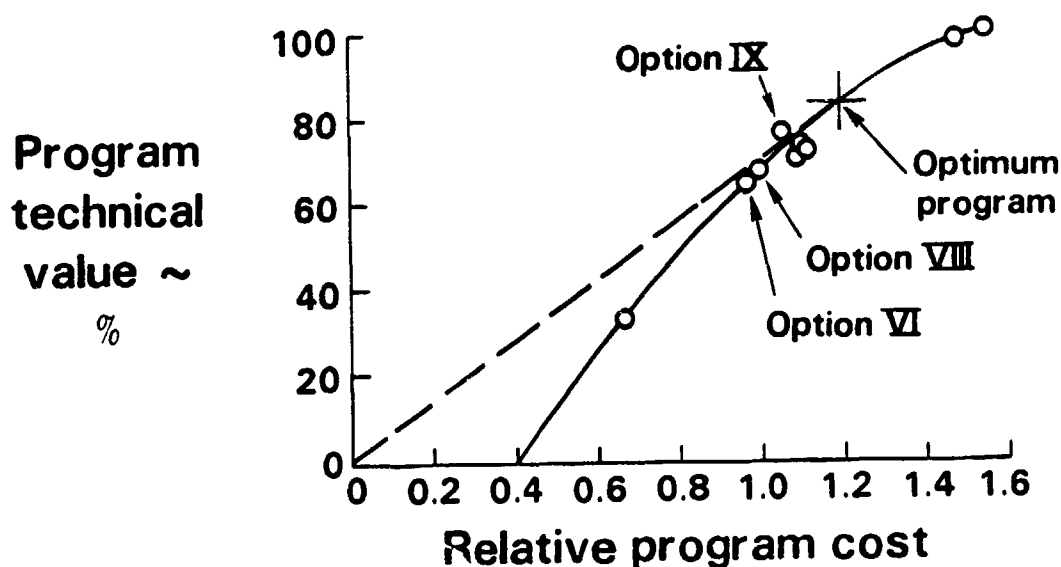


Figure 7.5-1 Cost Effectiveness Evaluation Results - Option IX is the most cost effective program.

TABLE 7.5-1

TECHNICAL MERIT VALUES ASSIGNED TO INSTRUMENTATION/DATA ELEMENTS
AND TO SPECIFIC FLIGHT TEST TYPES

RELATIVE DATA MERIT (Scale of 1 through 10)

Loads; maximum points = 23:

Pressure Loads, Inboard = 10 (396*), 9 (252*), 4 (126*)
g and gyro Loads, Inboard = 4 (18*), 2 (10*)
Pressure Loads, Outboard = 2
g and gyro Loads, Outboard = 7(18*), 6 (10*)

* Numbers in parentheses = number of static pressure
taps, accelerometers or rate gyros.

Engine Clearance Change; maximum points = 14:

Fan/High-Pressure Turbine, Both Inboard and Outboard; $8 + 6 = 14$
Fan/High-Pressure Turbine, Inboard; Fan, Outboard; $8 + 3 = 11$
Fan, Both Inboard and Outboard; $4 + 3 = 7$
Fan, Inboard Only; $4 + 0 = 4$

Performance Change and Analytical Build; maximum points = 6:

Expanded/Full Analytical (1 or 2 engines) = 6 (2 engines)
= 5 (1 engine plus
partial on 2nd)
Expanded/Partial Analytical (1 or 2 engines) = 2
Standard/No Analytical Build = 1

Case Temperature Thermocouples; maximum points = 3:

92 Thermocouples (2 engines) = 3
72 Thermocouples (1 engine) = 2
20 Thermocouples (1 engine) = 1

Total Relative Data Value = 46

RELATIVE FLIGHT TEST SCENARIO TECHNICAL VALUE

Data Quantity (Scale of 1 through 10):

Acceptance Flight Test = 10
Variations in Take-Off Conditions = 6
Variations in Landing Conditions = 3
Gust Loads = 5
Wind-Up (High g) Turns = 6

Total Relative Data Quantity Value = 30

TABLE 7.5-II
JT9D DIAGNOSTICS FLIGHT LOADS TEST PROGRAM OPTIONS

Program Option No.	I		II		III		IV		V		VI		VII	
	Inbd	Otbd	Inbd	Otbd	Inbd	Otbd	Inbd	Otbd	Inbd	Otbd	Inbd	Otbd	Inbd	Otbd
Flight Hours	33	33	33	33	15	15	15	15	15	15	15	15	7	7
Location														
Pressure Taps	396	45	396	45	396	0	396	45	396	0	252	0	126	0
Inertia Instrumentation	18	18	18	18	0	18	0	10	0	10	0	10	0	10
Proximity Probes	8	8	8	8	8	4	8	4	8	4	8	0	4	0
Thermocouples	72	20	72	20	20	0	0	0	0	0	0	0	0	0
Engine Performance	Exp	Exp	Exp	Exp	Exp	Std	Std	Std	Std	Std	Std	Std	Std	Std
Loads Rating Value	23	23	23	23	17	17	18	18	16	16	15	15	10	10
Engine Rating Value	23	23	22	22	14	14	12	12	12	12	9	9	5	5
Flight Rating Value	30	30	30	30	25	25	25	25	25	25	25	25	10	10
Total Rating Value	76	76	75	75	56	56	55	55	53	53	49	49	25	25
Program Technical Value (%)	100		97.8		73.7		72.4		69.8		64.5		32.9	

TABLE 7.5-III

ADDITIONAL PROGRAM OPTIONS EVALUATED

<u>Item</u>	<u>Option VIII</u>		<u>Option IX</u>	
	15		15	
Flight Hours	Inbd	Otbd	Inbd	Otbd
Location	Inbd	Otbd	Inbd	Otbd
Pressure Taps	252	45	252	45
Inertia Instrumentation	0	10	10	10
Proximity Probes	8	0	8	4
Thermocouples	0	0	20	0
Engine Performance	Std	Std	Exp	Std
Loads Rating Value	17		19	
Engine Rating Value	9		14	
Flight Rating Value	25		25	
Total Rating Value	51		58	
Program Technical Value (%)	67.2		76.3	

SECTION 8.0

RECOMMENDATIONS

It is concluded that a flight test program meeting the overall objective of determining the levels of aerodynamic and inertia loads to which the engine is exposed during the initial flight acceptance test and normal flight maneuvers is feasible and desirable. The concurrent measurement of engine clearance changes in the fan and first-stage high-pressure turbine, performance changes, and case thermal environment are also feasible and equally desirable.

The use of the NASA owned space shuttle carrier 747 aircraft, while technically feasible, is not recommended. There are technical and financial considerations, as well as the impact on the availability of the NASA airplane for its primary mission, that make the use of the aircraft undesirable. This recommendation is primarily based on the impact on program cost and the requirement to remove all instrumentation wiring and data recording equipment installed for the flight test program from the aircraft at the end of the program. The instrumentation and recording equipment cost might have been justifiable in terms of preparing the NASA 747 aircraft for long-term use on other potential research programs; however, the requirement for removal of the equipment/wiring negates this potential from consideration. The use of the BCAC RA001 airplane as the test vehicle for the flight loads test program is recommended.

The technical evaluations of the flight loads program options have been discussed in Section 7.0. The results of this analysis lead to the recommendation that Option IX be considered the preferred program. This program provides 15 hours of dedicated flight test time which will permit determination of the flight load levels encountered during the flight acceptance test, variation in take-off/landing conditions, and wind-up turns. The aerodynamic and inertia load instrumentation will provide data for both inboard and outboard engine installation positions to identify the variations in flight load levels between inboard/outboard engines and to correlate inertia loads at both locations with the aircraft center of gravity. This option will achieve 80 percent of the technical information sought in terms of flight load data type and quantity. This recommended program makes use of the available spare engine to permit instrumentation of the fan and high-pressure turbine for clearance changes on the inboard engine.

PRECEDING PAGE BLANK NOT FILLED

Exchange of the fan containment case by a P&WA team at Boeing will permit measurement of fan clearance changes on the outboard engine. The inboard engine would be prepared by installation at P&WA's Southington Service Center of an analytically prepared high-pressure turbine module and fan containment case. Expanded performance instrumentation would be utilized to assist in determining which flight load conditions are most deleterious to engine performance. Sufficient engine turbine case temperature information will be obtained to determine the variation in the high-pressure turbine case thermal environment between the X-ray Facility Load Test program and the Flight Test program. This option would obtain over 60 percent of the potentially achievable engine information.

In order to reduce estimated program costs, Option VIII was identified which eliminates the inertia loads instrumentation, expanded performance, and case thermocouples on the inboard engine and the fan clearance instrumentation on the outboard engine. This option retains the 15 hours of flight time and 74 percent of desired loads instrumentation for determination of flight load levels. The technical value for the engine instrumentation has been reduced to approximately 40 percent of the potential value related to determining the effect of loads, covering measurement of clearance changes related to loads on the fan and high-pressure turbine of the inboard engine alone.

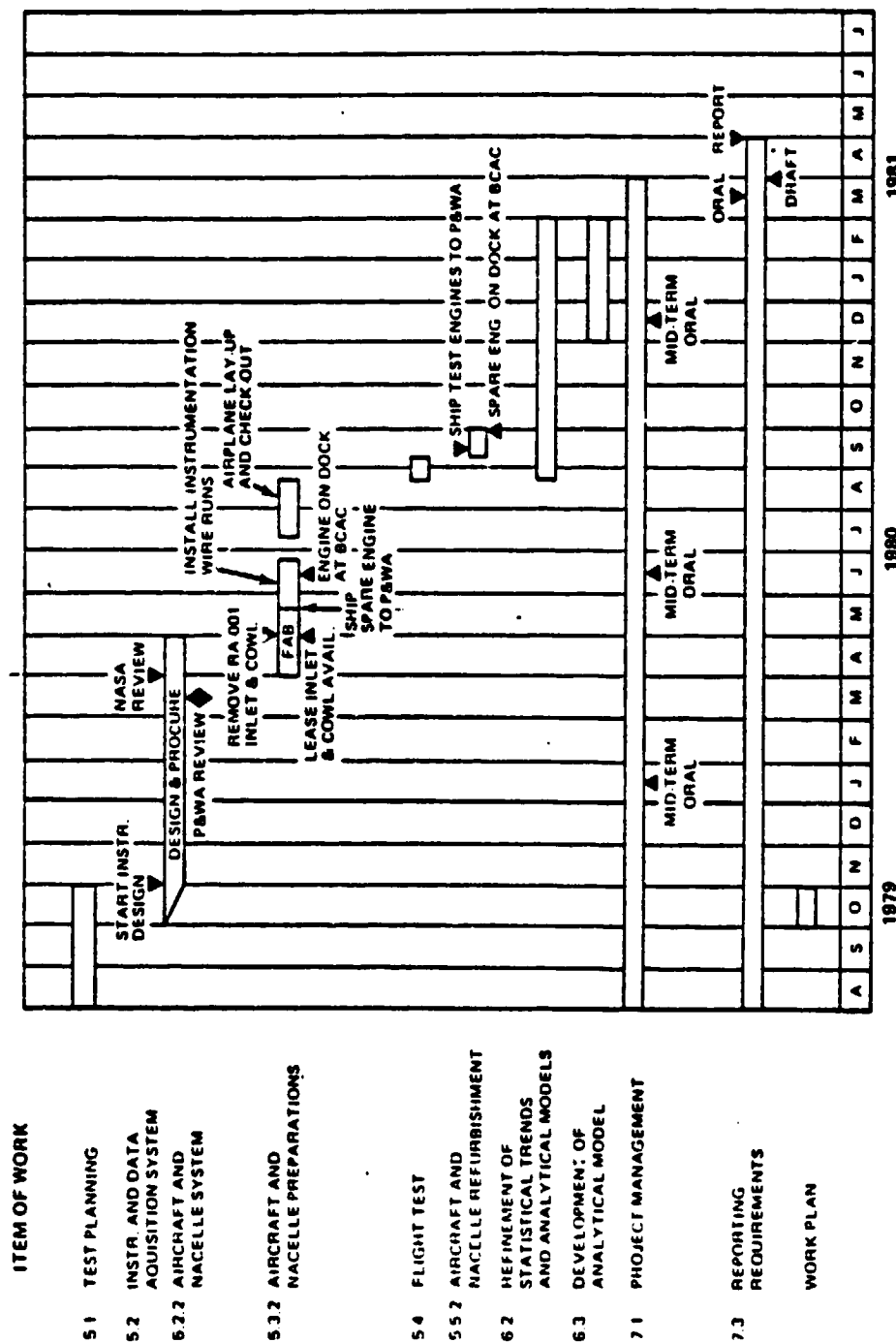
Option VI represents the third choice and is identical to Option VIII with the exception of removing the outboard nacelle pressure loads instrumentation. The dedicated 15 hour flight test program is retained, however, on a technical value basis. Only 65 percent of the potential loads information would be obtained.

Programs of lesser cost are not recommended. Further reduction of flight hours below the 15 hours recommended would represent significant and unwarranted risk in obtaining the desired flight loads data. Reduction in either loads instrumentation or engine instrumentation beyond that recommended in Option VI would further deteriorate the technical value of the program to a point that it would not be a cost effective investment on the part of NASA or an efficient use of resources by Pratt & Whitney Aircraft and the Boeing Commercial Aircraft Company.

APPENDIX A
SCHEDULE AND MILESTONES

C-2

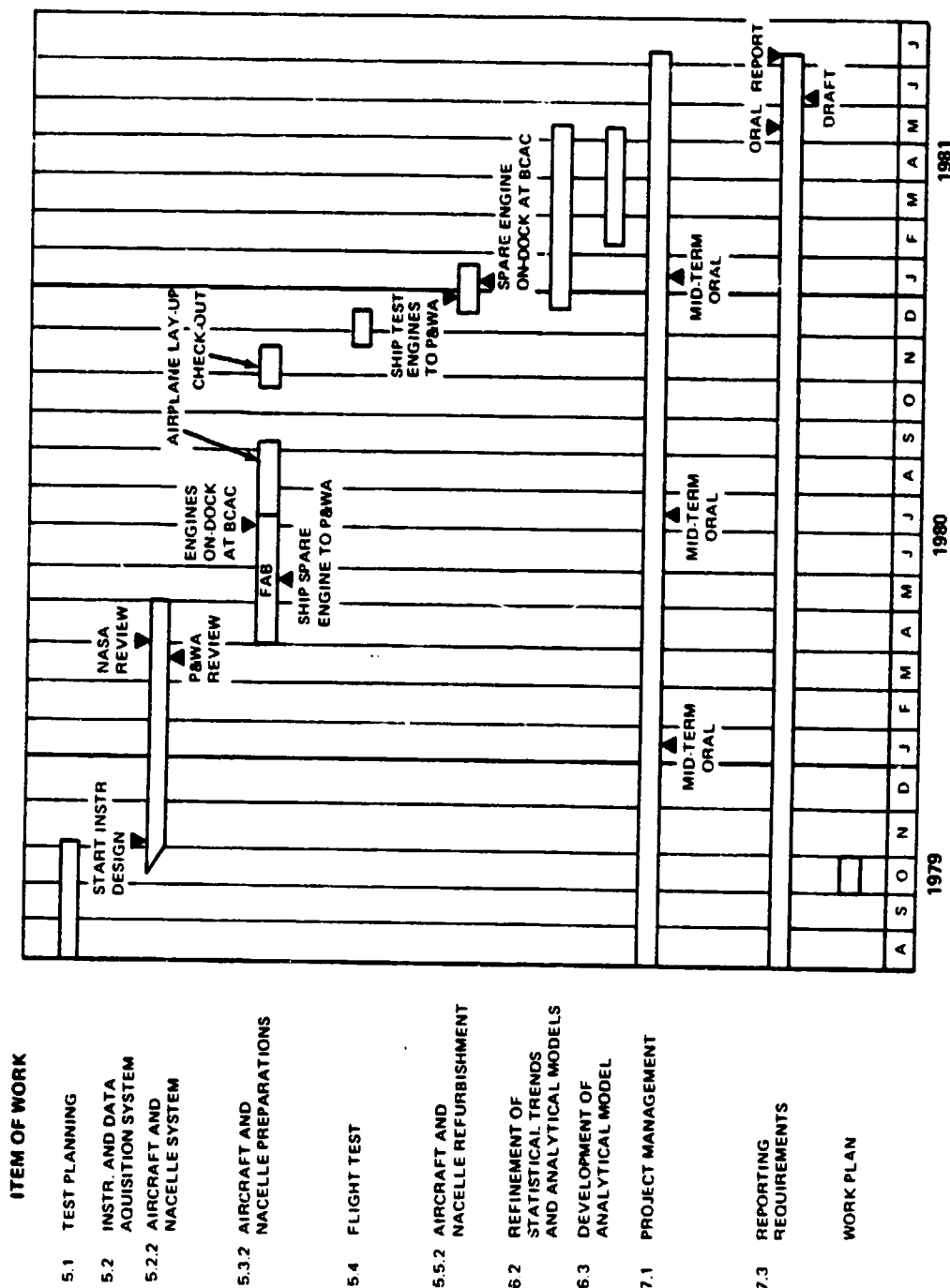
SCHEDULE I **747/JT9D FLIGHT LOADS FLIGHT TEST PROGRAM**



SCHEDULE II

DEFERRED

747/JT9D FLIGHT LOADS FLIGHT TEST PROGRAM



APPENDIX B
LIST OF ACRONYMS AND SYMBOLS

APPENDIX B

LIST OF ACRONYMS AND SYMBOLS

ADAMS	- Automatic Data Analysis and Monitoring System
APTDAC	- Automatic Production Test Data Acquisition and Control
BCAC	- Boeing Commercial Airplane Company
C.G. (or cg)	- Center of gravity
CDLA	- Condition lever angle
CRT	- Cathode ray tube
D/A	- Direct write
DAC	- Digital-to-analog converter
EB	- Environmental box (for T.V. camera)
EGT	- Exhaust gas temperature ($^{\circ}\text{C}$, $^{\circ}\text{F}$)
EVC	- Engine vane control
Fus	- Fuselage
g	- Acceleration of gravity (m/sec^2 or ft/sec^2)
GN ₂ (or GN2)	- Gaseous nitrogen
gyro	- Gyroscopic
HAPTS	- High Accuracy Pressure and Temperature (Data Acquisition) System
Hertz	- Frequency (cycles/sec)
HSD	- Hamilton Standard Division
HSPLM	- High-Speed Pulse Code Modulation
IGV	- Inlet guide vane
IRIG	- Inter-Range Instrumentation Group
LVDT	- Linear variable differential transducers
Man	- Manifold
mV	- Millivolt
NASA	- National Aeronautics and Space Administration
NBS	- National Bureau of Standards
PA	- Ambient pressure (psia)
PCM	- Pulse Code Modulation
PIC	- Plug-In Console (test system)
PLA	- Power lever angle
Pr	- Probe
psi	- Pounds per square inch
RMDU	- Remote Multiplier/De-Multiplier Units
RSS	- Root sum square
SCA	- Shuttle Carrier Airplane
TAI	- Thermal anti-icing (duct)

TC	- Thermocouple
TSFC	- Thrust specific fuel consumption (lb/hr-lb)
UTR	- Uniform temperature reference
V_d	- Design drive speed
V_{mo}	- Maximum operating speed
VAC	- Volts (alternating current)
β	- Stator vane angle
Ω	- Ohms